Aus dem Zentrum für Innere Medizin (Krehl Klinik) der Universität Heidelberg

(Geschäftsführender Direktor: Herr Prof. Dr. med. Hugo A. Katus)

Klinik für Hämatologie, Onkologie und Rheumatologie

(Ärztlicher Direktor: Herr Prof. Dr. med. Carsten Müller-Tidow)

# Blockade of CD95/CD95L Death Signaling Enhances CAR T Cell Persistence and Antitumor Efficacy

Inauguraldissertation

zur Erlangung des Doctor scientiarum humanarum

an der

Medizinischen Fakultät Heidelberg

der

Ruprecht-Karls-Universität Heidelberg

vorgelegt von

Bailin He

aus

Dongguan, China

2021

# CONTENT

# LIST OF ABBREVIATIONS

| | |
|---|---|
| 51Cr | Chromium-51 |
| 7AAD | 7-Aminoactinomycin D |
| ACT | Adoptive T cell therapy |
| AICD | Activation-induced cell death |
| AML | Acute myeloid leukemia |
| ALL | Acute lymphoid leukemia |
| ATCs | Activated T cells |
| ALPS | Autoimmune lymphoproliferative syndrome |
| ATP | Adenosine triphosphate |
| BCA assay | Bicinchoninic acid assay |
| BSA | Bovine serum albumin |
| CAR | Chimeric antigen receptor |
| Cas9 | CRISPR associated-9 |
| CBA | Cytometric Bead Array |
| CLL | Chronic lymphocytic leukemia |
| CR | Complete remission |
| CRISPR | Clustered regularly interspaced short palindromic repeats |
| crRNA | CRISPR RNA |
| CTG | Cell-titer-glo |
| CTLA-4 | Cytotoxic T-lymphocyte-associated protein 4 |
| DLBCL | Diffuse large B-cell lymphoma |
| DMSO | Dimethylsulfoxid |
| DSMZ | German Collection of Microorganisms and Cell Cultures |
| E:T | Effector to target |
| ELISA | Enzyme-linked immunosorbent assay |
| FACS | Fluorescence-activated cell sorting |
| FADD | Fas-associated death domain protein |
| FBS | Fetal bovine serum |
| FDA | Food and drug administration |
| FFluc | Firefly luciferase |
| FMO | Fluorescence minus one |
| GFP | Green fluorescence protein |
| gRNA | Guide ribonucleic acid |
| HD | Healthy donor |
| HD-CAR-1 | Heidelberg CAR T cell trial 1 |
| HSC | Hematopoietic stem cells |
| HSCT | Hematopoietic stem cell transplantation |
| IC50 | Half-maximal inhibitory concentration |
| ICS | Intracellular cytokine staining |
| IFN-γ | Interferon-gamma |
| IL | Interleukin |

| | |
|---|---|
| IL-2Rβ | Interleukin-2 receptor beta chain |
| IMDM | Iscove's modified dulbecco's medium |
| IVT | *in vitro* transcription |
| KO | Knockout |
| LAG3 | Lymphocyte-activation gene 3 |
| L-Gln | L -Glutamine |
| mCD95L | Membrane CD95L |
| MACS | Magnetic-activated cell sorting |
| MDS | Myelodysplastic syndrome |
| Near IR | LIVE/DEAD$^{TM}$ fixable near-infrared |
| NHL | Non-Hodgkin's lymphoma |
| NFAT | Nuclear factor of the activated T-cell |
| Oligos | Oligonucleotides |
| OR | Overall response |
| PBMCs | Peripheral blood mononuclear cells |
| PBS | Phosphate-buffered saline |
| PBT | Peripheral blood T cells |
| PCR | Polymerase chain reaction |
| PD1 | Programed cell death protein 1 |
| PR | Partial response |
| RLU | Relative light units |
| RIPA | Radio-immunoprecipitation assay |
| RNPs | Ribonucleoproteins |
| rpm | Revolutions per minute |
| r/r | Relapsed or refractory |
| RT | Room temperature |
| scFv | Single-chain variable fragment |
| SDS-PAGE | Sodium dodecyl sulphate–polyacrylamide gel electrophoresis |
| SEM | Standard error of the mean |
| sCD95L | Soluble CD95L |
| $T_{CM}$ | Central memory T cells |
| $T_E$ | Effector T cells |
| $T_{EM}$ | Effector memory T cells |
| $T_N$ | Naïve-like T cells |
| $T_{SCM}$ | Stem cell memory-like T cells |
| TBST | Tris buffered saline with tween 20 |
| TCR | T-cell-receptor |
| TIM3 | T cell immunoglobulin mucin-3 |
| TME | Tumor microenvironment |
| TNF-α | Tumor necrosis factor alpha |
| tracrRNA | Transactivating crRNA |
| TRUCK | T cell redirected for antigen-unrestricted cytokine-initiated killing |
| ζ | zeta |

# 1 INTRODUCTION

## 1.1 Hematologic malignancies

Hematopoiesis is based on a small pool of multi-potent hematopoietic stem cells (HSCs) which self-renew and differentiate into distinct cellular lineages of the blood (Morrison and Scadden 2014). Dysregulation of hematopoiesis results in the development of hematologic malignancies, which affect peripheral blood, bone marrow, and the lymphatic system (Vardiman et al. 2009). Hematologic malignancies, including leukemia, lymphoma, and myeloma, account for 6.6% of all newly diagnosed cancers in 2018 according to Global Cancer Statistics (Bray et al. 2018), making hematologic malignancies the fourth most common type of cancer in the world. Chemotherapy, targeted therapies and hematopoietic stem cell transplantation (HSCT) have dramatically improved the outcome of hematologic malignancies, especially for B cell malignancies like acute lymphoid leukemia (ALL) and diffuse large B cell lymphoma (DLBCL), with the 5-year survival rate ranging from 40% to 70% (Allemani et al. 2018). However, still 20-40% of patients with ALL relapse after initial treatment (Sive et al. 2012), and less than 10% of relapsed or refractory (r/r) ALL patients survive more than 5 years (Marks et al. 2019). Similarly, poor outcomes are also observed in patients with refractory DLBCL. Only 26% of patients achieve an objective response and 7% of patients obtain complete response (CR) to the later treatment (Crump et al. 2017). Thus, disease relapse after chemotherapy and hematopoietic stem cell transplantation remain a major challenge for the treatment of hematologic malignancies. Novel treatment approaches for patients with r/r hematologic malignancies are needed. Chimeric antigen receptor (CAR) T cell therapy is one of those new treatment options due to their ability to charge the immune system to attack cancer cells.

## 1.2 Chimeric antigen receptor (CAR) T cell therapy

CAR T cell therapy is a form of immunotherapy that uses genetically engineered T cells to fight cancer. T cells from a patient are isolated and genetically modified to

express a synthetic receptor called chimeric antigen receptors (CARs) that specifically binds to a tumor antigen, such as CD19, CD20, CD22 in B cell malignancies or CD33, CD123, CLL-1 in AML (Hofmann et al. 2019). CAR T cells are expanded *in vitro* and then infused back into the patient to attack the tumor cells (Feins et al. 2019). CARs are composed of an extracellular binding domain, a hinge region, a transmembrane domain, and one or more intracellular signaling domains (Cheng et al. 2019). Single-chain variable fragments (scFvs) derived from tumor antigen-reactive antibodies are commonly used as extracellular binding domains. The hinge region connects the scFv to the transmembrane segment and confers stability to the synthetic receptor. All CARs harbor the CD3 zeta chain domain as the intracellular signaling domain (Figure 1.1).
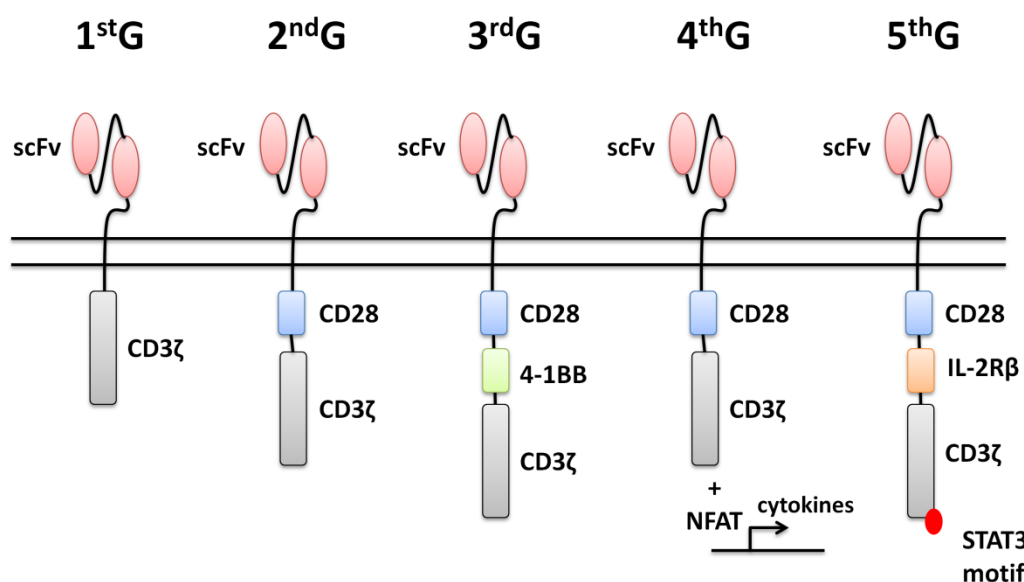


**Figure 1.1 The Current Landscape of Chimeric Antigen Receptor (CAR) Designs.**
The first generation CARs (1stG) contain the target domain scFv and the intracellular CD3ζ domain. Second generation CARs (2ndG) incorporate a costimulatory domain, such as CD28, 4-1BB or OX40, in addition to the 1stG CARs properties. Third generation CARs (3ndG) incorporate two costimulatory domains. Fourth-generation CARs (4thG) contain one co-stimulatory domain and a nuclear factor of the activated T-cell (NFAT) to direct the cell to express transgenic products, such as cytokines IL-12 or IL-18. Fifth-generation CAR (5thG) is based on 2G CARs with the IL-2 receptor beta chain (IL-2Rβ) and a STAT3-binding motif.

First-generation CARs comprise only the CD3 zeta intracellular signaling domain and displayed low clinical efficacy in patients (Jensen et al. 2010). Second-generation

CARs contain a co-stimulatory domain such as CD28, 4-1BB (CD137) or OX40 (CD134) adjacent to the CD3 ζ-domain and achieve enhanced clinical efficacy (Hu et al. 2016). Currently, the most commonly used costimulatory signals of CARs involve 4-1BB and CD28. The 4-1BB signal induces moderate expansion and prolonged persistence of CAR T cells, while the CD28 signal induces robust expansion and greater functionality of CAR T cells (Zhao et al. 2015). Third-generation CARs contain two co-stimulatory domains, like CD28 and 4-1BB, exhibit advanced proliferative capacity, has been reported improved effector functions and *in vivo* persistence as compared to second-generation CAR (Enblad et al. 2018; Ramos et al. 2018). Fourth-generation CAR T cells also known as T cell redirected for antigen-unrestricted cytokine-initiated killing (TRUCK) T cells encode genes for cytokine production (like IL-12, IL-15 or IL-18) to augment CAR T cell activity or suicide genes to prevent toxicity (Chmielewski and Abken 2015; Chmielewski and Abken 2020). Recently, a fifth-generation CAR has been reported that CAR encoding a IL-2 receptor beta-chain and a STAT3-binding motif, together with the CD3zeta and CD28 domains, showed superior *in vivo* persistence and antitumor effects in models of liquid and solid tumors (Hyrenius-Wittsten and Roybal 2019; Kagoya et al. 2018). However, the efficacy and toxicity of fourth- and fifth-generation CARs have not yet been evaluated in the clinical setting to date.

## 1.2.1 CD19.CAR T cell therapy in B cell malignancies

CD19 is a specific B-cell surface marker that plays a crucial role in the differentiation of naive B cells into pre-B cells and maintains the balance of mature B cells in peripheral blood (Xu et al. 2019). CD19 is expressed on the cell surface of normal B cells as well as most B-cell malignancies, which makes it an effective target for CAR T cell therapy. Anti-CD19 CAR T cell therapy has shown very promising clinical efficacy for treating relapse and refractory CD19^{+} B cell malignancies, including ALL, CLL and DLBCL (Table 1.1, adapted from (Skorka et al. 2020)). In 2017, the United States Food and Drug Administration (FDA) has approved two CD19.CAR T cell

therapies for patients with relapsed/refractory B cell malignancies, which are tisagenlecleucel (Kymriah®, CD3ζ-41BB) for r/r B-ALL and axicabtagene ciloleucel (Yescarta®, CD3ζ-CD28) for r/r DLBCL.

**Table 1.1 Selected clinical trials for CD19.CAR T therapy in B cells malignancies**

| Study | Phase | Disease | Costimulatory | Outcome (n/n) | References |
|---|---|---|---|---|---|
| NCT01593696 | I | ALL | CD28 | CR: 70% (14/20) | (Lee et al. 2015) |
| NCT01044069 | I | ALL | CD28 | CR: 83% (44/53) | (Park et al. 2018) |
| NCT02028455 | I/II | ALL | 4-1BB | CR: 93% (40/43) | (Gardner et al. 2017) |
| NCT02772198 | I/II | ALL | CD28 | CR: 90% (18/20) | (Jacoby et al. 2018) |
| NCT02435849 | II | ALL | 4-1BB | CR: 81% (61/75)[*] | (Maude et al. 2018) |
| NCT01029366 | I | CLL | 4-1BB | OR: 57% (8/14; 4 CR and 4 PR) | (Porter et al. 2015) |
| NCT01416974 | I | CLL | CD28 | OR: 38% (3/8; 2 CR and 1 PR) | (Geyer et al. 2018) |
| NCT01865617 | I/II | CLL | 4-1BB | OR: 74% (14/19; 4 CR and 10 PR) | (Turtle et al. 2017) |
| NCT03331198 | I/II | CLL | 4-1BB | OR: 87% (13/15; 7 CR and 8 PR) | (Siddiqi et al. 2019) |
| NCT00924326 | I | DLBCL | CD28 | OR: 68% (13/19; 9 CR and 4 PR) | (Kochenderfer et al. 2017) |
| NCT02631044 | I | DLBCL | 4-1BB | OR: 68% (89/131; 64 CR and 25 PR) | (Abramson et al. 2020) |
| NCT02348216 | I/II | DLBCL | CD28 | OR: 83% (84/101; 59 CR and 25 PR)[#] | (Locke et al. 2019) |
| NCT02445248 | II | DLBCL | 4-1BB | OR: 52% (48/93; 37 CR and 11 PR)[*] | (Schuster et al. 2019) |

Abbreviations: ALL, acute lymphoblastic leukemia; CLL, chronic lymphocytic leukemia; DLBCL, difuse large B-cell lymphoma; OR, overall response; CR, complete response; PR, Partial response; *, tisagenlecleucel; #, axicabtagene ciloleucel.

### 1.2.1.1 CD19.CAR T cell therapy in ALL

Acute lymphoid leukemia (ALL) is a hematological malignancy characterized by a transformation and proliferation of lymphoid progenitor cells (Skorka et al. 2020).

Although the 5-year survival for pediatric B cell ALL is up to 90%, the survival rate for adults is estimated at about 40% (Paul et al. 2016). The prognosis for the relapsing and refractory ALL is much worse and currently available treatment options being unsatisfactory. Anti-CD19 CAR T cell therapy has shown promising outcomes for r/r ALL. In the updated analysis of the phase II clinical trial with tisagenlecleucel (Kymriah ®) in pediatric and adult patients with r/r B-cell ALL, 81% (61/75) of patients obtained complete remission with at least 3 months of follow-up after an infusion. The remissions were durable, with a 6-month overall survival rate of 90% and relapse-free survival rate of 80% (Maude et al. 2018). The median duration of persistence of CAR T cells in blood was 168 days (range, 20 to 617 days) after a single infusion of tisagenlecleucel. High rates of complete remission have also been found in pediatric and adult patients with r/r ALL treated with other anti-CD19 CAR T cell therapies, ranging from 70% to 93% (Table 1.1) (Gardner et al. 2017; Jacoby et al. 2018; Lee et al. 2015; Park et al. 2018).

## 1.2.1.2    CD19.CAR T cell therapy in DLBCL

Diffuse large B cell lymphoma (DLBCL) is the most common type of non-Hodgkin's lymphoma in adults and it accounts for approximately 30-40% of all lymphomas. The 5-year overall survival rate of DLBCL is 60-70% after standard therapy, but primary refractory disease or relapse after therapy is not rare (Li et al. 2018). Surface B cell antigens CD19, CD20 and CD22 have the potential to be therapeutic targets for DLBCL. Currently, most of CAR T clinical trials in DLBCL focus on CD19 antigen and axicabtagene ciloleucel CD19.CAR T cells (Yescarta ®) containing the CD28 costimulatory domain has been approved for r/r DLBCL by the FDA in 2017. Long-term study of axicabtagene ciloleucel in refractory large B-cell lymphoma (ZUMA-1) including DLBCL, reported a total of 101 patients in phase 2 with a median of 27.1 months follow-up. The 2-year follow-up data showed that 83% (84/101) of patients achieved an objective response, 58% (59/101) of patients received complete response and 25% (25/101) of patients had a partial response, with median duration of response of 11.1 months (Locke et al. 2019). A second anti-CD19

CAR T cell product, Tisagenlecleucel (Kymriah ®), approved by the FDA for r/r ALL, has also been evaluated in r/r DLBCL. In the phase 2 study of tisagenlecleucel in adult patients with r/r DLBCL, a total of 93 patients who were ineligible for HSCT or had disease progression after autologous HSCT received an infusion with median time of 14 months follow-up. The best overall response rate was 52%, 40% of the patients achieved complete responses and 12% patients had partial responses (Schuster et al. 2019). Another trial also showed promising results of CD19.CAR T therapy for DLBCL (Abbasi et al. 2020; Kochenderfer et al. 2017), like lisocabtagene maraleucel with 73% (89/131) best overall responded rate and 49% complete remission rate (Viardot et al. 2019).

### 1.2.1.3 CD19.CAR T cell therapy in CLL

CLL is a hematological malignancy occurring in adults, characterized by a clonal proliferation of mature lymphocytes. CD19.CAR T cell therapy has proven to be effective in CLL patients who either did not respond to standard therapy or developed drug resistance over time, with approximately 74-87% best overall response rate and 21-47% CR rate (Siddiqi et al. 2019; Turtle et al. 2017). There have also been clinical trials that enrolled CLL patients who did not receive previous treatment. Patients who did not achieve complete remission after chemotherapy received CD19.CAR T cell infusion as a form of consolidative therapy. There are 3 out of 8 (38%) patients that responded to the CAR T therapy, with 2 (25%) patients achieving clinical CR and one (13%) achieving partial remission of disease (Geyer et al. 2018).

### 1.2.2 Limitations and improvements of CAR T cell therapy

Despite of the high overall response rate with CD19.CAR T cell therapy in patients with relapsed or refractory B cell malignancies, there are still 33-57% of ALL patients (Park et al. 2018; Turtle et al. 2017) and 18-47% of DLBCL patients (Neelapu et al. 2017; Schuster et al. 2019) relapsing after the cell therapy, mostly within 1 year of treatment (Song et al. 2019). Thus, understanding the limitations of CAR T cell therapy will be critical to realize the full potential of this novel treatment approach.

Growing evidence showed the limitations of the treatment including CD19-positive and -negative relapses. CD19-positive relapse is mostly due to poor persistence CAR T cell *in vivo*. CD19-negative relapses are associated with CD19 mutations, epitope masking, and trogocytosis in which CAR T cells "rip off" the CD19 molecules from the leukemic blasts by membrane transfer (Frigault and Maus 2020; Song et al. 2019). Across clinical trials, *in vivo* CAR T cell expansion and persistence have correlated with superior outcome in patients following the cell therapy. Poor CAR T cell persistence is often associated with an early relapse of leukemia or lymphoma within a few months after induction of successful remission (Song et al. 2019).

Multiple factors may influence the survival of CAR T cells following infusion, including the CAR construct, the state of T cell differentiation and local immuno-suppressive factors within the tumor-bearing host (Cheng et al. 2019). Third-generation CARs have been produced by incorporation of both CD28 and 4-1BB costimulatory signals, expecting to obtain good anti-tumor potency and prolonged persistence at the same time. Clinical data confirmed third-generation CD19.CAR T cells had superior expansion and longer persistence than second-generation CD19.CAR T cells (Ramos et al. 2018). The safety and favorable outcome of third-generation CD19.CAR T cell therapy in B cell malignancies has also been proven by the phase I/II clinical trial undertaken by our study group (NCT03676504, (Schubert et al. 2019)). Additionally, infusion of less differentiated CAR T cell subsets (like stem cell memory and central memory T cells) has been shown superior antitumor efficacy and long-term persistence of CAR T cells in multiple preclinical (Gattinoni et al. 2011; Klebanoff et al. 2005; Sommermeyer et al. 2016) and clinical studies (Blaeschke et al. 2018; Louis et al. 2011). Immuno-suppressive factors, including the inhibitory receptors (PD1, TIM3 and CTLA4) and pro-apoptotic genes (Fas and FasL), that negatively regulate T cell function and survival might be the potential therapeutic targets for enhancing adoptive immunotherapies (Mamonkin and Heslop 2017; Wang et al. 2019). Immune checkpoint inhibitors, such as anti-PD1 and anti-CTLA4 antibodies, have shown

remarkable benefit in the treatment of a range of cancer types, especially in solid tumors (Navani et al. 2020; Sharma and Allison 2020). The combination therapy with CAR T cells and immune checkpoint blockade have yielded encouraging results, with several clinical trials ongoing (Grosser et al. 2019).

## 1.3  CD95/CD95L death signaling

CD95 (also known as Fas) is an apoptosis-inducing TNF-family receptor and is expressed on most of immune cells, either constitutively or after activation. Its cognate ligand, CD95L (FasL) is predominantly expressed in activated T cells and NK cells. CD95L can be cleaved by metalloproteases upon activation and so exists in two different forms: membrane bound (mCD95L, 40 kD) and soluble (sCD95L, 26 kD). Interaction of mCD95L to CD95 promotes the recruitment of Fas-associated death domain protein (FADD) and caspase-8 and leads to the activation of caspase-3, which finally induces apoptosis of CD95 expressing T cells (Green and Ferguson 2001; Le Gallo et al. 2017).

It was recently observed that death receptor CD95 was highly expressed by the third-generation anti-CD19 CAR T cells used in our lab. This CD95 expression might trigger activation-induced cell death (AICD) through interaction with CD95L. The CD95-CD95L pathway plays an important role in the regulation of immune homeostasis (Lynch et al. 1995) as well as the progression of cancer (Maher et al. 2002). CD95L was reported to be overexpressed by solid tumors, including melanoma (Redondo et al. 2002), gastric carcinoma (Lim 2002), colon carcinoma (Nozoe et al. 2003), and breast carcinoma (Muschen et al. 2000), as a mechanism to evade immune surveillance and promote tumor progression and metastasis. However, CD95L is rarely expressed in hematologic malignancies, especially in B cell malignancies (Yamamoto et al. 2019). Recent evidence indicated that other cells within tumor microenvironment (TME) can also express CD95L and trigger apoptosis of tumor infiltrating lymphocytes expressing CD95, thus contributing to tumor immune evasion (Zhu et al. 2019; Zhu et al. 2017).

## 1.4 CD95L inhibitor APG101

CD95L inhibitor APG101 (Asunercept ®), a human fusion protein consisting of the extracellular domain of human CD95 and Fc domain of human IgG antibody, has been designed to selectively bind to CD95L and therefore disrupt CD95/CD95L signaling (Krendyukov and Gieffers 2019). CD95L is overexpressed on glioblastoma cells, which contributes to the invasion of glioblastoma cells, and APG101 can reduce this invasiveness via neutralizing CD95L (Blaes et al. 2018). Moreover, treatment with APG101 has shown promising clinical outcome in patients with relapsed glioblastoma (NCT01071837) (Wick et al. 2014). CD95 is found to be expressed on CD34$^+$ hematopoietic progenitors and erythrocytes in patients with myelodysplastic syndrome (MDS), which might negatively regulate erythrocyte production in the bone marrow. APG101 administration results in a reduction of transfusion need and frequency in transfusion-dependent MDS patients (NCT01736436) (Boch et al. 2018). Therefore, CAR T cells highly express death receptor CD95, which might be sensitive to CD95L-mediated apoptosis and thus impair their persistence and antitumor efficacy.

Based on the knowledge that the interaction of CD95 and CD95L leads to AICD, we hypothesize that CD95 and CD95L interaction within CAR T cells or within the TME might limit CAR T cell persistence and thus impair their antitumor activity and inhibition of CD95-CD95L pathway through the CD95L inhibitor APG101 could prevent CAR T cells from CD95L-mediated apoptosis and thus improve their persistence (Figure 1.2).
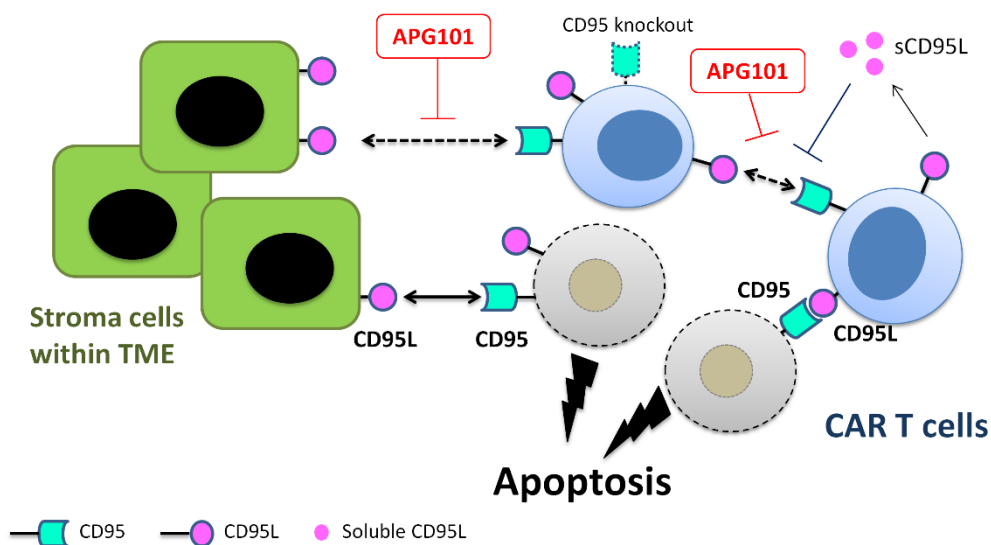
**Figure 1.2 Role of CD95-CD95L signaling in CAR T cells and tumor microenvironment.**

CD95 and CD95L are both expressed on the cell surface of activated CAR T cells following interaction with tumor cells. The binding of CD95 and CD95L within CAR T cells can trigger the activation-induced cell death (AICD) in CAR T cells expressing CD95 receptor. Stroma cells within tumor microenvironment (TME) expressing CD95L can also induce apoptosis of CAR T cells via CD95 binding. Soluble CD95L (sCD95L) is cleaved from surface of activated CAR T cells by matrix metalloproteinases, which can also bind to CD95 receptor and thus competitively inhibit the CD95L-mediated apoptosis in CAR T cells. Disruption of CD95-CD95L signaling by CD95L inhibitor APG101 or via genome editing might protect CAR T cells from CD95-mediated apoptosis thus improve their persistence.

## 1.5 Aims of this work

Despite the encouraging outcome of anti-CD19 chimeric antigen receptor T (CAR T) cell therapy in patients with B cell malignancies, CAR T cell persistence remains a major clinical challenge. CAR T cells highly express death receptor CD95, which might be sensitive to CD95L-mediated apoptosis and thus impair their persistence. The aim of this study was to investigate whether disruption of the CD95-CD95L pathway within CAR T cells through pharmacologic and genetic approaches would prevent CAR T cells from CD95L-mediated apoptosis and improve their persistence.

The present work aims to address the following issues:

1) Whether CD95L inhibitor APG101 would influence the production of CD19.CAR T cells.

2) Whether $CD95^+$ CAR T cells experience activation-induced cell death (AICD) upon tumor stimulation and APG101 could protect CAR T cells from AICD.

3) Whether APG101 could improve the persistence of CAR T cells after repeated stimulation with tumor cells.

4) Whether APG101 could enhance the anti-tumor efficacy of CAR T cells.

5) Whether CD95 knockout in CD19.CAR T cells via CRISPR-Cas9 would result in better persistence and superior cytotoxicity.

# 2 MATERIALS AND METHODS

## 2.1 Materials

### 2.1.1 Consumables

| | |
|---|---|
| Amersham Protran 0.2 NC Nitrocellulose Western blotting membranes | Cat. No.: 10600001<br>GE Healthcare, Little Chalfont, UK |
| Axygen® Filter- Pipette Tips, 10µl NC | Cat. No.: 320-05-151<br>Axygen (Corning), Union City, USA |
| Axygen® Filter- Pipette Tips, 20µl NC | Cat. No.: 320-03-151<br>Axygen (Corning), Union City, USA |
| Axygen® Filter- Pipette Tips, 100µl NC | Cat. No.: 320-08-151<br>Axygen (Corning), Union City, USA |
| Axygen® Filter- Pipette Tips, 200µl NC | Cat. No.: 320-04-151<br>Axygen (Corning), Union City, USA |
| Axygen® Filter- Pipette Tips, 1000µl NC | Cat. No.: 320-01-151<br>Axygen (Corning), Union City, USA |
| BD Plastikpak Disposable Syringe 1 ml | Ref.: 300013; BD Biosciences,<br>Franklin Lakes, NJ, USA |
| BD Plastikpak Disposable Syringe 5 ml | Ref.: 300911; BD Biosciences,<br>Franklin Lakes, NJ, USA |
| BD Plastikpak Disposable Syringe 10 ml | Ref.: 300912; BD Biosciences,<br>Franklin Lakes, NJ, USA |
| BD Plastikpak Disposable Syringe 20 ml | Ref.: 300629; BD Biosciences,<br>Franklin Lakes, NJ, USA |
| C-Chip Counting Chamber | Cat. NO.: 2N13202<br>NanoEnTek, Seoul, South Korea |
| Cellstar® 96 Well Cell Culture Plate, U-bottom | Cat. NO.: 650180, Greiner Bio-One,<br>Frickenhausen, Germany |
| Cryo.s$^{TM}$ 2ml Freezing Tubes, PP | Cat. NO.: 122263, Greiner Bio-One,<br>Frickenhausen, Germany |
| Falcon® 24-well Polystyrene Clear Flat Bottom Not Treated Cell Culture Plate | Cat. NO.: 351147,<br>Falcon®, NY, USA |
| Falcon® Round Bottom Polystyrene Tubes 5ml | Cat. NO.: 352054,<br>Corning, Corning, NY, USA |
| Griptips, 125µl, 5 Racks of 96 Tips, S,F | Cat. NO.: 4425, Integra Biosciences,<br>Zizers, Switzerland |
| Griptips, 300µl, 5 Racks of 96 Tips, S,F | Cat. NO.: 4435, Integra Biosciences,<br>Zizers, Switzerland |
| Invitrogen$^{TM}$ NuPAGE 4-12% Bis-Tris Gel 1.0mm*12 well | Cat. NO.: NP0322BOX<br>Invitrogen, Waltham, MA, USA |
| Liquid Scintillation Vials, 6ml | Cat. NO.: 3020001, Zinsser Analytic,<br>Frankfurt am Main, Germany |

| | |
|---|---|
| LS Columns | Cat. NO.: 130-042-401; Miltenyi Biotec, Bergisch-Gladbach, Germany |
| Millex-HV 0.45µm Filter, Durapore PVDF Membrane | Cat. NO.: SLHV033RS Merck Millipore, Darmstadt, Germany |
| Multiwell 6 Well Plate | Cat. NO.: 83.3920, Sarstedt, Nümbrecht, Germany |
| Multiwell 12 Well Plate | Cat. NO.: 83.3921 Sarstedt, Nümbrecht, Germany |
| Multiwell 24 Well Plate | Cat. NO.: 83.3922 Sarstedt, Nümbrecht, Germany |
| Parafilm M® Laboratory Film | Cat. NO.: PM-996, Bemis, Neenah, WI, USA |
| PP Greiner Centrifuge Tubes, 15ml, Conical (V) Bottom | Cat. NO.: 188271, Greiner Bio-One, Frickenhausen, Germany |
| PP Greiner Centrifuge Tubes, 50ml, Conical (V) Bottom | Cat. NO.: 227261, Greiner Bio-One, Frickenhausen, Germany |
| PP Screw Cap Tube, 10ml, Concial Base, PP With Assembled Yellow Cap | Cat. NO.: 629924284, Greiner Bio-One, Frickenhausen, Germany |
| Pre-Separation Filters | Cat. NO.: 130-041-407; Miltenyi Biotec, Bergisch-Gladbach, Germany |
| Reagent Low Banding, 1.5ml | Ref.: 72.706.600 Sarstedt, Nümbrecht, Germany |
| Rotilabo® Aluminum Foil | Cat. NO.: 2596.1 Carl Roth, Karlsruhe, Germany |
| SafeSeal Reagent, 0.5ml, PP | Ref.: 72.704, Sarstedt, Nümbrecht, Germany |
| SafeSeal Reagent, 1.5ml, PP | Ref.: 72.706 Sarstedt, Nümbrecht, Germany |
| SafeSeal Reagent, 2.0ml, PP | Ref.: 72.695.500 Sarstedt, Nümbrecht, Germany |
| Serological Pipettes, 5ml | Cat. NO.: 4487 Corning Incorporated, NY, USA |
| Serological Pipettes, 10ml | Cat. NO.: 4488 Corning Incorporated, NY, USA |
| Serological Pipettes, 25ml | Cat. NO.: 4489 Corning Incorporated, NY, USA |
| Serological Pipettes, 50ml | Cat. NO.: 4490 Corning Incorporated, NY, USA |
| Sterile Pasteur Pipettes | Cat. NO.: S0957A LP Italiana Spa, Mailand, Italy |
| 100 mm Tissue Culture-Treated Dishes | Cat. NO.: 83.3902 Sarstedt, Nümbrecht, Germany |
| T25 TC Flasks with Vented Cap | Cat. NO.: 83.3910.002 Sarstedt, Nümbrecht, Germany |

| T75 TC Flasks with Vented Cap | Cat. NO.: 83.3911.002<br>Sarstedt, Nümbrecht, Germany |
|---|---|
| T175 TC Flasks with Vented Cap | Cat. NO.: 83.3912.002<br>Sarstedt, Nümbrecht, Germany |
| TouchNTufff® Nitrile Gloves | Cat. NO.: 112-0997<br>Ansell, Brüssel, Belgien |

## 2.1.2 Media, solutions and buffers

| Annexin V Binding Buffer | Cat. NO.: 422201; Biolegend, San Diego, CA, USA |
|---|---|
| AutoMACS Rinsing Solution | Cat. No.: 130-091-222, Miltenyi Biotec, Bergisch-Gladbach, Germany |
| BD Horizon BrilliantTM Stain Buffer | Cat. NO.: 563794; BD Biosciences, New Jersey, U.S. |
| Clicks (EHAA) Medium | Cat. NO.: 9195; Irvine Scientific, Santa Ana, CA, USA |
| Dulbecco's Phosphate Buffered Saline (PBS) | Cat. NO.: D8537-500ml; Sigma-Aldrich, St. Louis, MO, USA |
| Fetal Bovine Serum, Heat Inactivated (FBS) | Thermo Fisher Scientific, Waltham, MA, USA |
| Lymphoprep | Cat. NO.: 07851; STEMCELL Technologies, Germany |
| Fixation Buffer | Cat. NO.: 420801; Biolegend, San Diego, CA, USA |
| Foxp3 Staining Buffer Set | Cat. NO.: 130-093-142; Miltenyi Biotec, Bergisch-Gladbach, Germany |
| Iscove's Modified Dulbecco's Medium (IMDM) + GlutaMAX | Cat: 31980-022; Thermo Fisher Scientific, Waltham, MA, USA |
| L-Glutamine (200 mM) | Cat. No.: 25030081, Gibco, Grand Island, NY, USA |
| MACS Bovines Serumalbumin (BSA) stock solution | Cat No.: 130-091-376, Miltenyi Biotec, Bergisch-Gladbach, Germany |
| Nuclease-Free Water | Cat No.: 129114, Qiagen, Hilden, Germany |
| NuPAGE LDS Sample Buffer (4X) | Cat. NO.: NP008; Thermo Fisher Scientific, Waltham, MA, USA |
| NuPAGE™ MES SDS Running Buffer (20X) | Cat. NO.: NP0002; Thermo Fisher Scientific, Waltham, MA, USA |
| Protease Inhibitor Cocktail Tablet | Sigma Aldrich, Steinheim, Germany |
| RIPA Lysis and Extraction Buffer | Cat. NO.:89900; Thermo Fisher Scientific, Waltham, MA, USA |
| ReBlot Plus Strong Antibody Stripping Solution, 10X | Cat. No.: 2504, Millipore, Burlington, Massachusetts, USA |

| Roswell Park Memorial Institute (RPMI) 1640 Medium | Cat. NO.: 21875-034, Thermo Fisher Scientific, Waltham, MA, USA |
|---|---|
| Tris Buffered Saline with Tween® 20 (TBST-10X) | Cat. NO.: #9139, Cell Signaling Technology, Danvers, MA, USA |
| Trypsin-Ethylenediaminetetraace tic acid (EDTA) 0.05%, phenol red | Cat. No.: 25300054, Gibco, Grand Island, NY, USA |
| 10X Transfer Buffer | 288g Glycine + 60.4g Tris-base + 2L ddH2O |

## 2.1.3 Reagents and chemicals

| APG101 | Apogenix, Heidelberg, Germany |
|---|---|
| APG122 | Apogenix, Heidelberg, Germany |
| BD™ Cytometric Bead Array (CBA) Human Th1/Th2/Th17 Cytokine Kit | Cat. NO.: 560484; BD Biosciences, New Jersey, U.S. |
| Bovine Serum Albumin (BSA) | Serva Electrophoresis, Heidelberg, Germany |
| Brefeldin A Solution (1,000X) | Cat. NO.: 420601; Biolegend, San Diego, CA, USA |
| CaspGLOW Fluorescein Active aspase-8 staining kit | Cat. NO.: 88-7005; Thermo Fisher Scientific, Waltham, MA, USA |
| CellTiter-Glo® 2.0 Cell Viability Assay | Cat. NO.: G9242; Promega, Fitchburg, WI, USA |
| CD3 MicroBead, human | Cat. NO.: 130-050-101, Miltenyi Biotec, Bergisch Gladbach, Germany |
| Chromium 51, 74MBq (2,000Ci/2000µl) | Cat. NO.: 17216210, Hartmann Analytic, Braunschweig, Germany |
| Dead Cell Removal Kit | Cat. NO.: 130-090-101, Miltenyi Biotec, Bergisch Gladbach, Germany |
| Dimethyl sulfoxide (DMSO) | Cat. No.: 4540, Sigma-Aldrich, St. Louis, Missouri, USA |
| GeneArt™ Precision gRNA Synthesis Kit | Cat. NO.: A29377; Thermo Fisher Scientific, Waltham, MA, USA |
| Gene Juice Transfection Reagent | Cat. No.: 70967, Merck Millipore, Burlington, Massachusetts, USA |
| Geneticin Selective Antibiotic (G418 Sulfate) | Cat. No.: 10131027, Gibco, Grand Island, NY, USA |
| Glycine | Cat. No.: G8898-1KG. Sigma-Aldrich, St. Louis, Missouri, USA |
| Interleukin 17 (IL-7) | Cat. No.: 207-IL-005, R&D systems, Minneapolis, USA |
| Interleukin 15 (IL-15) | Cat. No.: 247-ILB-005, R&D systems, Minneapolis, USA |

| | |
|---|---|
| Isopropanol | Cat. No.: I9516, Sigma-Aldrich, St. Louis, Missouri, USA |
| LEAF® anti-Human CD3 OKT3, 1mg/ml | Cat. NO.: 317315; Biozol, Eching, Germany |
| LEAF® anti-Human CD28 clone 28.2, 1mg/ml | Cat. NO.: 302923; Biozol, Eching, Germany |
| LIVE/DEADTM Fixable Near-Infrared (Near-IR) | Cat. NO.: L34976; Thermo Fisher Scientific, Waltham, MA, USA |
| Methanol | Cat. No.: 4627.1, Carl Roth, Karlsruhe, Germany |
| Monensin Solution (1,000X) | Cat. NO.: 420701; Biolegend, San Diego, CA, USA |
| Na-Pyruvate, 100mM | Cat. NO.: 11360-070; Thermo Fisher Scientific, Waltham, MA, USA |
| Neon™ Transfection System 10-µL Kit | Cat. NO.: MPK1025; Thermo Fisher Scientific, Waltham, MA, USA |
| QIAprep® Spin Miniprep Kit | Cat. NO.: 27104; QIAGEN, Hilden, Germany |
| Quantikine® ELISA kit (Human Fas Ligand/TNFSF6 Immunoassay) | Cat. NO.: DFL00B; R&D systems, Minneapolis, USA |
| PageRulerTM Prestained Protein Ladder | Cat. No.: 26616, Thermo Fisher Scientific, Waltham, MA, USA |
| PegPam3 Packaging Plasmid | Provided by Professor Malcolm Brenner, Center for Cell and Gene Therapy, Houston, Texas |
| Penicillin Streptomycin (Pen/Strep) | Cat. NO.: A 2212; Biochrom GmbH, Berlin, Germany |
| RetroNectin®, 1mg/ml | Cat. NO.: T100B; Takara Bio, Shiga, Janpan |
| RDF Plasmid Envelope Plasmid | Provided by Professor Malcolm Brenner, Center for Cell and Gene Therapy, Houston, Texas |
| SUPERFASLIGAND® Protein (soluble) (human), (recombinant) | Cat. NO.:ALX-522-020-C005; Enzo Life Sciences, New York, USA |
| Triton X-100 | Cat. NO.: 108603; Merck Millipore, Darmstadt, Germany |
| TrueCut™ Cas9 Protein v2 | Cat. NO.: A36497; Thermo Fisher Scientific, Waltham, MA, USA |
| Trypanblue Solution | Cat. NO.: L6323; Biochrom, Berlin, Germany |
| Ultima Gold® Liquid Scintillation Cocktail | Cat. No.:6013329; PerkinElmer, Waltham, MA, USA |
| XenoLight D-Luciferin - K+ Salt Bioluminescent Substrate | Cat. No.: 122799; PerkinElmer, Waltham, MA, USA |

## 2.1.4  Antibodies

| | |
|---|---|
| Annexin V APC | Cat. NO.: 640920; Biolegend, San Diego, CA, USA |
| Anti-mouse IgG, HRP-linked Antibody | Cat. NO.: 7076S; Cell Signaling Technology, Massachusetts, USA |
| Anti-rabbit IgG, HRP-linked Antibody | Cat. No.: 7074s, Cell signaling Technology, Massachusetts, USA |
| Anti-human CD3 Alexa Flour 700, Mouse IgG1($\kappa$) Clone: UCHT1 | Cat. NO.: 300424; Biolegend, San Diego, CA, USA |
| Anti-human CD3 APC, Mouse IgG1($\kappa$) Clone: UCHT1 | Cat. NO.: 300412; Biolegend, San Diego, CA, USA |
| Anti-human CD3 APC/Cy7, Mouse IgG1($\kappa$) Clone: SK7 | Cat. NO.: 344818; Biolegend, San Diego, CA, USA |
| Anti-human CD3 FITC, Mouse IgG1($\kappa$) Clone: SK7 | Cat. NO.: 344804; Biolegend, San Diego, CA, USA |
| Anti-human CD3 Pacific Blue, Mouse IgG2a($\kappa$) Clone: HIT3a | Cat. NO.: 300330; Biolegend, San Diego, CA, USA |
| Anti-human CD3 PerCP, Mouse IgG1($\kappa$) Clone: SK7 | Cat. NO.: 344814; Biolegend, San Diego, CA, USA |
| Anti-human CD3 PE, Mouse IgG2a($\kappa$) Clone: HIT3a | Cat. NO.: 300308; Biolegend, San Diego, CA, USA |
| Anti-human CD3 PE-Cyanine7, Mouse IgG1($\kappa$) Clone: UCHT1 | Cat. NO.: 25-0038-42; eBioscience, San Diego, CA, USA |
| Anti-human CD3 PE eFluor 610, Mouse IgG1($\kappa$) Clone: UCHT1 | Cat. NO.: 61-0038-42; eBioscience, San Diego, CA, USA |
| Anti-human CD4 Alexa Fluor 700, Mouse IgG1($\kappa$) Clone: RPA-T4 | Cat. NO.: 560049-42; eBioscience, San Diego, CA, USA |
| Anti-human CD8 PerCP, Mouse IgG1($\kappa$) Clone: SK1 | Cat. NO.: 344708; Biolegend, San Diego, CA, USA |
| Anti-human CD19 PerCP, Mouse IgG1 $\kappa$ Clone: HIB19 | Cat. NO.: 302228; Biolegend, San Diego, CA, USA |
| Anti-human CD20 Brilliant Violet 510™, Mouse IgG2b $\kappa$ Clone: 2H7 | Cat. NO.: 302340; Biolegend, San Diego, CA, USA |
| Anti-human CD25 PerCP, Mouse IgG1($\kappa$) Clone: M-A251 | Cat. NO.: 356132; Biolegend, San Diego, CA, USA |
| Anti-human CD45RA FITC, Mouse IgG2b $\kappa$ Clone: HI100 | Cat. NO.: 304106; Biolegend, San Diego, CA, USA |
| Anti-human CD45 RA APC, Mouse IgG2b($\kappa$) Clone: HI100 | Cat. NO.: 304112; Biolegend, San Diego, CA, USA |
| Anti-human CD69 APC, Mouse IgG1($\kappa$) Clone: FN50 | Cat. NO.: 310910; Biolegend, San Diego, CA, USA |
| Anti-human CD95(Fas) BV510, Mouse IgG1($\kappa$) Clone: DX2 | Cat. NO.: 305640; Biolegend, San Diego, CA, USA |

| | |
|---|---|
| Anti-human CD107a FITC Antibody, Mouse IgG1(κ), Clone: H4A3 | Cat. No.: 555800, BD Biosciences, Franklin Lakes, New Jersey, USA |
| Anti-human CD178 (FasL) BV421, Mouse IgG1(κ) Clone: NOK-1 | Cat. NO.: 306412; Biolegend, San Diego, CA, USA |
| Anti-human CD197 (CCR7) PE-Cy7, Rat IgG2a (κ) Clone: 3D12 | Cat. NO.: 25-1979-42; eBioscience, San Diego, CA, USA |
| Anti-human CD223 (LAG-3) APC, Mouse IgG1(κ) Clone: 7H2C65 | Cat. NO.: 369212; Biolegend, San Diego, CA, USA |
| Anti-human CD279 (PD-1) Alexa Fluor 488, Mouse IgG1(κ) Clone: EH12.2H7 | Cat. NO.: 329935; Biolegend, San Diego, CA, USA |
| Anti-human CD366 (Tim-3) BV421, Mouse IgG1(κ) Clone: F38-2E2 | Cat. NO.: 345007; Biolegend, San Diego, CA, USA |
| Anti-human F(ab)2 IgG (H+L) PE, Goat F(ab)2 Polyclonal | Cat. NO.: 109-116-088; Dianova, Hamburg, Germany |
| Anti-human IFN-gamma Alexa Fluor 488, Mouse IgG1(κ) Clone: 4S.B3 | Cat. NO.: 502515; Biolegend, San Diego, CA, USA |
| Anti-human IFN-gamma APC, Mouse IgG1 κ Clone: B27 | Cat. NO.: 554702; BD Biosciences, Franklin Lakes, NJ, USA |
| Anti-human TNF-α BV421Antibody, Mouse IgG1(κ) Clone: MAb11 | Cat. No.: 562783, BD Biosciences, Franklin Lakes, New Jersey, USA |
| β-actin Antibody (C4) HRP, Mouse IgG1(κ) Clone: C4 | Cat. NO.: sc-47778; Santa Cruz Biotechnology, California, USA |
| Caspase-8 (1C12) Mouse mAb | Cat. No.: 9746, Cell signaling Technology, Massachusetts, USA |
| Fas (4C3) Mouse mAb #8023 | Cat. No.: 8023, Cell signaling Technology, Massachusetts, USA |
| FasL (D1N5E) Rabbit mAb #68405 | Cat. No.: 68405, Cell signaling Technology, Massachusetts, USA |

## 2.1.5   Equipments

| | |
|---|---|
| Amersham Imager 600 | GE Healthcare, Little Chalfont, UK |
| Applied Biosystems 2720 Thermal Cycler | Thermo Fisher Scientific, Waltham, MA, USA |
| Aqualine AL 12 Water bath | Lauda, Lauda-Königshofen, Germany |
| Autoklav | Tuttnauer, Breda, Nederland |
| Centrifuge Hermle Z300 | Hermle Labortechnik, Wehingen, Germany |
| DIAVERT Microscope | Leica, Wetzlar, Germany |
| DM3000 Microscope | Leica, Wetzlar, Germany |
| EnSight Multimode plate reader | PerkinElmer, Waltham, MA, USA |
| FACS BD LSRII | Becton Dickinson, Franklin Lakes, NJ, USA |

| | |
|---|---|
| Finnpipette 300µl labsystems L13410 | Thermo Fisher Scientific, Waltham, MA, USA |
| GIOSON Pipette 20 µl | Gilson, Middleton, WI, USA |
| GIOSON Pipette 100 µl | Gilson, Middleton, WI, USA |
| GIOSON Pipette 200 µl | Gilson, Middleton, WI, USA |
| GIOSON Pipette 1000 µl | Gilson, Middleton, WI, USA |
| Herasafe* KS, Class II Biological Safety Cabinet | Thermo Fisher Scientific, Waltham, MA, USA |
| Heraeus* Megafuge* 16 Centrifuge | Thermo Fisher Scientific, Waltham, MA, USA |
| Heraeus Pico17 Centrifuge | Thermo Fisher Scientific, Waltham, MA, USA |
| LABOVERT Microscope | Leica, Wetzlar, Germany |
| M-20 microplate swing bucket rotor grotor | Thermo Fisher Scientific, Waltham, MA, USA |
| Memmert* In CO2 Incubators | Thermo Fisher Scientific, Waltham, MA, USA |
| Mini MACS, MultiStand | Miltenyi Biotec, Bergisch-Gladbach, Germany |
| Mr. Frosty Freezing Container | Thermo Fisher Scientific, Waltham, MA, USA |
| NanoDrop one | Thermo Fisher Scientific, Waltham, MA, USA |
| Neno Transfection System | Thermo Fisher Scientific, Waltham, MA, USA |
| Pipetus® Pipette Boy | Hirschmann Laborgeräte, Eberstadt Germany |
| Precision Balance | Sartorius, Göttingen, Germany |
| Research® plus (fixed) Pipette Eppendorf 0.1-2.5 µl | Eppendorf, Hamburg, Germany |
| Research® Pipette Eppendorf 0.5 µl-10 µl | Eppendorf, Hamburg, Germany |
| Research® Pipette Eppendorf 10 µl-100 µl | Eppendorf, Hamburg, Germany |
| Research® Pipette Eppendorf 100 µl-1000 µl | Eppendorf, Hamburg, Germany |
| Roller Mixer Stuart SRT6 | Cole- Parmer, Vernon Hills, IL, USA |
| TECAN Spark microtiterplate reader | TECAN, Männedorf, Zürich, Switzerland |
| Thermomixer comfort | Eppendorf, Hamburg, Germany |
| Vortexer | Heidolph Instruments, Schwabach, Germany |

### 2.1.6 Cell lines

CD19-positive (CD19$^+$) Nalm6 (acute lymphoblastic leukemia, ALL) and Daudi (Burkitt lymphoma), CD19-negative (CD19$^-$) K562 cells (chronic myeloid leukemia in blast crisis) and 293T (embryonal kidney) were obtained from DSMZ (German Collection of Microorganisms and Cell Cultures). Nalm6 cells transduced with lentivirus vector expressing green fluorescence protein (GFP) were selected by flow cytometry. Nalm6, Nalm6-GFP, Daudi and K562 cells were cultured in RPMI 1640 (Thermo Fisher Scientific) supplemented with 10% heat-inactivated fetal bovine serum (FBS) at 37°C and 5% $CO_2$. 293T cells were cultured in Iscove's modified Dulbecco's medium (IMDM) supplemented with 10% FBS and 0,1% sodium pyruvat. All cell lines were authenticated at DSMZ and were free from mycoplasma tested by PCR (VenorGeM, Minerva Biolabs GmbH, Berlin, Germany).

## 2.2    Methods

### 2.2.1  Isolation of PBMCs

Fresh patient blood and buffy coats were diluted 2:1 and 1:1 with PBS containing 2% FBS, respectively. 15 ml of Lymphoprep Density gradient medium was loaded into 50 ml vertical centrifuge tube then carefully layering 20 ml of diluted sample. The 50 ml tubes were centrifuged at 400 g for 30 min at room temperature (RT) without brake. Draw off the upper layer containing plasma and platelets using a sterile pipette, leaving the mononuclear cell layer undisturbed at the interface. The layer of mononuclear cells was transferred to a 50 ml sterile centrifuge tube using a sterile pipette. The transferred peripheral blood mononuclear cells (PBMC) were washed twice by using 20 ml of PBS + 2% FBS and centrifuge at 500 g for 10 min. Cell viability and cell number were determined by trypan blue staining. The PBMCs were cryopreserved as described below.

### 2.2.2  Cryopreservation of PBMCs

PBMCs were resuspended at $1 \times 10^7$ cells/ml for patient sample and $2\text{-}5 \times 10^7$ cells/ml for healthy donor (HD) samples in cold freezing medium containing 90% FBS and 10% DMSO and then aliquoted in 2 ml cryovials. Samples were kept in Cryo-Safe Cooler and maintained at -80°C overnight, followed by long-term storage in liquid nitrogen.

### 2.2.3  Thawing of PBMCs

Frozen PBMCs were thawed at 37°C in water bath until a small ice was left. Thawed PBMCs were immediately transferred into warm complete medium by dropwise. After centrifugation at 500 g for 5 minutes, cell pellets were resuspended in media appropriate for the application.

### 2.2.4  Generation of CD19.CAR T cells

#### 2.2.4.1    Preparation of plasmid DNA

CD19 specific retroviral vector plasmid (RV-SFG.CD19.CAR.CD28.CD137zeta),

PegPam3 plasmid containing gag-pol and RDF plasmid containing the envelope were kindly provided by Professor Malcolm Brenner, Baylor College of Medicine, Houston, USA. Plasmid DNA (100 ng) was mixed into 50 ul of competent cells (DH5α) in a microcentrifuge tube and incubated on ice for 20-30 mins. 25 ul of the competent cell/DNA mixture was plated onto a 10 cm LB agar plate containing 25 ug/ml Ampicillin antibiotic and incubated at 37°C overnight. The individual colonies of the transformed DH5α were picked and inoculated into 3 ml of LB media supplemented with Ampicillin in 13 ml sterile polypropylene snap-cap tubes. The bacterial cultures were incubated overnight (18-20 h) at 37 °C in a shaker for uniform growth. The bacteria containing plasmid DNA were harvested by centrifugation at 5000 rpm for 10 min at RT. Plasmid DNA from bacteria was isolated and purified by Miniprep Kit according to the instructions. DNA concentration was measured using Nanodrop.

### 2.2.4.2    Production of retrovirus

Cryopreserved 293T cells were thawed and resuspended in Iscove's modified dulbecco's medium (IMDM) containing L-glutamine, supplied with 10% FBS, 0.1mM Na-Pyruvate and 500μg/ml antibiotic geneticin (termed as complete IMDM). $2.0 \times 10^6$ of 293T cells were seeded in a 10 cm tissue culture-treated dish and incubated at 37°C, 5% CO2. The cultured medium was replaced by fresh complete IMDM after overnight culture. One day later, 293T cells were digested by 0.05% Trypsin and 0.02 % EDTA and then resuspended in 10 ml of complete IMDM, followed by seeding in a new dish at 1:10 dilution. 3 days later, 293T cells were digested by Trypsin-EDTA and seeded in new dishes at a density of $2.0 \times 10^6$ per dish. One day later, CD19 specific retroviral vector plasmids (3.75μg), packaging plasmid PegPam3 (3.75μg) and envelope plasmid RDF (2.5μg) were mixed in a 1.5 ml eppendorf tube (plasmid DNA mixture). 470μl IMDM and 30μl GeneJuice transfection reagent were mixed and incubated at RT for 5 minutes before adding into the plasmid DNA mixture (mix gently by tapping). After 15 mins of incubation, 510μl of the mixture was added dropwise into the 293T cells dish. Retrovirus rich culture supernatant was harvested at 48 hr and 72 hr post-transfection and aliquoted at -80°C

until being used.

### 2.2.4.3    Activation of T cells

The PBMCs from healthy donors or patient samples were thawed and resuspended in the complete medium containing 45% (vol/vol) Clicks Medium (EHAA), 45% (vol/vol) RPMI 1640 Medium, 10% (vol/vol) FBS, and 2 mmol/l L-glutamine. $1 \times 10^6$ of PBMCs were seeded in the anti-CD3 (1μg/ml) and anti-CD28 (1μg/ml) antibodies pre-coated well of non-treated 24-well plates, which considered as day 0. After two days cultivation, half of cultured medium was replaced by fresh complete medium containing IL-7 (10 ng/ml) and IL-15 (5 ng/ml), which led to an expansion of T cells in the culture plate.

### 2.2.4.4    Retroviral transduction of T cells

On day 3 of cultivation, activated T cells (ATCs) were harvested and resuspended in complete medium at the density of 1.0 x 106/ml. 0.5 ml of ATCs were mixed with 1.5ml of thawed retroviral supernatant and seeded in a non-treated 24-well plates which pre-coated with 7μg/ml retronectin and then incubated for 3 days in the presence of IL-7 and IL-15.

### 2.2.4.5    Expansion of CAR T cells

Post transduced T cells were expanded in 6-well plates or T75 flasks with complete medium in the presence of IL-7 (10 ng/ml) and IL-15 (5 ng/ml) and changed the medium every 3-4 days. The transduction efficacy was determined on indicated times by flow cytometry.

## 2.2.5  Flow cytometry

The fluorochrome-conjugated antibodies: CD3 (clone UCHT1 or HIT3a), CD4 (clone RPA-T4), CD8 (clone SK1), CD25 (clone BC96), CD69 (clone FN50), CD95 (clone DX2), CD95L (clone NOK-1), CD45RA (clone HI100), CCR7 (clone 3D12), PD1 (clone EH12.2H7), TIM3 (clone F38-2E2) and LAG3 (clone 7H2C65) from BioLegend or eBioscience were used for cell surface staining. Dead cells were

excluded with the LIVE/DEAD™ fixable near-infrared (IR) dead cell stain kit (Thermo Fisher Scientific) or 7AAD (BD Biosciences). The anti-human goat F(ab)$_2$ IgG (H+L) PE antibody (Dianova, Hamburg, Germany) was used to identify CD19-specific CAR expression. To ensure the accuracy of measurement, fluorescence compensation was applied before acquisition. Appropriate fluorescence minus one (FMO) control or non-transduced control were included. All flow cytometric data were acquired using a BD LSRII flow cytometer (BD Biosciences) and analyzed using FlowJo v.10 software.

### 2.2.5.1 Cell surface staining

Cells were harvested into 12 x 75 mm test tubes and washed with cell staining buffer. Cells were resuspended in 100 ul of Staining Buffer (5-10 x $10^5$ cells/tube) and stained with indicated antibodies at predetermined optimum concentrations. After washing twice with 2ml of Cell Staining Buffer by centrifugation at 400g for 5 minutes, cell pellets were resuspended in 0.5ml of Cell Staining Buffer. 5µl of 7-AAD Viability Staining Solution was added into the test tubes before flow cytometric analysis.

### 2.2.5.2 Annexin V staining

After surface marker staining, cells were resuspended in 100 µl Annexin V staining solution, which consists of 98 µl Annexin V binding buffer and 2 µl Annexin V, followed by a 15 minutes incubation at RT in dark. After washing with 400µl Annexin V binding buffer, cells were resuspended in 400 µl Annexin V binding buffer for acquisition.

### 2.2.5.3 CaspGLOW Fluorescein Active Caspase-8 staining

The CaspGLOW Fluorescein Active Caspase-8 staining kit (Thermo Fisher Scientific) was used to detect the active caspase-8 in cells, which utilizes the caspase 8 inhibitor, IETD-FMK, conjugated to FITC (FITC-IETD-FMK) as a marker. Cells were harvested, washed and resuspended in 300 µl of complete medium. 1 µL of FITC-IETD-FMK was added into each tube and incubate for 30 minutes in a 37°C

incubator with 5% CO2. After washing twice with 500 ul wash buffer, the cells were analyzed using flow cytometry.

### 2.2.5.4    Intracellular cytokine staining

For cytokine release analysis, CD19.CAR T cells were stimulated with CD19 positive Daudi cells for 4-6 hours in the presence of two secretion inhibitors, monensin and brefeldin A, and CD107a antibody. For the unstimulated control, CAR T cells were treated with the secretion inhibitors and CD107a, but not tumor cells. Degranulating cells are identified by their surface expression of CD107a. After the incubation, cells were harvested in test tubes and stained with surface markers for 30 minutes. After cell fixation and permeabilization with the FoxP3 staining buffer set, cells were stained with interferon gamma (IFN-γ) and tumor necrosis factor alpha (TNF-α) for 30 minutes on ice in the dark. After washing once with 1 ml of FACS buffer, cells were resuspended in 400 µl FACS buffer for acquisition.

### 2.2.6    Chromium release assay

The potency of CD19.CAR-T cells was determined by chromium-51 (51Cr) release assay. Briefly, effector CD19.CAR T cells were co-cultured with $5 \times 10^3$ 51Cr-labeled tumor cells at the indicated effector to target (E:T) ratio in 96-well U-bottom plate at 37°C with 5% CO2 for 4 hours. The spontaneous release and maximal release were determined by incubating 51Cr-labeled tumor cells with medium and 1% Triton-100, respectively. K562 cells were used as negative control. The percentage of specific lysis was calculated as follows: [experimental release - spontaneous release] / [maximal release - spontaneous release] × 100.

### 2.2.7    CellTiter-Glo luminescent cell viability assay

Cell viability was assessed by CellTiter-Glo Luminescent Cell Viability Assay (Promega), which determines the number of viable cells in culture based on quantitation of the ATP present, an indicator of metabolically active cells. CAR T cells or Peripheral blood T cells (PBT) isolated by CD3 MicroBeads (Miltenyi Biotec)

were seeded in 96-well tissue culture plates and incubated with indicated concentration of recombinant human CD95 ligand (Peprotech) for 24 hours in the presence of APG101 or APG122 (Apogenix) or not. 100 ul of CellTiter-Glo Reagent was added to each well, including control wells containing medium without cells to obtain a value for background luminescence. After 10 minutes incubation at room temperature, luminescence in each well was recorded by Ensight Multimode Plate Reader. Relative viability was normalized to untreated cells control.

### 2.2.8 *In vitro* co-culture stress test assay

Effector T cells CD19.CAR T cells ($5 \times 10^5$) were co-cultured with CD19 positive target cells, i.e. Daudi or Nalm-6 cells at effector/target (E:T) ratio of 1:4 (round I) in the presence of indicated concentration of APG101. Additional tumor cells were supplied to the co-culture every 24 hours. After 3 rounds of stimulation (72 hours), CAR T cells ($CD3^+ CD19^-$) and tumor cells ($CD3^- CD19^+$) were harvested for analysis by flow cytometry (Figure 2.1) and culture supernatants were assayed by ELISA for soluble CD95L detection. Absolute numbers of cells in the coculture were calculated by CountBright absolute counting beads via flow cytometer.
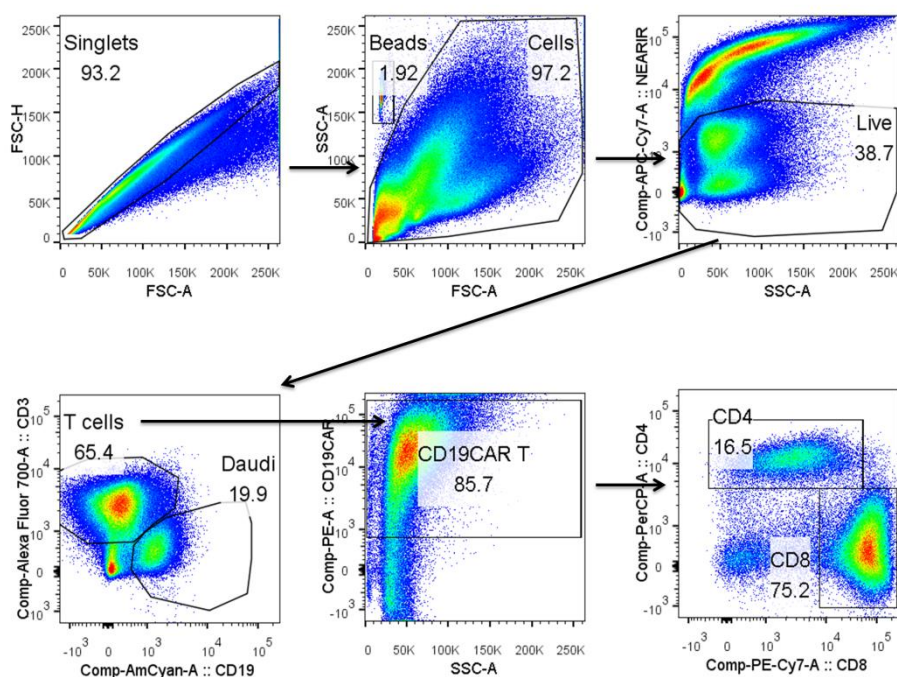


**Figure 2.1 Flow cytometry gating strategy for CAR T cells in coculture with tumor cells.**

FSC-A vs. FSC-H was used for getting singlets from FACS data. Dead cells were then excluded by Live/Death NearIR staining. The CD3⁻CD19⁺ population was tumor cells, and CD3⁺CD19⁻ T cells were further analyzed with CAR expression and then CD4 and CD8 markers.

## 2.2.9 Human Fas/CD95 Ligand Immunoassay

The quantitative determination of human Fas/CD95 ligand concentrations in cell culture were detected by Human Fas Ligand/TNFSF6 Quantikine enzyme-linked immunosorbent assay (ELISA) Kit (R&D Systems) according to the manufacturer's instructions. Briefly, 100 ul of Assay Diluent RD1S was added into indicated wells from 96 well polystyrene microplate coated with a monoclonal antibody specific for human FasL before adding 50 ul of standards, control, or samples per well. After 2 hours incubation at RT, liquid from each well was removed completely and washed the wells with 400ul Wash Buffer for a total of four times. Subsequently, 200 ul of Human FasL conjugate was added to each well for 2 hours incubation at RT. After washing the wells for 4 times, 200 ul of Substrate Solution was added to each well and incubated for 30 minutes at RT in the dark. The optical density of each well was determined within 30 minutes after adding 50 ul of Stop Solution, using a microplate reader set to 450 nm. A standard curve was generated for each set of samples assayed.

## 2.2.10 Magnetic-activated cell sorting (MACS)

Magnetic cell separation is based on antibodies coupled to magnetic beads. During incubation with a cell suspension, the antibody/bead complex binds to cells expressing the corresponding epitope. When the cell suspension is placed into a magnetic field, magnetically labeled cells are retained, while unlabeled cells can be removed.

### 2.2.10.1 CD3⁺ T cell isolation using CD3 MicroBeads

MACS buffer was prepared by diluting MACS BSA Stock Solution 1:20 with autoMACS™ Rinsing Solution. Cells were harvested in a FACS tube by centrifugation at 300g for 10 minutes and resuspended in 80 ul of MACS buffer per

$10^7$ total cells. 20 ul of CD3 MicroBeads was added into the test tubes and mixed well. After 15 minutes incubation at 4 °C, cells were washed with 2 ml MACS buffer and resuspended in 500 ul of MACS buffer for magnetic separation. LS column was placed in the magnetic field of MACS Separator. Cell suspension was applied onto the column which has been rinsed with 3 ml MACS buffer before. Unlabeled cells (CD3 negative) which pass through were collected in a 15 ml Falcon tube. The column was washed by 3 ml MACS buffer for 3 times, each time once the column reservoir is empty. Column was removed from the separator and placed on another 15 ml collection tube. 5 ml of MACS buffer was added onto the column and the magnetically labeled cells (CD3 positive) were flushed out by firmly applying the plunger supplied with the column. The unlabeled cell fraction and labeled cell fraction were stained with CD3 FITC antibody and analyzed by flow cytometry.

### 2.2.10.2    Elimination of dead cells using Dead Cell Removal MicroBeads

Dead Cell Removal MicroBeads recognize a moiety in the plasma membrane of apoptotic as well as dead cells. For the dead cell depletion, cells were resuspended in 1 x Binding Buffer and stained with 100 ul of Dead Cell Removal MicroBeads for 15 minutes at RT. Cell suspension was passed through a LS column. The magnetically labeled dead cells are retained within the column. The unlabeled living cells run through and this cell fraction is thus depleted of dead cells. After removing the column from the magnetic field, the magnetically retained dead cells was eluted as the positively selected cell fraction. The labeled and unlabeled cell fraction were proceed to microscopic analysis of dead cells with membrane exclusion dyes, such as Trypan Blue, as well as to flow cytometric analysis using 7-AAD Staining Solution.

## 2.2.11   Western blot

### 2.2.11.1    Cell lysis and protein extraction

For lysis of CAR T cells cultured with tumor cells, live CD3 positive T cells were collected by CD3 MicroBeads after removal of dead cells using Dead Cell Removal MicroBeads. Cells were harvested in 1.5 ml microfuge tubes and washed with cold

PBS by centrifuging at 2000g for 5 min at 4°C. Ice-cold lysis buffer (RIPA buffer with adequate protease and phosphatase inhibitors) was added to the cell pellet and incubated for 30 minutes in the ice or at 4°C. The supernatant was collected in fresh tube after centrifuging at 16000g for 20 minutes at 4°C. 10 ul of lysate was used for protein estimation by bicinchoninic acid assay (BCA) assay. The protein concentration of unknown samples was determined by comparison with the standards. Adequate volume of loading buffer was added to cell lysate and incubated at 95°C for 5 minutes. These samples were stored at -20°C or used to proceed with gel electrophoresis.

### 2.2.11.2    Western blotting

30 ug of protein samples and 5 ul of prestained molecular weight markers were loaded onto SDS-PAGE gel. The proteins and markers were separated under the indicated voltage for 1-2 hours. The proteins were electrotransferred on nitrocellulose membrane at 300 mA for 2 hours in the cold room. After transfer, nitrocellulose membrane was washed with 25 ml tris-buffered saline with tween 20 (TBS-T) buffer for 5 min at room temperature, followed by incubated in 25 ml of blocking buffer (5% milk in TBS-T) for 1 hr at room temperature. After washing with TBS-T, membrane was incubated with primary antibody at the recommended dilution (1:1000) with gentle agitation overnight at 4°C. After washing 3 times for 5 min each with TBS-T, membrane was incubated with anti-rabbit/-mouse IgG HRP-linked antibody at recommended dilution in blocking buffer with gentle agitation for 1 hour at RT. The membrane was washed and incubated with appropriate enzyme substrate solution for 2 minutes. Proteins were visualized in an Amersham Imager 600. Quantification of the intensity of protein bands was performed by using software ImageJ.

## 2.2.12    Long-term co-culture assay

$1 \times 10^5$ CD19.CAR T cells were cocultured with $CD19^+$ Nalm6 cells expressing GFP at a E:T ratio of 1:1, 1:2 or 1:4 on day 0. Additional Nalm6 GFP cells were daily supplied to the co-culture by indicated E:T ratio till day 6. AGP101 administration

(100 ug/ml) was at day 0 and day 3. Cells were harvested for flow cytometric analysis every 24 hours and culture supernatants were harvested on day 6 of co-culture for quantitative determination of multiple cytokines using Cytometric Bead Array (CBA). Absolute numbers of CAR T cells ($CD3^+ GFP^-$) and tumor cells ($CD3^- GFP^+$) in the coculture were calculated by CountBright absolute counting beads via flow cytometer. The phenotype of CAR T cells after coculturing were assessed on day 6, Naïve-like T ($T_N$) cells were defined as $CD45RA^+ CCR7^+$, central memory T ($T_{CM}$) cells as $CD45RA^- CCR7^+$, effector memory T ($T_{EM}$) cells as $CD45RA^- CCR7^-$ and effector T ($T_E$) cells as $CD45RA^+ CCR7^-$. Flow cytometry gating strategy was showed in Figure 2.2.
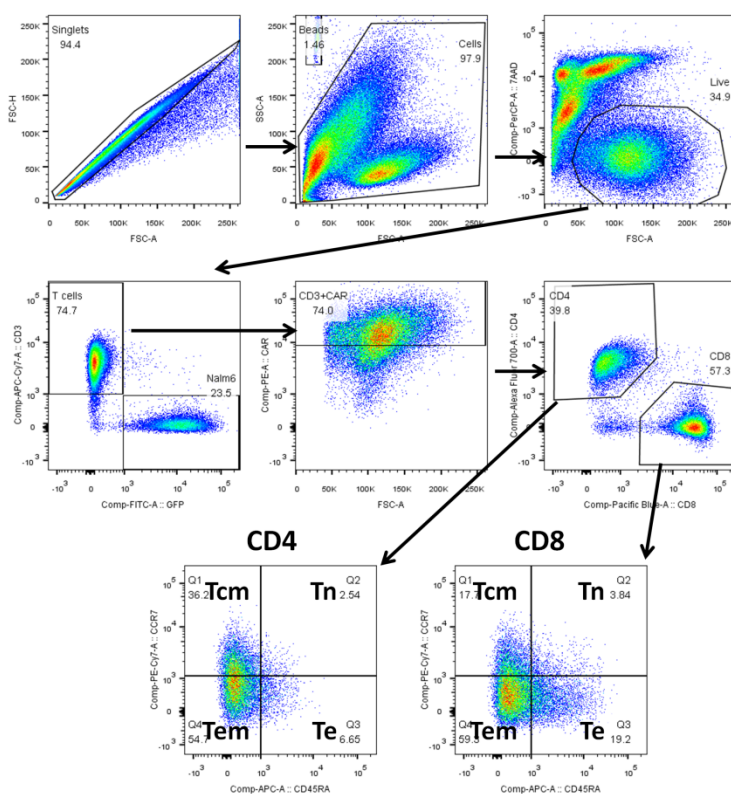


**Figure 2.2 Flow cytometry gating strategy for different subsets of CAR T cells after cocultured with tumor cells.**
FSC-A vs. FSC-H was used for getting singlets from FACS data. Dead cells were then excluded by 7AAD. The $CD3^- GFP^+$ population was tumor cells, and $CD3^+ GFP^-$ T cells were further analyzed with CAR expression and then CD4 and CD8 markers. CCR7 together with CD45RA were used to identify Naïve-like T ($T_N$) cells, central memory T ($T_{CM}$) cells, effector memory T ($T_{EM}$) cells and effector T ($T_E$) cells.

### 2.2.13 Luminescence assay

Luciferase enzymes are ideally suited for reporter assays with simple light-based detection and high sensitivity that can quantify even small changes in expression. To assess the cytotoxic capacity of CD19.CAR T cells in the long-term co-culture assay, we used luciferase reporter rather than Chromium-51 because luciferase vector is safer and easier to be introduced into cultured cells and detected with substrate D-luciferin for measuring changes over time. Thus, GFP-Firefly Luciferase retrovirus (provided by Professor Malcolm Brenner, Baylor College of Medicine) was used to transduce $CD19^+$ tumor cell line Nalm6 by spin-transduction in the presence of retronectin. Nalm6 cells expressing luciferase were collected by FACS sorting GFP positive cells. CAR T cells were repeatedly stimulated with Nalm6 expressing firefly luciferase (Nalm6 FFluc) in 96 well plate (E:T=1:2 ratio) every 24 hours for a total of 6 times. Luminescence intensity was measured every day after addition of D-Luciferin substrate using luminescence microplate reader. The luminescence readings are expressed as relative light units (RLU). % specific lysis = (1 − RLU in the coculture well / RLU in untreated Nalm6 FFluc well) × 100.

### 2.2.14 Cytometric Bead Array (CBA)

The BD CBA Human Th1/Th2/Th17 Cytokine Kit uses bead array technology to simultaneously detect multiple cytokine proteins in research samples. Seven bead populations with distinct fluorescence intensities have been coated with capture antibodies specific for IL-2, IL-4, IL-6, IL-10, TNF, IFN-γ, and IL-17A proteins. The seven bead populations are mixed together to form the bead array, which is resolved in a red channel of a flow cytometer (Figure 2.3 A). Thus, cytokines released by CAR T cells in co-culture supernatant were detected by this CBA Human Th1/Th2/Th17 Cytokine Kit. Fresh cytokine standards were prepared to run with each experiment. A 10 ul aliquot of each Capture Bead into a single tube and vortex the bead mixture thoroughly. 50 ul of Human Th1/Th2/Th17 Cytokine Standard dilutions were added to the control tubes. The negative control tube is with Assay Diluent only. 50 ul of

each unknown sample (1:1000 dilution by Assay Diluent) were added to the appropriately labeled sample tubes. 50 ul of the Human Th1/Th2/Th17 PE Detection Reagent were added to all assay tubes and incubated for 3 hours at RT in the dark. Subsequently, each assay tube was washed with 1 ml wash buffer by centrifuge at 200g for 5 minutes. The supernatant from each tube was carefully aspirated and discarded. The bead pellets were resuspended by 300 ul of Wash Buffer. The samples were acquired on the flow cytometer according to the instruction. The concentration of each cytokine was determined by comparison with the standards (Figure 2.3 B).
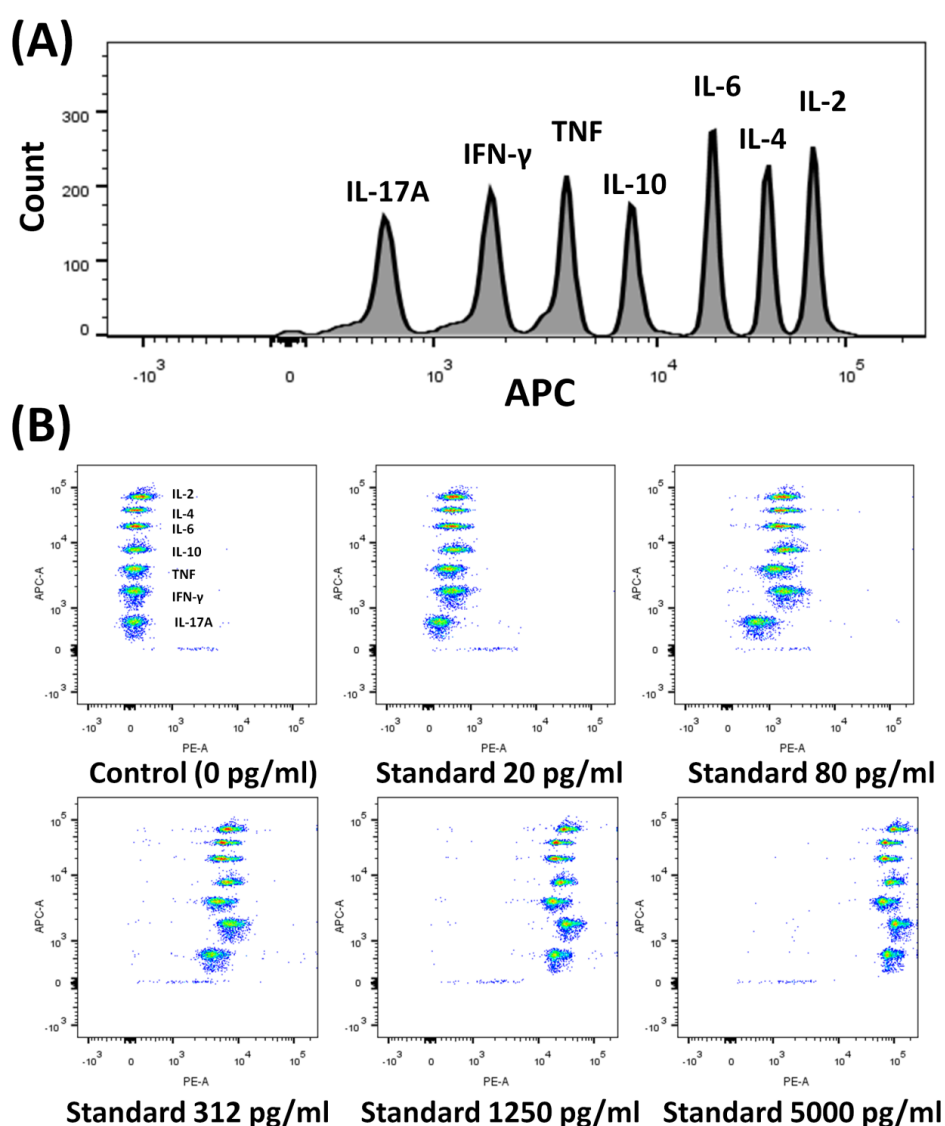


**Figure 2.3 Flow cytometric analysis of the standards using Cytometric Bead Array**

(A) The seven bead populations, IL-2, IL-4, IL-6, IL-10, TNF, IFN-γ, and IL-17A, were displaced in a red channel (APC) of a flow cytometer. (B) The dot plots, acquired using BD LSR II, shows standards and detectors alone.

## 2.2.15    Knockout of CD95/Fas in CAR T cells via CRISPR-Cas9

The CRISPR (clustered regularly interspaced short palindromic repeats) system is a prokaryotic adaptive immune system that uses the RNA-guided DNA nuclease Cas9 to silence viral nucleic acids (Jinek et al. 2012), and it has been shown to function as a gene editing tool in various organisms including mammalian cells (Cong et al. 2013; Mali et al. 2013). The CRISPR system consists of a short non-coding guide RNA (gRNA) made up of a target complementary CRISPR RNA (crRNA) and an auxiliary transactivating crRNA (tracrRNA). The gRNA guides the Cas9 endonuclease to a specific genomic locus via base pairing between the crRNA sequence and the target sequence, and cleaves the DNA to create a double-strand break (Cong et al. 2013).

### 2.2.15.1    gRNA design and assembly

The CRISPR sequences against human Fas gene were designed using the CRISPR Guide RNA design tool Benchling (www.benchling.com/crispr). Three different target sequences within the first 3 exons were chosen following the guidelines (table 2.1). The full-length gRNA was synthesized by the GeneArt™ Precision gRNA Synthesis Kit. The gRNA DNA template sequence is composed of the T7 promoter sequence, the sequence coding the target-specific gRNA, and the constant region of the crRNA/tracrRNA. Thus, two 34- to 38-bp oligonucleotides were orded to assemble the synthetic gRNA template: a target forward primer harboring the T7 promoter sequence (TAATACGACTCACTATAG) and a target reverse primer that overlaps with the target primer and the 5' end of the crRNA/tracrRNA constant sequence (TTCTAGCTCTAAAAC). The forward and reverse oligonucleotides were PCR assembled with the Tracr Fragment + T7 Primer Mix included in the kit to generate the Fas gRNA DNA template according to the recommended PCR protocol (table 2.2).

**Table 2.1 CRISPR sequences against human Fas gene**

| No. | Name | Sequence 5' to 3' | Exon |
|---|---|---|---|
| 1 | Target sequence | GTGACTGACATCAACTCCAA | 2 |
| | Forward primer | taatacgactcactataGGTGACTGACATCAACTCCAA | |
| | Reverse primer | ttctagctctaaaacTTGGAGTTGATGTCAGTCAC | |
| 2 | Target sequence | GGAGTTGATGTCAGTCACTT | 2 |
| | Forward primer | taatacgactcactataGGAGTTGATGTCAGTCACTT | |
| | Reverse primer | ttctagctctaaaacAAGTGACTGACATCAACTCC | |
| 3 | Target sequence | TAGGGACTGCACAGTCAATG | 3 |
| | Forward primer | taatacgactcactataGTAGGGACTGCACAGTCAATG | |
| | Reverse primer | ttctagctctaaaacCATTGACTGTGCAGTCCCTA | |

**Table 2.2 PCR protocol for the gRNA template DNA**

| Cycle step | Temperature | Time | Cycles |
|---|---|---|---|
| Initial denaturation | 98°C | 10 seconds | 1X |
| Denaturation | 98°C | 5 seconds | 32X |
| Annealing | 55°C | 15 seconds | |
| Final extension | 72°C | 1 minute | 1X |
| Hold | 4°C | Hold* | 1X |

### 2.2.15.2    Generation of gRNA by *in vitro* transcription (IVT)

To perform *in vitro* transcription reaction, gRNA DNA template (from PCR assembly) was mixed with the reaction components (NTP mix, 5X TranscriptAid Reaction Buffer and TranscriptAid Enzyme Mix) thoroughly and incubated at 37°C for 4 hours. To prevent the template DNA from interfering with downstream applications of the RNA transcript, the DNA template was removed by DNase I digestion directly after the IVT reaction. A control IVT reaction was performed in parallel using the Control gRNA (targets the human HPRT locus) forward and reverse primers included in the kit.

### 2.2.15.3    Purification of the in vitro transcribed gRNA

The gRNA generated by IVT was purified using the gRNA Clean Up Kit (Box 2 of the GeneArt™ Precision gRNA Synthesis Kit) according the protocol. The gRNA Clean Up Kit contains preassembled GeneJET™ RNA Purification Micro Columns

and all the necessary buffers to effectively remove primers, dNTPs, unincorporated nucleotides, enzymes, and salts from PCR and IVT reaction mixtures. The concentration of the purified gRNA was determined using the NanoDrop™ spectrophotometer (table 2.3). The eluted gRNA was used immediately or stored at –20°C until use, for prolonged storage (>1 month), it was stored at –80°C.

**Table 2.3 The concentration of the purified Fas gRNAs**

| Sample | Concentration (ng/ul) | A260 | A280 | 260/280 |
|---|---|---|---|---|
| Fas gRNA_1 | 1085.87 | 27,147 | 12,445 | 2,18 |
| Fas gRNA_2 | 1175.66 | 29,392 | 13,817 | 2,13 |
| Fas gRNA_3 | 1067.75 | 26,694 | 12,492 | 2,14 |
| Control gRNA | 1018.57 | 25,464 | 12,622 | 2,02 |

### 2.2.15.4 Generation of Fas knockout CAR T cells via Neon Transfection System

The Neon Transfection System is a novel, benchtop electroporation device that employs an electroporation technology by using the pipette tip as an electroporation chamber to efficiently transfect mammalian cells including primary and immortalized hematopoietic cells, stem cells, and primary cells. The Neon Transfection System efficiently delivers nucleic acids, proteins, and gRNA into all mammalian cell types including primary and stem cells with a high cell survival rate.

T cells from PBMC derived from healthy donors were activated by plate-bound anti-CD3/CD28 antibodies and transduced with the CD19.CAR.CD28.CD137zeta retroviral vector. CD19.CAR T cells were cultured in the presence of IL-7 and IL-15 for 4-6 days before electroporation. The Neon™ Transfection System 10-µL Kit was used for CAR T cells electroporation with Cas9 and gRNA. In brief, 1 ug of TrueCut Cas9 Protein v2 and 1 ug of gRNA were mixed in Resuspension Buffer R (up to 6 ul in total). The Cas9/gRNA complex was incubated in Resuspension Buffer R at room temperature for 20 minutes. CAR T cells were harvested and washed once with PBS in 1.5 ml centrifuge tube and then resuspended in Buffer R at density of $4 \times 10^7$ - $6 \times 10^7$ cells/ml. 5 ul of CAR T cells ($2 \times 10^5$ - $3 \times 10^5$) was then gently mixed with 6 ul

of Cas9/gRNA complex. 10 μL of the CAR Tcells mixed with Cas9/gRNA complexes was pipette into the Neon 10-ul tip slowly. After electroporation with the program of 1600 V/10ms/3 pulses, the electroporated cells were immediately transferred into a 24-well plate containing 1 ml of pre-warmed culture medium. The electroporated CAR T cells were cultured in the presence of IL-7 and IL-15 for 8-9 days, the editing efficiency was verified by determination of Fas expression using flow cytometry.

### 2.2.16    Statistical analysis

Statistical analysis was performed using GraphPad Prism v7 (GraphPad Software Inc., San Diego, CA). *P* values were calculated using the pared t-test for comparison between two groups or the on-eway ANOVA with Dunnett's multiple comparisons test for comparison more than two groups. *P* values $< 0.05$ were considered as statistically significant. The half-maximal inhibitory concentration (IC50) was calculated using nonlinear regression analysis in GraphPad Prism. Where not otherwise indicated, results are presented as mean $\pm$ standard error of the mean (SEM). *, $P < 0.05$; **, $P < 0.01$; ***, $P < 0.001$; NS, no significant difference.

# 3 RESULTS

## 3.1 Effects of the CD95L inhibitor APG101 on CD19.CAR T cell products.

To assess whether the CD95L inhibitor APG101 could influence the production of CD19.CAR T cells, CD19.CAR T cells were generated in the presence of APG101. PBMCs from healthy donor were stimulated by plate-bound CD3 and CD28 antibodies, and then transduced with a CD19-specific 3$^{rd}$ generation retroviral CAR. Cells were treated with different doses of APG101 (0, 1, 10 and 100 µg/ml) twice a week for 14 days of cultivation in the presence of IL7 and IL-15 (Figure 3.1.1 A). The evolution of subpopulations within CD19.CAR T cells over time was assessed by phenotypic analyses on days 0, 3, 7, 10 and 14. CAR T cells generated with APG101 exhibited similar high transduction efficiency as CAR T cells without APG101 (74.27 ± 3.00 %, $P > 0.05$, Figure 3.1.1 B). APG101 did not affect the viability and expansion of CAR T cells (Figure 3.1.1 C). The phenotype of CAR T cells was analyzed by FACS staining with CD45RA and CCR7, CD4$^+$ or CD8$^+$ subpopulations like naïve T cells (CD45RA$^+$ CCR7$^+$), central memory T cells (CD45RA$^-$ CCR7$^+$), effector memory T cells (CD45RA$^-$ CCR7$^-$) and effector T cells (CD45RA$^+$ CCR7$^-$) were not influenced by APG101 treatment (Figure 3.1.1 D). The expression of the exhaustion markers PD1, TIM3 and LAG3 on both CD4$^+$ and CD8$^+$ T cells were upregulated transiently on day 3 during activation with anti-CD3/CD28 antibodies and then gradually declined to basal levels on day 14 except for TIM3 which remained at a high level. APG101 did not affect the expression of exhaustion markers on CAR T cells during the cultivation ($P > 0.05$, Figure 3.1.2 A). CD95L expression was very low on CAR T cells during the cultivation, and APG101 did not affect its expression ($P > 0.05$, Figure 3.1.2 B). Given that membrane-bound CD95L (mCD95L) could be cleaved into a soluble form by a metalloprotease upon activation, soluble CD95L (sCD95L) was analyzed in the culture supernatants by ELISA. We found that peak secretion of sCD95L occurred at day 3 and fell to a low level at day 14, whereas sCD95L remained unaffected by APG101 treatment ($P > 0.05$, Figure

3.1.2 C). In addition, the function of these CAR T cells was assessed by intracellular TNF-α and IFN-γ staining, as well as degranulation analysis (CD107a staining). APG101 did not affect the secretion of TNF-α, IFN-γ or CD107a by CAR T cells in response to CD19$^+$ Daudi cells ($P > 0.05$, Figure 3.1.2 D). Moreover, Cr-51 release assay was also used to analyze the antitumor activity of these CAR T cells. CD19.CAR T cells killed CD19$^+$ target cells Daudi effectively but not CD19$^-$ target cells K562, and this antigen-specific cytotoxic capacity was comparable in APG101 pre-treated CAR T cells ($P > 0.05$, Figure 3.1.2 E). Taken together, the presence of CD95L inhibitor APG101 has no negative effect on CAR T cell production, nor does APG101 change phenotype or function of CAR T cells.
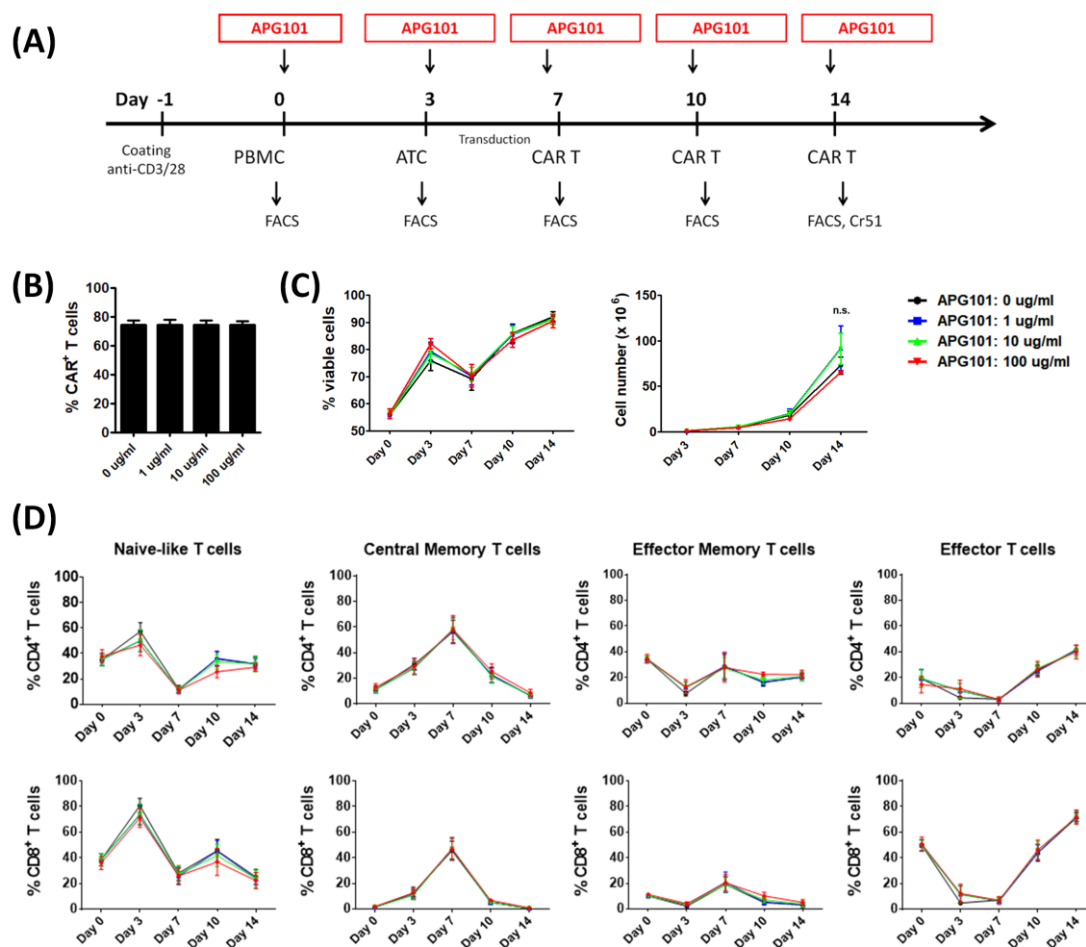
**Figure 3.1.1 CD95L inhibitor APG101 did not change the phenotype of CAR T cells.**

(A) Workflow of CD19.CAR T cells generated with APG101. (B) CD19-specific CAR expression was detected by FACS staining with anti-human goat $F(ab)_2$ IgG (H+L) PE antibody on day 4 post transduction. (C) Cell viability was analyzed by LIVE/DEAD fixable near-infrared (IR) dead cell stain kit, and viable cell numbers were counted at indicated time points. (D) The phenotype of $CD4^+$ or $CD8^+$ CAR T cells was analyzed by FACS staining with CD45RA and CCR7, like naïve T cells ($CD45RA^+ CCR7^+$), central memory T cells ($CD45RA^- CCR7^+$), effector memory T cells ($CD45RA^- CCR7^-$) and effector T cells ($CD45RA^+ CCR7^-$). Results are presented as mean ± standard error of the mean (SEM). n.s., no significant difference.
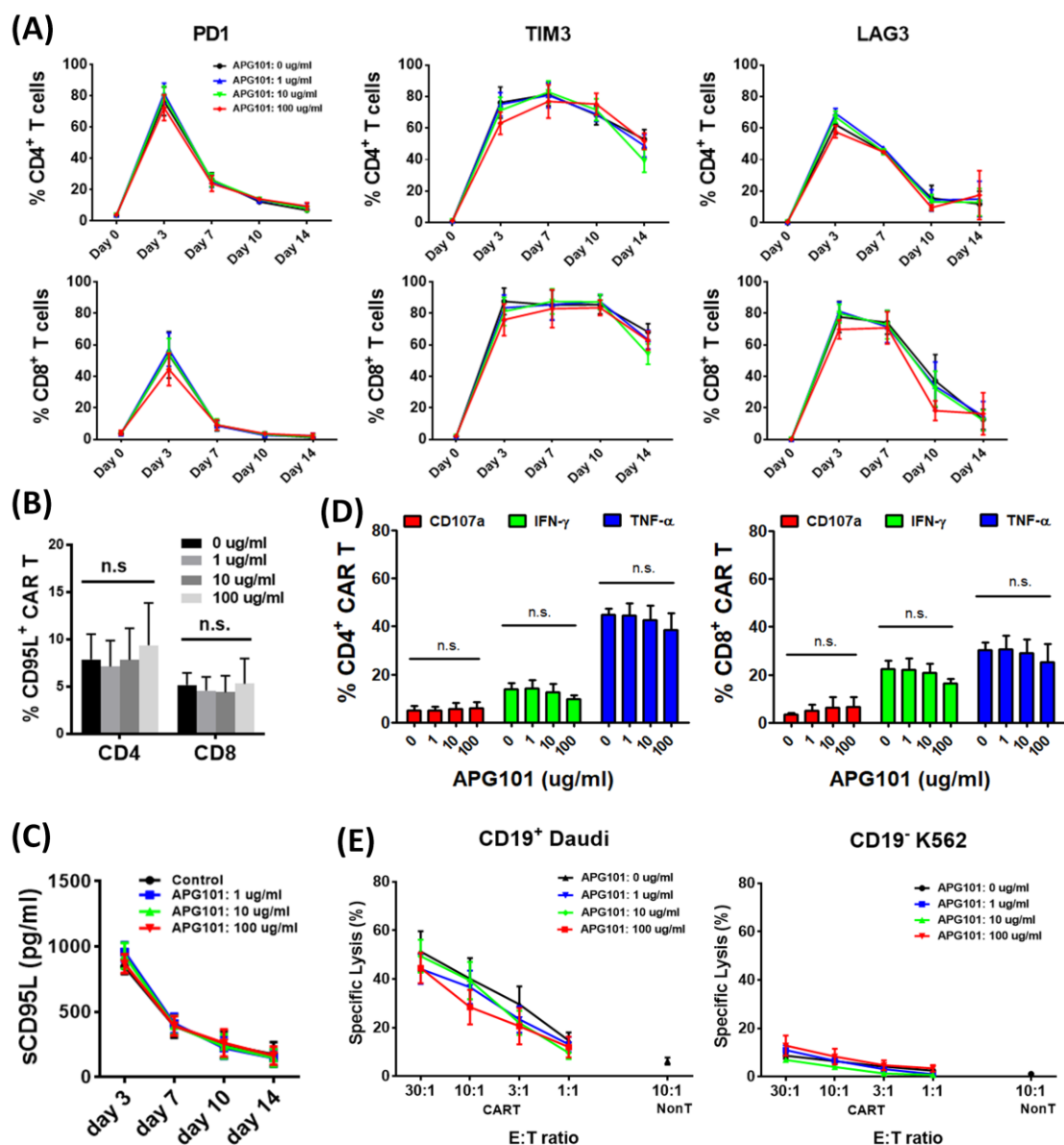
**Figure 3.1.2 The function of CD19.CAR T cells was not impaired by APG101.**

(A) The expression of exhaustion markers PD1, TIM3 and LAG3 on CD4^{+} and CD8^{+} CAR T cells were analysed by FACS. (B) Surface CD95L expression on CD4^{+} and CD8^{+} CAR T cells were analysed by FACS. (C) Soluble CD95L expression in cell culture supernatants at indicated time was measured by ELISA. (D) Intracellular TNF-α and IFN-γ staining, as well as degranulation analysis (CD107a staining) of CAR T cells in response to CD19^{+} Daudi cells. (E) Cytotoxic capacity of CAR T cells generated with APG101 or not was analyzed by Cr-51 release assay. Results are presented as mean ± standard error of the mean (SEM). n.s., no significant difference.

## 3.2 CD19.CAR T cells express high levels of CD95 and are susceptible to CD95L-mediated cell death.

In the next step, it was determined whether CD95 death receptor is expressed on the surface of CD19.CAR T cells. Interestingly, CD95 was expressed on all CAR T cells from healthy donors (n = 4). The expression of CD95 was much higher on CAR T cells compared to peripheral blood CD3$^+$ T cells (PBT) (100 ± 0 % vs 56.93 ± 3.31 %, $P < 0.001$, Figure 3.2 A). To assess their susceptibility to CD95L-induced apoptosis, CAR T cells or PBT cells were incubated with different concentrations of recombinant CD95L protein for 24 hours. Compared with PBT cells, CAR T cells were more sensitive to apoptosis induced by recombinant CD95L (IC50 value was 194.4 ng/ml and 26.54 ng/ml, respectively), in a dose-dependent manner (Figure 3.2 B). Next, it was investigated whether blockade of CD95/CD95L signaling by CD95L inhibitor APG101 could protect CAR T cells from this CD95L-mediated apoptosis. CAR T cells were treated with increasing concentrations of CD95L inhibitor APG101 (0.1, 1, 10, 100 and 1000 ng/ml) in the presence of recombinant CD95L protein (100 ng/ml) for 24 hours. The viability of CAR T cells in the presence of 100 ng/ml CD95L protein without APG101 treatment was 27.39 ± 8.51 % (Figure 3.2 C). The viability of CAR T cells treated with 10, 100 and 1000 ng/ml of APG101 in the presence of CD95L protein was 102.50 ± 8.41 %, 105.77 ± 6.47 % and 107.96 ± 7.15 %, respectively, which indicated that the apoptosis mediated by CD95L was effectively inhibited by the addition of APG101 ($P < 0.05$, Figure 3.2 C, red bar). Of note, APG101 by itself did not affect the viability of CAR T cells, as the viability of APG101 treated CAR T cells without CD95L protein were unaffected ($P > 0.05$, Figure 3.2 C, blue bar). The effect of APG122, a CD95L binding defective CD95-Fc mutant, on apoptosis inhibition was also tested as a negative control. APG122 did not show any effect on CAR T cells in the absence or presence of CD95L (Figure 3.2 D). These data indicated that CAR T cells expressing CD95 were highly sensitive to apoptosis induced by the recombinant CD95L, which can be reversed by CD95L inhibitor APG101.
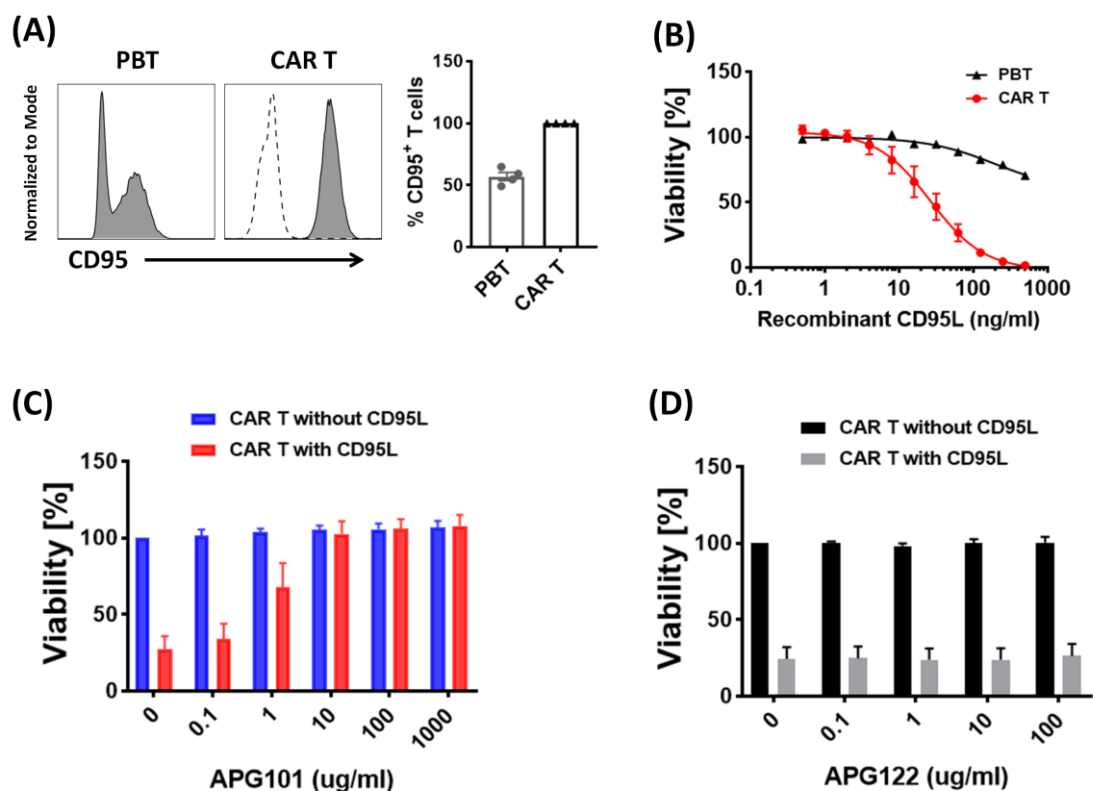
**Figure 3.2 CD19.CAR T cells express high levels of CD95 and are susceptible to CD95L-mediated cell death.**

(A) Freshly isolated peripheral blood CD3^{+} T (PBT) cells and CD19.CAR T cells both from the same healthy donors were stained with anti-CD95-BV421 (solid line) or isotype control (dashed line). The expression of CD95 detected by flow cytometry in PBT and CAR T cells were shown. FACS plot are representative of 4 different donors. (B) 1 x 10^5 PBT cells or CAR T cells were incubated with increasing concentration of recombinant human CD95 ligand protein (0, 0.5, 1, 2, 4, 8, 16, 31.75, 62.5,125, 250 and 500 ng/ml) for 24 hours. Cell viability was assessed by CellTiter-Glo Luminescent Cell Viability Assay and data was presented as relative to untreated control. (C) 1 x 10^5 CAR T cells were treated with increasing concentration of APG101 (0.1, 1, 10, 100 and 1000 ng/ml) or media alone in the presence of 100 ng/ml recombinant CD95L protein or not, and cell viability was measured at 24 hours. (D) 1 x 10^5 CAR T cells were treated with increasing concentration of APG122 (0.1, 1, 10 and 100 ng/ml) or media alone in the presence of 100 ng/ml recombinant CD95L protein or not, and cell viability was measured at 24 hours.

## 3.3 Repetitive antigen stimulation promoted CD95L expression and results in AICD on CD95+ CAR T cells.

For better understanding of the role of CD95/CD95L pathway on CAR T cells, an *in vitro* co-culture stress test assay was employed to assess the functional status and viability of CD19.CAR T cells upon repetitive stimulation with CD19+ tumor cells. CAR T cells were stimulated with target cells Nalm6 for 0, 1, 2, or 3 times in a 3 days period (Figure 3.3 A). A progressive increase of dead CAR T cells was observed following serial antigenic stimulation ($P < 0.05$, Figure 3.3 A). In addition to CD95, CD95 ligand is also an essential effector molecule for triggering T cell apoptosis. It was found, that CD19.CAR T cells expressed little mCD95L under normal conditions, however, mCD95L was rapidly expressed following antigen stimulation. The relative mean fluorescence intensity (MFI) of mCD95L on CAR T cells after 1st, 2nd, and 3rd round stimulations were $2.18 \pm 0.03$, $2.30 \pm 0.12$ and $2.46 \pm 0.03$, respectively, much higher than that on CAR T cells without stimulation ($1.06 \pm 0.06$, $P < 0.05$, Figure 3.3 C). Further, we analyzed sCD95L which releases from cell surface upon activation in the cell co-culture supernatant. The production of sCD95L in the supernatant of the coculture of CAR T cells with tumor cells was 13-fold higher than that in CAR T cells monoculture for 72 hours (Figure 3.3 C). Both mCD95L and sCD95L were dramatically up-regulated upon the 1st round stimulation, and were stably expressed after 2nd and 3rd round stimulations. Repetitive stimulation often drives T cell exhausted and lose their antitumor activity. Thus, the exhaustion markers PD1, TIM3 and LAG3 on CAR T cells after serial antigenic stimulation were analyzed. As expected, PD1, TIM3 and LAG3 were up-regulated in CAR T cells upon stimulation with tumors (Figure 3.3 E-G). Taken together, these data indicate that repetitive antigen stimulation promotes CD95L expression and results in activation-induced cell death (AICD) on CD95+ CAR T cells.
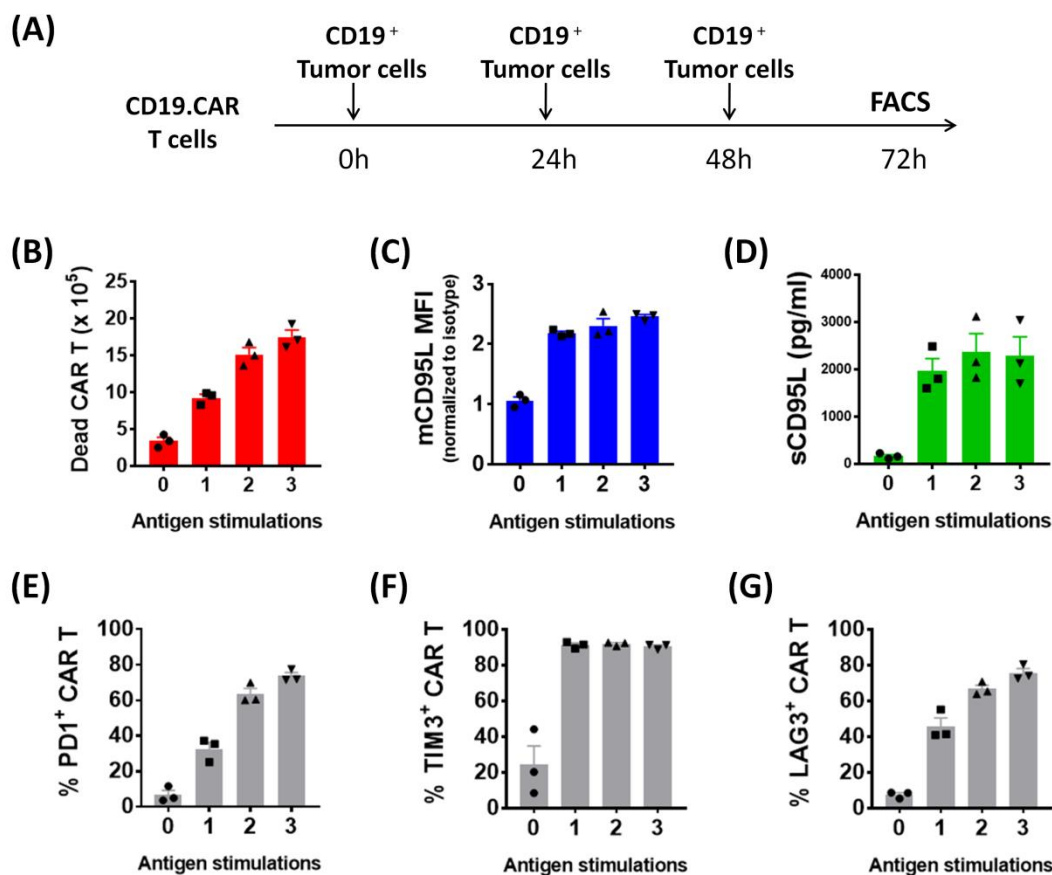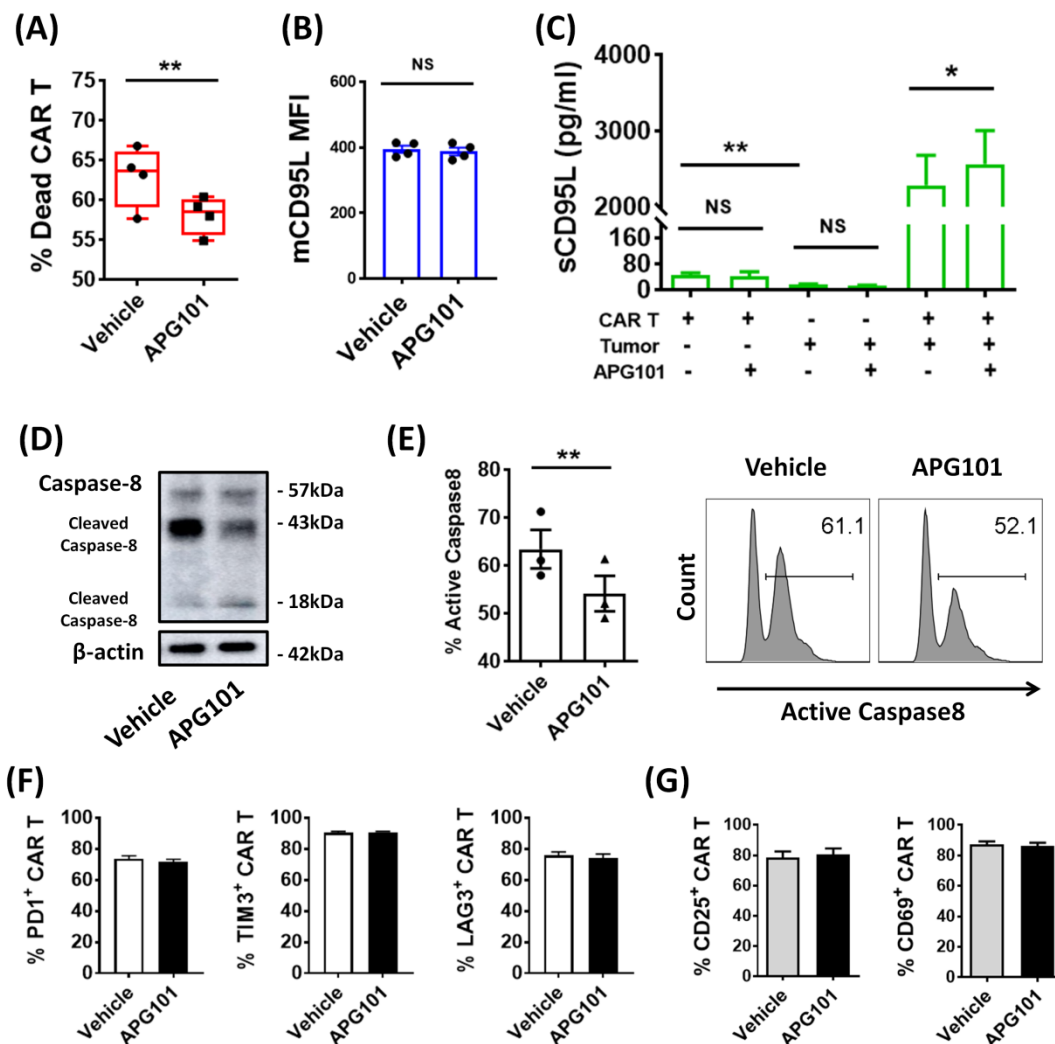
**Figure 3.3 Repeated antigen stimulation promotes CD95L expression and results in AICD on CD95+ CAR T cells.**

(A) Schematic diagram of the *in vitro* co-culture stress test assay in which 5 x 10⁵ CD19.CAR T cells were repeatedly stimulated with CD19⁺ target cells at E:T=1: 4 ratio for 72 hours. (B) Apoptosis of CAR T cells were analyzed after stimulation with CD19⁺ Nalm6 for 0, 1, 2, or 3 times in a 3 days period; bars represent the absolute numbers of dead CAR T cells. (C) Expression of membrane CD95L (mCD95L) was detected by flow cytometry in CAR T cells cultured with or without tumor cells; bars represent mean fluorescence intensity (MFI) of mCD95L normalized to isotype control. (D) The concentration of soluble CD95L (sCD95L) in the cell culture supernatants was measured by ELISA. (E-F) The expression of PD1, TIM3 and LAG3 in CAR T cells following stimulations were detected using flow cytometry. Data shown are from 3 different healthy donors. *, $P < 0.05$; **, $P < 0.01$; ***, $P < 0.001$; NS, no significant difference.

## 3.4   APG101 protects CAR T cells from CD95L-mediated cell death through blockade of CD95/CD95L pathway.

To evaluate whether the CD95L inhibitor APG101 could protect CAR T cells from AICD, CAR T cells were repeatedly stimulated with tumor cells in the presence of APG101 or vehicle control. The APG101 concentration of 100 µg/ml was chosen based on the data obtained from previous experiments (Figure 3.2 C) and 100 ug/ml of APG101 was found to be superior to 10 ug/ml of APG101 in terms of CAR T cell protection. It is found that a significant reduction of apoptosis in CAR T cells after stimulation with tumor cells in the presence of 100 ug/ml APG101 ($P < 0.01$, Figure 3.4 A). No significant differences of mCD95L expression were observed between CAR T cells treated with or without APG101 ($P > 0.05$, Figure 3.4 B). However, an increased level of sCD95L was found in the co-culture supernatant with APG101 ($P < 0.05$, Figure 3.4 C). This increase was not caused by APG101 itself as the level of sCD95L was comparable in the supernatants of CAR T cells cultured with or without APG101, nor from tumor cells because both sCD95L and mCD95L were hardly expressed on hematological tumor cells like Nalm6 and Daudi cells ($P > 0.05$, Figure 3.4 C). The engagement of CD95 with mCD95L promotes the recruitment of adaptor protein FADD and pro-caspase-8 and leads to the activation of caspase-8 and caspase-3, which finally induces apoptosis of CD95 expressing T cells (Yi et al. 2018). To further demonstrate that APG101 reduces CD95-mediated apoptosis in CAR T cells, we evaluated the activity of caspase-8, the downstream effector of CD95/CD95L pathway, in cells treated with or without APG101. As shown in Figure 3.4 D, the full-length caspase-8 protein (57 kDa) was cleaved into two stable 43 kDa and 18 kDa fragments after stimulation with tumor cells, while the cleavage process was significantly inhibited in cells treated with APG101. The inhibition of caspase-8 activity by APG101 was also confirmed by flow cytometry (Figure 3E). Additionally, the expression of activation markers (CD25 and CD69; Figure 3.4 G) and exhaustion markers (PD1, TIM3 and LAG3; Figure 3.4 F) of CAR T cells was also analyzed after co-culture. APG101 neither hampers the activation of CAR T cells nor affects the T

cell exhaustion, but was able to preserve CAR T cells after repeated antigen stimulation. Thus, these data indicated that APG101 protects CAR T cells from AICD through disruption of CD95/CD95L signaling.



**Figure 3.4 APG101 protects CAR T cells from CD95L-mediated cell death through disruption of CD95/CD95L pathway.**
(A) CAR T cell death was analyzed by FACS after repeated antigen stimulation in the presence of 100 ug/ml APG101 or vehicle control. (B) The mCD95L MFI was shown in CAR T cells co-cultured with CD19$^+$ Nalm6 cells with or without the addition of APG101. (C) The sCD95L concentration was measured in the cultured supernatants where CAR T cells or tumor cells alone or together in the presence or absence of APG101. (D) The protein levels of caspase-8 in CAR T cells were assessed by western blot. (E) The active caspase-8 of CAR T cells was detected by flow cytometry; summary plot and representative histogram are shown. (F) The expression of exhaustion markers PD1, TIM3 and LAG3 and (G) activation markers CD25 and CD69 on CAR T cells after repetitive stimulation with tumor cells with or without APG101 were analyzed by flow cytometry. *, $P < 0.05$; **, $P < 0.01$; ***, $P < 0.001$; NS, no significant difference.

## 3.5 APG101 enhances CAR T cell survival and preserves the effector memory T cell subset

Based on the above observation, a long-term co-culture assay was used to assess the *in vitro* survival of CAR T cells after repeated antigen stimulation in the presence of APG101. 1 x $10^5$ CD19.CAR T cells were cocultured with $CD19^+$ Nalm6 cells at 1:1, 1:2 or 1:4 E:T ratio at day 0. Additional Nalm6 cells were added daily to the co-culture in the appropriate ratio till day 6. AGP101 administration (100 ug/ml) was at day 0 and day 3. Figure 3.5 A displays the absolute cell number of CAR T cells during co-culture with Nalm6 in the presence or absence of APG101. CAR T cells expanded notably from day 3 to day 6 when stimulated with Nalm6, and a higher expansion level was found at lower E:T ratio (overall fold expansion: 18-fold at E:T=1:1, 15-fold at E:T=1:2, 6-fold at E:T=1:4). Addition of APG101 to the co-culture resulted in a significant increase of CAR T cell number from day 2 until the end of the culture under Nalm6 stimulation, and this increase was more pronounced on day 6 at the E:T ratio of 1:4 (approximately 1-fold increase at E:T=1:1, 2-fold increase at E:T=1:2, 3-fold increase at E:T=1:4) (Figure 3.5 A). Of note, APG101 itself has no impact on viability or proliferation of CAR T cell when cultured alone. In addition, after 6 days of co-culture, CAR T cell death was significantly lower in the presence of APG101 compared with vehicle control (Figure 3.5 B), which indicated that the enhanced persistence of CAR T cells was attributed to the reduction of AICD on CAR T cells mediated by APG101. Next, the expansion of CAR T cell subpopulations on day 6 of co-culture, i.e., $CD4^+$ and $CD8^+$ CAR T cells, was investigated. We observed that APG101 preserved both CD4 and CD8 subpopulations (Figure 3.5 C). The preservation of $CD4^+$ and $CD8^+$ CAR T cells induced by APG101 was comparable as CD4/CD8 ratio was similar with or without APG101 ($0.53 \pm 0.07$ *vs.* $0.50 \pm 0.08$, $P = 0.13$, Figure 3.5 D). Subsequently, the distribution of CAR T cell subsets defined by CD45RA and CCR7 T cell expression profiles after coculturing and the effect of APG101 on these subsets was analyzed. The effector memory T cell subset ($T_{EM}$, $CD45RA^-$ $CCR7^+$) was the dominant cell type of $CD4^+$ or $CD8^+$ CAR T

cells after the coculture (CD4$^+$ T$_{EM}$: 66.51 ± 1.75%, CD8$^+$ T$_{EM}$: 52.68 ± 2.33%, Figure 3.5 E). Addition of APG101 resulted in significantly higher percentages of CD4$^+$ T$_{EM}$ cells (without *vs.* with APG101: 66.51 ± 1.75% *vs.* 71.06 ± 3.00%, *P* < 0.05) and CD8$^+$ T$_{EM}$ cells (without *vs.* with APG101: 52.68 ± 2.33% *vs.* 62.00 ± 3.77%, *P* < 0.01) on day 6 of coculture. In contrast, CD45RA$^+$ CCR7$^+$ naïve-like T cells (T$_N$), also defined as "stem cell memory" T cells (T$_{SCM}$) due to their CD95 expression, were decreased when cultivated with APG101 (CD4$^+$ T$_N$ cells: without *vs.* with APG101: 2.10 ± 0.16% *vs.* 1.54 ± 0.30%, *P* < 0.05; CD8$^+$ T$_N$ cells: without *vs.* with APG101: 4.53 ± 0.65% *vs.* 2.96 ± 0.60, *P* < 0.01). The central memory T cell fraction (T$_{CM}$; CD45RA$^-$ CCR7$^+$) was declined in CD8$^+$ CAR T cells but not in CD4$^+$ CAR T cells after treated with APG101. The proportion of effector T cells (T$_E$; CD45RA$^+$ CCR7$^-$) in both CD4$^+$ and CD8$^+$ CAR T cells were hardly affected by APG101 on day 6 (Figure 3.5 D). Together, these results suggested that APG101 enhanced the long-term survival of CD19.CAR T cells after repeatedly encountered with CD19$^+$ Nalm6 cells and resulted in an accumulation of effector memory T cell subsets.
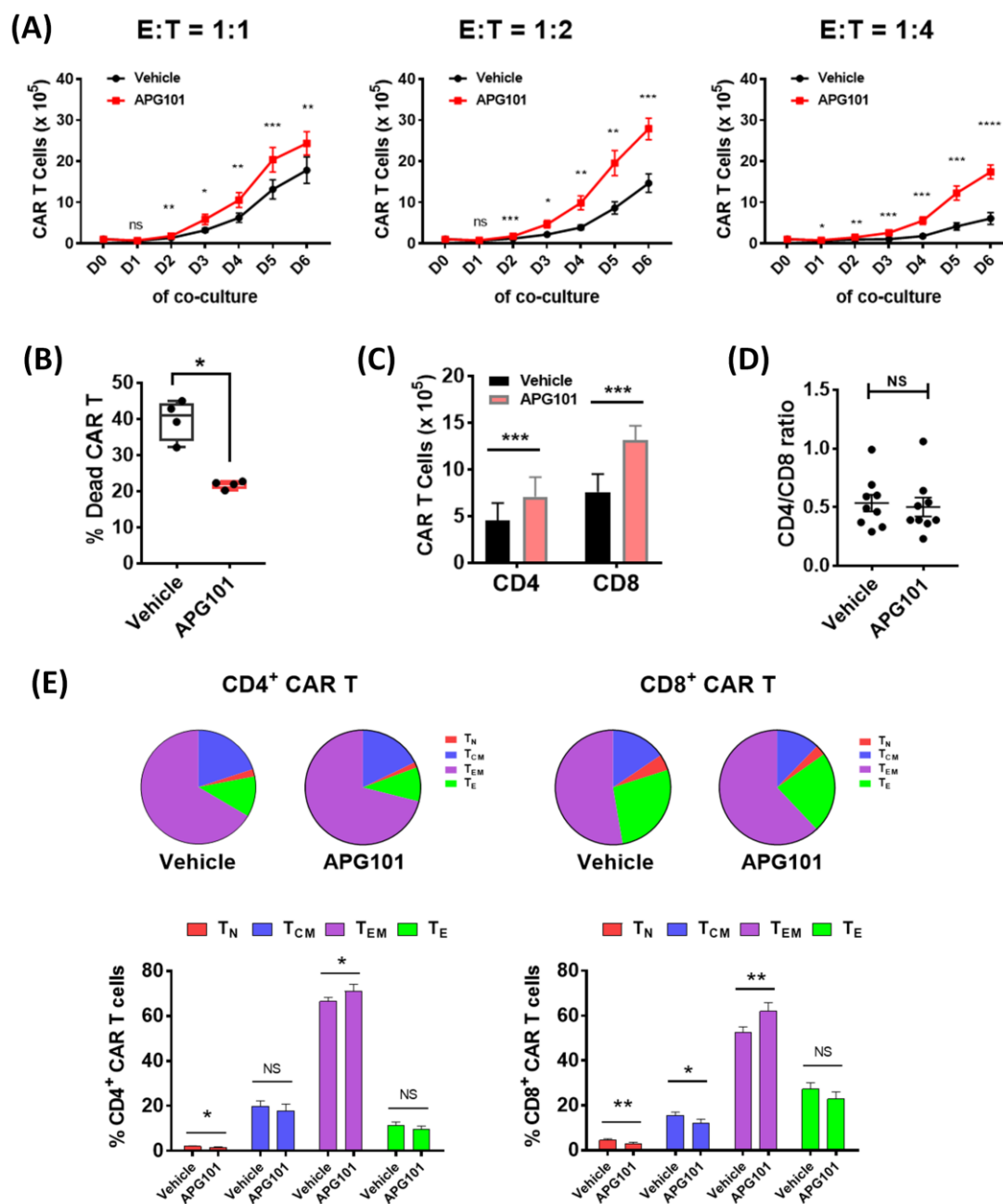
**Figure 3.5 APG101 enhances CAR T cell survival and preserves the effector memory T cell subset.**

(A) *In vitro* expansion of CAR T cells following repetitive stimulation with Nalm6 cells at indicated E:T ratios in the presence of APG101 (100 ug/ml) or vehicle control, viable CAR T cells were assessed by flow cytometry at day 1 to day 6. (B) Dead CAR T cells were assessed on day 6 after coculture (at E:T=1:4 ratio). (C) The absolute numbers of CD4$^+$ and CD8$^+$ CAR T cells on day 6 after coculture were determined by flow cytometry. (D) The CD4:CD8 ratio of CAR T cells on day 6 after coculture was analyzed by FACS. (E) The percentage of different CAR T cell subsets after coculture were assessed on day 6, Naïve-like T (T$_N$) cells were defined as CD45RA$^+$ CCR7$^+$, central memory T (T$_{CM}$) cells as CD45RA$^-$ CCR7$^+$, effector memory T (T$_{EM}$) cells as CD45RA$^-$ CCR7$^-$ and effector T (T$_E$) cells as CD45RA$^+$ CCR7$^-$. *, $P < 0.05$; **, $P < 0.01$; ***, $P < 0.001$; NS, no significant difference.

## 3.6 CD95L blockade by APG101 enhanced the long-term antitumor effect of CAR T cells *in vitro*.

After showing an improved persistence of CAR T cells induced by APG101, the influence of APG101 on the function of CAR T cells was investigated. Firstly, intracellular production of TNF-α and IFN-γ was assessed on CD19.CAR T cells after incubation with CD19$^+$ Daudi cells for 4 hours with or without APG101. No significant differences of TNF-α and IFN-γ expression on CAR T cells were observed between APG101 treatment and vehicle control (data not shown). The intracellular cytokine staining assay is a short term coculture assay, thus, a long-term coculture assay in which CAR T cells were repeatedly stimulated with target cells Nalm6 GFP for 6 days was performed. Nalm6 GFP cells in the long-term coculture were dramatically reduced in the presence of APG101 from day 5 to 6 at E:T=1:1 and 1:2 ratio, from day 2 to day 6 at E:T=1:4 ratio (Figure 3.6 A). At day 6 of co-culture, a 82% decrease of the number of tumor cells was found in the presence of APG101 at E:T=1:1 ratio, a 81% decrease at E:T=1:2 ratio and a 51% decrease at E:T=1:4 ratio, as compared to the untreated control (Figure 3.6 B). Of note, the better control of tumor cells was not caused by APG101 itself, as APG101 alone has no cytotoxic effect on tumor cells, i.e. Nalm6 and Daudi cells. In a next step, the cytotoxic capacity of CD19.CAR T cells against CD19+ Nalm6 GFP cells expressing firefly luciferase (FFluc) in the presence of APG101 was evaluated. Repetitive stimulation with fresh tumor cells resulted in a trend towards decreased lytic activity in CAR T cells from day 4 to day 6 (Figure 3.6 C). However, this effect was reversible in CAR T cells when treated with 100 ug/ml APG101 every three days. The enhanced anti-leukemia efficacy of CAR T cells mediated by APG101 was CD19 antigen dependent, because these effects were also observed in the co-culture of CAR T cells with CD19$^+$ Daudi cells but not CD19$^-$ K562 cells (data not shown). In addition, cytokines released by CAR T cells in the co-culture supernatant were measured on day 6 by flow cytometry with the BD™ CBA Human Th1/Th2/Th17 Cytokine Kit, which includes Interleukin-2 (IL-2), Interleukin-4 (IL-4), Interleukin-6

(IL-6), Interleukin-10 (IL-10), Tumor Necrosis Factor (TNF), Interferon-γ (IFN-γ), and Interleukin-17A (IL-17A). As shown in Figure 3.6 D, IFN-γ was the highest one among these cytokines secreted by CAR T cells and a further increase of IFN-γ was observed in the presence of APG101 (without *vs.* with APG101: 11819.55 pg/ml ± 2057.09 pg/ml *vs.* 17038.06 pg/ml ± 2174.98 pg/ml, $P = 0.009$). Significantly higher levels of TNF was also observed in the co-culture supernatant under APG101 treatment (without *vs.* with APG101: 225.71 pg/ml ± 80.66 pg/ml *vs.* 441.71 pg/ml ± 109.56 pg/ml, $P = 0.002$). Although the level of IL-10 was low in the co-culture supernatant, its expression was increased by APG101(without *vs.* with APG101: 23.78 pg/ml ± 2.02 pg/ml *vs.* 34.19 pg/ml ± 4.51 pg/ml, $P = 0.019$). In contrast, the high expressed IL-2 in the supernatant was decreased by APG101, although there was no statistically difference (without *vs.* with APG101: 689.63 pg/ml ± 433.62 pg/ml *vs.* 140.76 pg/ml ± 64.97 pg/ml, $P = 0.202$). No remarkable differences of IL-4, IL-6 and IL-17A expression were found between APG101 treatment and untreated control. Together, these data indicated that blockade of CD95/CD95L pathway by APG101 not only improves CAR T cell persistence *in vitro* but also enhances their long-term antitumor activity.
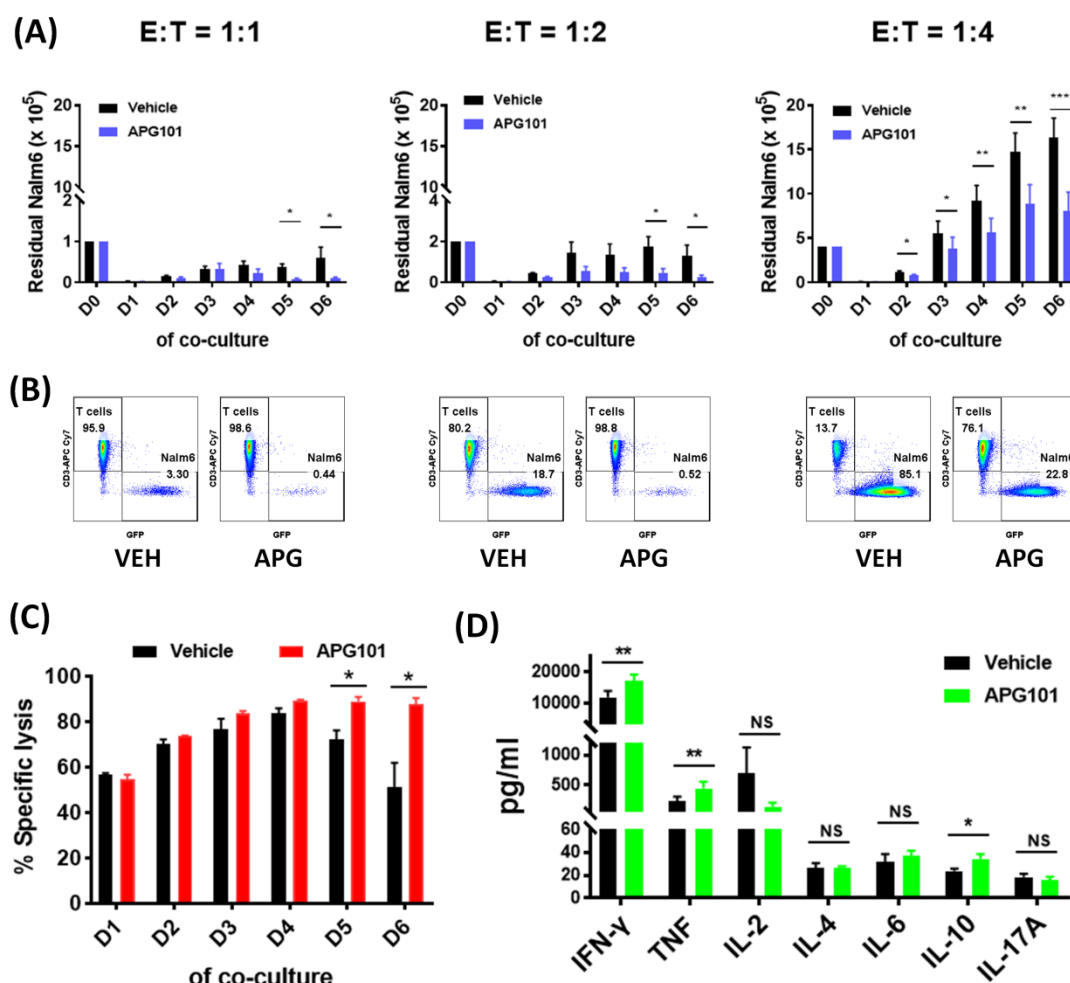
**Figure 3.6 CD95L blockade enhances the long-term antitumor effect of CAR T cells *in vitro*.**

(A) CAR T cells were daily stimulated with Nalm6 GFP cells at indicated E:T ratios in the presence of APG101 (100 ug/ml) or vehicle control for 6 days and the absolute number of residual Nalm6 GFP cells was assessed by flow cytometry every day. (B) FACS data showed the viable cells at day 6 of coculture at E:T=1:1, 1:2 and 1:4 ratios in the presence of APG101 treatment or not. FACS dot plots are representative data of 6 different donors. (C) CAR T cells were repeatedly stimulated with Nalm6 GFP cells expressing firefly luciferase (Nalm6 GFP FFluc) in 96 well plates (E:T=1:2 ratio) and luminescence intensity was measured after addition of D-Luciferin substrate. The luminescence readings are expressed as RLU (Relative Light Unit). % specific lysis = (1 – RLU in the coculture well / RLU in untreated Nalm6 FFluc well) × 100. (D) Cytokine secretion in the coculture supernatant were measured by flow cytometry after 6 days of coculture (E:T=1:4 ratio). VEH, vehicle; APG, APG101; *, $P <$ 0.05; **, $P < 0.01$; ***, $P < 0.001$; NS, no significant difference.

## 3.7 Knockout of CD95 (Fas) in CD19.CAR T cells.

Based on these data, it was further investigated whether disruption of CD95/CD95L signaling within CAR T cells might prevent their apoptosis and improve their persistence. Given that CD95 (also known as Fas) is highly expressed on CD19.CAR T cells, CRISPR-Cas9 was used to knockout Fas gene in these CAR T cells. Cas9 protein and 3 different gRNAs targeting human Fas gene or a control gRNA targeting the human HPRT locus were introduced into CD19.CAR T cells via electroporation (Figure 3.7 A). As Figure 3.7 B shows, the expression of Fas (CD95) on CAR T cells transfected with Fas gRNA 1, 2 or 3 were significantly down-regulated, whereas Fas expression on CAR T cells transfected with control gRNA was hardly affected compared to wild type (WT) CAR T cells. The knockout efficiency of these 3 different Fas gRNA in CAR T cells were approximately 60 %, 70 % and 80% ($P <$ 0.05), respectively, as analyzed by flow cytometry. Knockout efficiency of Fas in protein level of CAR T cells was also confirmed by western blot (Figure 3.7 C). As anticipated, Fas protein was dramatically diminished in CAR T cells transfected with Fas gRNA 1, 2 or 3, but not in control CAR T cells that transfected with control gRNA. In addition, knockout of Fas in CAR T cells has no impact on their viability and CAR expression, as no significant difference of cell viability and CAR transduction efficiency were observed among Fas KO CAR T cells and wild type CAR T cells (Figure 3.7 D-E). Overall, Fas knockout CAR T cells were successfully generated with high efficiency using CRISPR-Cas9 and found that the viability and CAR expression were not dramatically changed during *in vitro* culture.
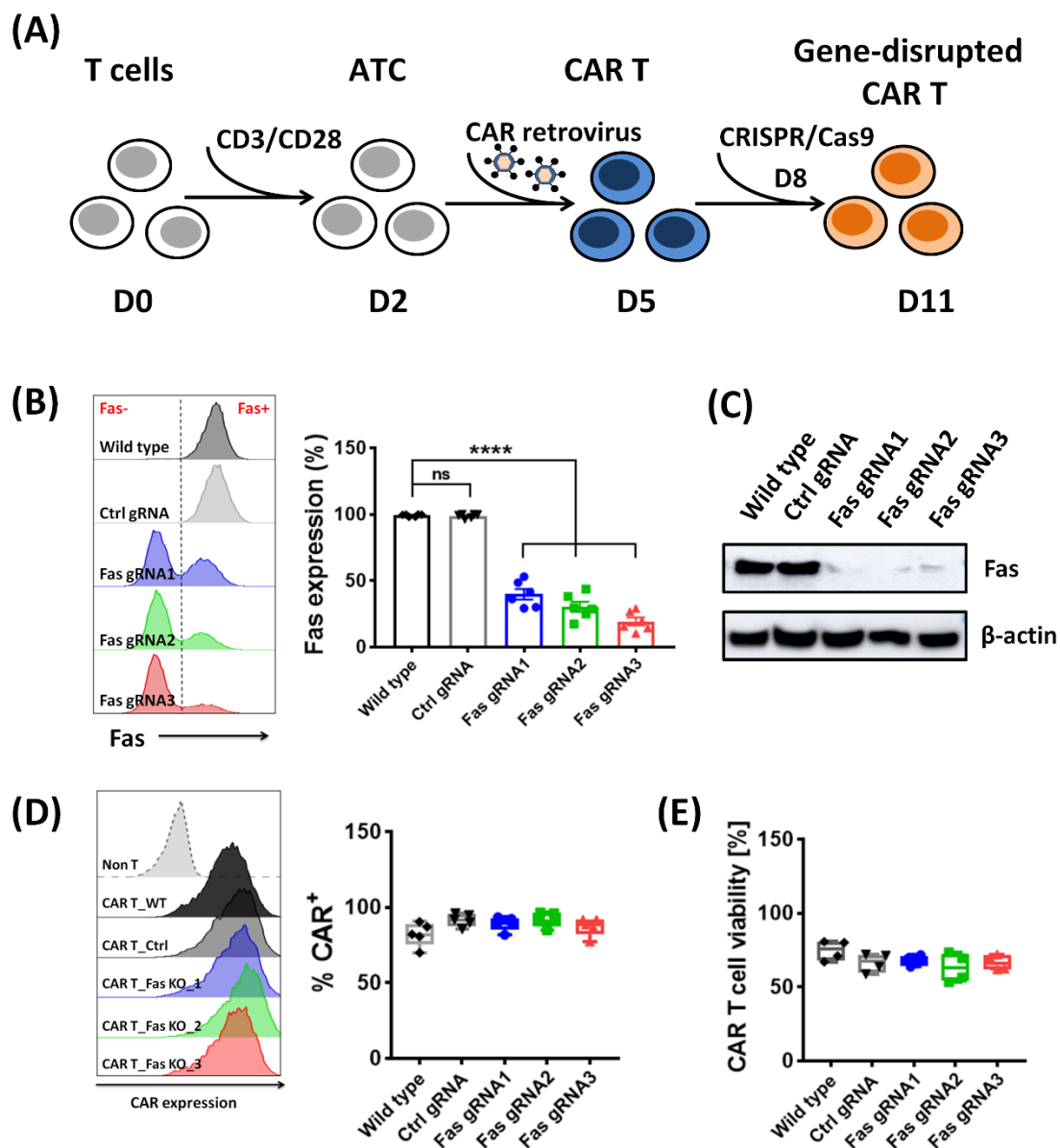
**Figure 3.7 Knockout efficiency of Fas in CD19.CAR T cells.**

(A) Schematic diagram of generation of Fas knockout CD19.CAR T cells. (B) Fas expression on gene-disrupted and wild type CD19.CAR T cells were analyzed by flow cytometry on day 8 or 9 after electroporation with indicated gRNAs and Cas9 protein. Representative data of 6 healthy donors is shown. (C) The expression of Fas protein on gene-disrupted and wild type CD19.CAR T cells were measured by western blot. (D) CAR expression on gene-disrupted CAR T cells, wild type CD19.CAR T cells and non-transduced T cells (Non T) were analyzed by flow cytometry. (E) Cell viability of gene-disrupted and wild type CD19.CAR T cells were analyzed by flow cytometry on day 8 or 9 after electroporation with indicated gRNAs and Cas9 protein. Mean values were calculated for each group (n = 6); error bars indicate standard error deviation. ATC, activated T cells. *, $P < 0.05$; **, $P < 0.01$; ***, $P < 0.001$; NS, no significant difference.

## 3.8    Characterization of CD95 (Fas) knockout CD19.CAR T cells.

The phenotype of the gene modified CAR T cells including Fas KO CAR T cells, control CAR T cells and WT CAR T cells were analyzed by flow cytometry on day 8 or 9 after electroporation with indicated gRNAs and Cas9. We found the CD4/CD8 ratio were comparable among the gene-modified CAR T cells and WT CAR T cells (CD4/CD8 ratio for CAR T transfected with Fas gRNA 1, 2 and 3 was 0.82, 0.72 and 0.84, respectively; WT CAR T was 0.88; $P > 0.05$, Figure 3.8 B). Next, the CD45RA and CCR7 expression in $CD4^+$ and $CD8^+$ subsets of CAR T cells was investigated. Based on the expression of CD45RA and CCR7, naïve-like ($T_N$), central memory ($T_{CM}$), effector memory ($T_{EM}$) and effector ($T_E$) $CD4^+$ and $CD8^+$ T cells were identified in Fas KO CAR T cells and WT CAR T cells. For $CD4^+$ Fas KO CAR T cells, $T_{EM}$ subset was the dominant cell type, followed by $T_{CM}$, $T_E$ and $T_N$ subset. For $CD4^+$ WT CAR T cells, $T_E$ subset was the dominant cell type, followed by $T_N$, $T_{EM}$ and $T_{CM}$ subset (Figure 3.8 B). $CD8^+$ Fas KO CAR T cells and $CD8^+$ WT CAR T cells displayed similar phenotypic features with $T_E$ subset being the dominant cell type, followed by $T_N$, $T_{EM}$ and $T_{CM}$ subset. Furthermore, for both $CD4^+$ and $CD8^+$ CAR T cells, higher percentages of $T_{EM}$ and $T_{CM}$ cells and a lower percentage of $T_E$ were found in Fas KO CAR T cells, compared to WT CAR T cells (Figure 3.8 C). The proportion of $CD4^+$ $T_N$ cells in Fas KO CAR T cells was lower than that in WT CAR T cells, but $CD8^+$ $T_N$ proportion was comparable among Fas KO and WT CAR T cells. In addition, expression of exhaustion markers on these gene-disrupted and WT CAR T cells were analyzed by flow cytometry. As Figure 3.8 D shown, the Fas KO CAR T cells did not show any change in the expression of PD1 and TIM3 compared with WT CAR T cells as well as control CAR T cells electroprated with control gRNA. However, upregulation of LAG3 was found in $CD8^+$ Fas KO CAR T cells, as well as $CD8^+$ control CAR T cells. Higher expression of LAG3 was also found in $CD4^+$ gene-disrupted CAR T cells, but there was no statistical difference. Taken together, knockout of Fas in CAR T cells results in a memory-like phenotype, characterized by a higher fraction of $T_{CM}$ and $T_{EM}$, compared with WT CAR T cells.
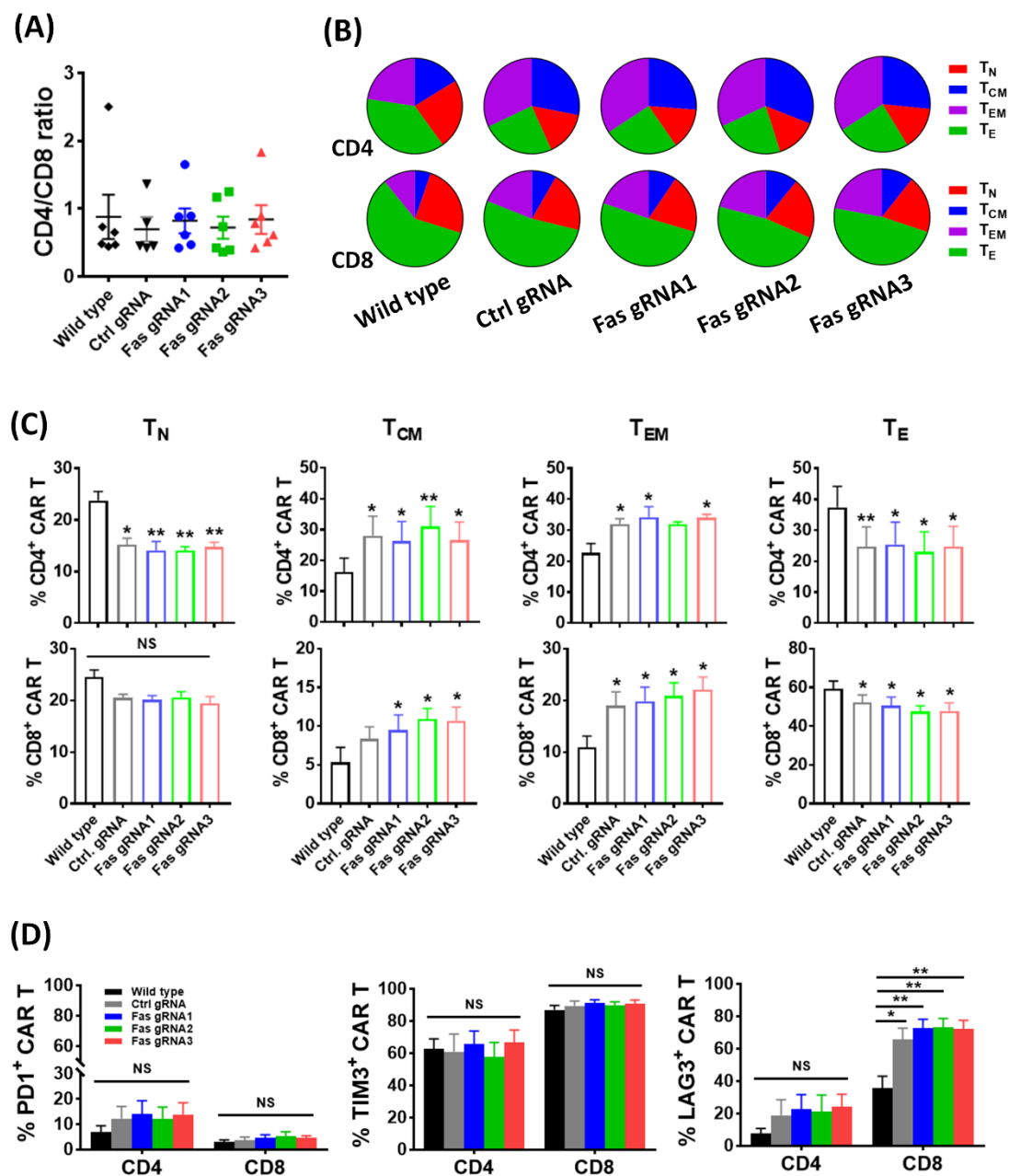
**Figure 3.8 Phenotypic analysis of CD95 (Fas) knockout CD19.CAR T cells.**

(A) $CD4^+$ and $CD8^+$ T cell subpopulations were analyzed in wild type and gene-disrupted CAR T cells transfected with either control gRNA, Fas gRNA1, Fas gRNA2 or Fas gRNA3 by electroporation. Immunophenotypic profiles such as naïve T ($T_N$, $CD45RA^+$ $CCR7^+$), central memory T ($T_{CM}$, $CD45RA^-$ $CCR7^+$), effector memory T ($T_{EM}$, $CD45RA^-$ $CCR7^-$) and effector T cells ($T_E$, $CD45RA^+$ $CCR7^-$) of Fas KO CAR T cells and WT CAR T cells were shown as pie charts (B) and histograms (C). (D) Exhaustion markers PD1, TIM3 and LAG3 were analyzed within wild type and gene-disrupted CAR T cells by flow cytometry. Mean values were calculated for each group (n = 6); error bars indicate standard error deviation. vs. wild type, *, $P < 0.05$; **, $P < 0.01$; ***, $P < 0.001$; NS, no significant difference.

## 3.9 CD95L-mediated apoptosis is prevented in Fas KO CAR T cells.

Further, the T cell function of these Fas KO CAR T cells was determined. WT or Fas KO CD19.CAR T cells were stimulated with CD19 positive Nalm6 as target cells at the E:T ratio of 2:1 for 4h and then harvested for intracellular TNF-α and IFN-γ staining, as well as the degranulation marker CD107a. No significant difference was observed among Fas KO CAR T cells and WT CAR T cells in terms of expression of TNF-α, IFN-γ and CD107a (Figure 3.9 A). Subsequently, in order to test their susceptibility to CD95L-induced apoptosis, WT or Fas KO CAR T cells were incubated with 100 ng/ml recombinant CD95L protein for 24 hours. The Fas expressing CAR T cells WT CAR T cells as well as control CAR T cells were highly sensitive to CD95L mediated apoptosis, as confirmed by the increase of apoptotic cells in the presence of CD95L protein (Figure 3.9 B). However, Fas KO CAR T cells were resistant to this CD95L-mediated apoptosis, due to a lack of the binding partner CD95. Thus, these data indicated that knockout of Fas in CAR T cells did not impair their cytokine production, and was able to protect them from CD95L-mediated apoptosis.
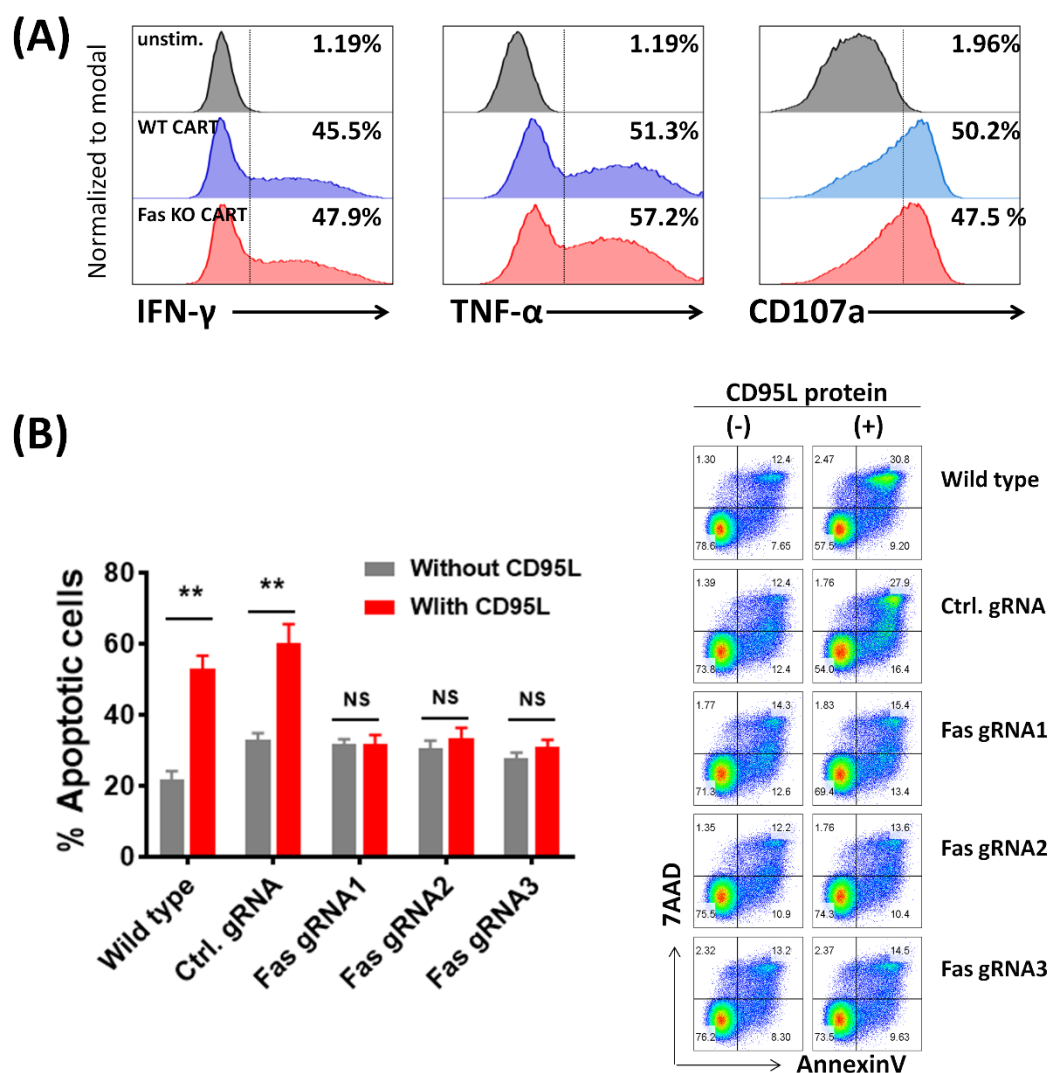
**Figure 3.9 Fas KO CAR T cells are resistant to CD95L-mediated apoptosis.**

(A) WT or Fas KO CD19.CAR T cells transfected with Fas gRNA 1 were stimulated with CD19 positive target cells Nalm6 at 2:1 E:T ratio for 4h and then harvested for intracellular TNF-α and IFN-γ staining, as well as degranulation marker CD107a. WT CAR T cells without antigen stimulation were used as control. (B) WT or Fas KO CAR T cells were incubated with or without 100 ng/ml recombinant CD95L protein for 24 hours and then stained with Annexin V and 7-AAD for apoptosis analysis. Summary plot and representative FACS dot plots are shown. Mean values were calculated for each group (n = 6); error bars indicate standard error deviation *, $P < 0.05$; **, $P < 0.01$; ***, $P < 0.001$; NS, no significant difference.

## 3.10 Fas knockout CAR T cells show better persistence upon repetitive antigen stimulation.

To assess whether Fas KO CAR T cells show better survival upon repeated tumor stimulation, WT CAR T or gene edited CAR T cells ($1 \times 10^5$) were co-cultured with target cells Nalm6 for 6 days at the E:T ratio of 1:4. Fas KO CAR T cell number were dramatically increased from day 3 to day 5 and stabilized on day 6 of coculture, whereas expansion level of WT CAR T and control CAR T cells was moderate (Figure 3.10 A). By the end of the co-culture on day 6, Fas KO CAR T cells transfected with Fas gRNA 1, 2, 3 were expanded over 9-fold, 14-fold, 11-fold, respectively, compared with 2-fold expansion for both WT CAR T cells and control CAR T cells. No statistical differences were found among the 3 different Fas KO CAR T cells on day 6. Moreover, the Fas negative population within Fas KO CAR T cells significantly increased comparing the time-points before and after co-culture. This phenomenon was not found in WT CAR T and control CAR T cells (Figure 3.10 B), suggesting that Fas negative CAR T cells were resistant to AICD in CAR T cells. In fact, the enhanced persistence of Fas KO CAR T cells was attributed to the reduction of AICD in Fas KO CAR T cells, as a reduction of cell death was observed for the Fas KO CAR T cells that were repetitively challenged by Nalm6 cells (Figure 3.10 C). Additionally, the phenotype of the CAR T cells after co-culture with Nalm6 was analyzed on day 6. CD4/CD8 ratio of WT CAR T cells was comparable to that of gene-disrupted CAR T (Figure 3.10 D). A similar distribution of T cell subsets, like $T_N$, $T_{CM}$, $T_{EM}$ and $T_E$, was found in WT and gene-disrupted CAR T cells (Figure 3.10 E). However, a significantly higher percentage of $CD4^+$ $T_{CM}$ was found in Fas KO CAR T cells but not in control CAR T cells when compared to WT CAR T cells. In contrast, the proportion of $CD4^+$ $T_E$ in Fas KO CAR T cells was significantly lower, as compared to WT CAR T cells. No significant difference of $CD4^+$ $T_N$ and $T_{EM}$ were found among gene-disrupted CAR T and WT CAR T cells. For $CD8^+$ CAR T cells, Fas KO CAR T had a significantly lower percentage of $T_E$ ($P < 0.05$) and a higher percentage of $T_{EM}$ ($P > 0.05$) compared with WT CAR T cells. The proportion of

CD8$^+$ T$_N$ and T$_{CM}$ did not show any difference among Fas KO CAR T cells and WT CAR T cells. Together, knockout of Fas in CAR T cells prevented CAR T cells from undergoing AICD and thus enhanced their survival upon repetitive tumor stimulation.
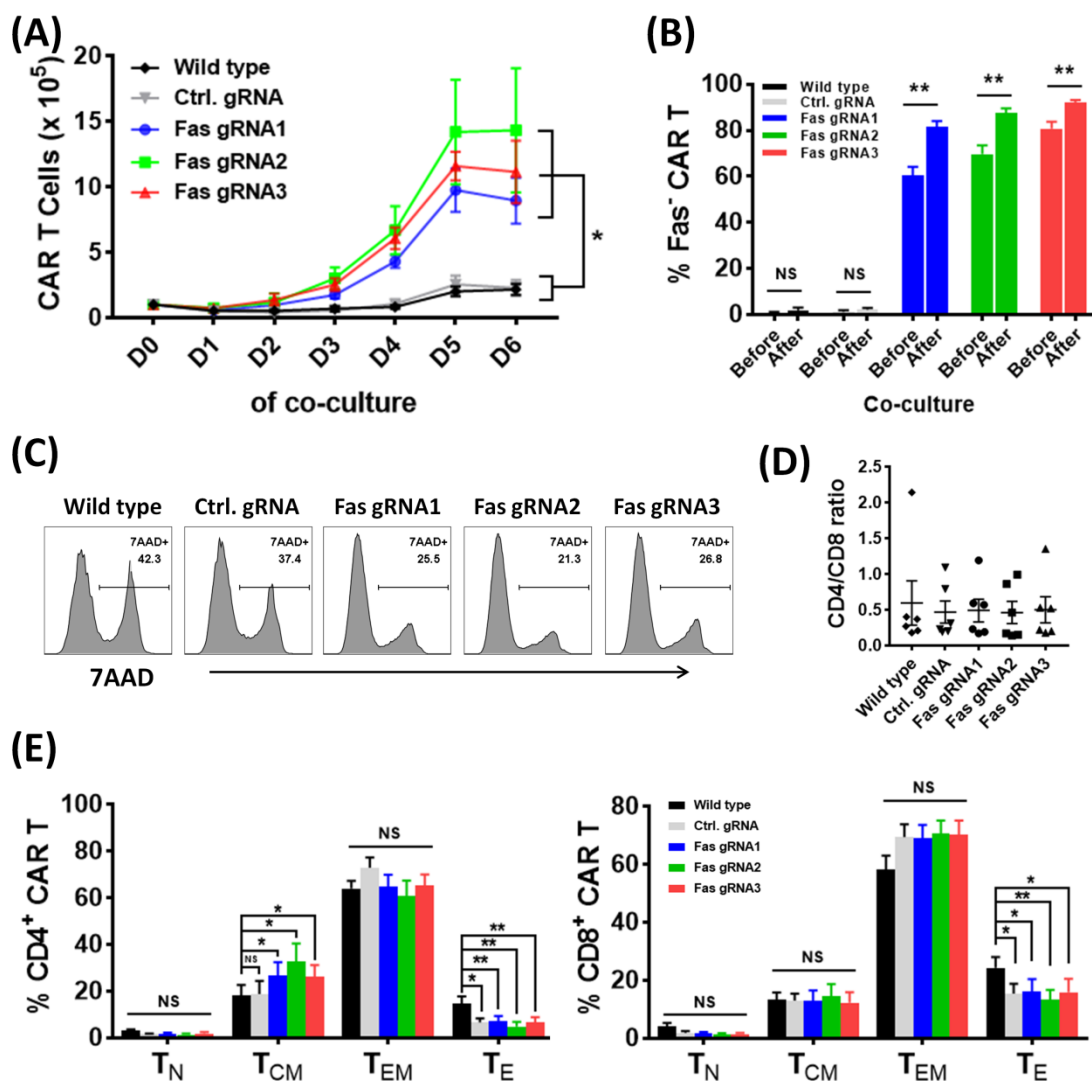


**Figure 3.10 Fas KO CAR T cells show better persistence upon repetitive antigen stimulation.**

(A) WT or gene-disrupted CAR T cells (1 x 10$^5$) were re-stimulated with CD19$^+$ target cells Nalm6 at 1:4 E:T ratio for 6 days, the absolute number of viable CAR T cells were assessed by flow cytometry from day 1 to day 6. (B) Fas expression on CAR T cells before or after co-culture (6 days) were measured by flow cytometry. (C) Dead CAR T cells on day 6 of co-culture were analyzed by staining with 7AAD. Representative FACS histograms were shown (n=6). (D) The ratio of CD4/CD8 in different CAR T cells were analyzed on day 6. (E) Phenotype profiles like Naïve-like (T$_N$, CD45RA$^+$ CCR7$^+$), central memory (T$_{CM}$, CD45RA$^-$ CCR7$^+$), effector memory (T$_{EM}$, CD45RA$^-$ CCR7$^-$) and effector (T$_E$, CD45RA$^+$ CCR7$^-$) subsets of Fas KO CAR T cells and WT CAR T cells were analyzed on day 6. Mean values were calculated for each group (n = 6).

## 3.11 Fas knockout CD19.CAR T cells exhibits superior killing efficiency against CD19^{+} leukemia cells.

Having established that knockout of Fas in CAR T cells results in enhanced persistence, the antitumor efficacy of these cells was evaluated. WT CAR T or gene edited CAR T cells (1 x 10$^5$) were daily stimulated with Nalm6 GFP cells (4 x 10$^5$). After 6 days of re-stimulation, the residual Nalm6 GFP cells were counted using absolute counting beads by flow cytometry. No significant difference of residual tumor cells on day 1 and day 2 were found after coculture with WT or gene-disrupted CAR T cells. CAR T cells engineered with Fas gRNAs showed better control of tumor cells starting from day 3 of co-culture, as significantly lower numbers of Nalm6 GFP cells were found after coculture with Fas KO CAR T cells compared with WT or control CAR T cells (Figure 3.11 A). After 6 days of coculture, the percentage and absolute number of residual Nalm6 GFP cells were lower in the coculture with Fas KO CAR T cells (Figure 3.11 A, C). The killing efficacy from control engineered CAR T cells did not differ from WT CAR T cells. It was reported that repetitive stimulation often drives T cell exhausted and lose their antitumor activity. Thus, we also analyzed the exhaustion marker PD1 on CAR T cells after repeated stimulation with tumor cells. An enhanced antitumor activity mediated by Fas KO CAR T cells did not result in T cell exhaustion in this study. In contrast, lower level of PD1 was found in CD4$^+$ and CD8$^+$ CAR T cells engineered with Fas gRNAs (Figure 3.11 B). In addition, cytokine production of CAR T cells were also detected after being co-cultured with target Nalm6 cells for 6 days (Figure 3.11 D). Interferon gamma (IFN-γ) and tumor necrosis factor (TNF), key cytokines for effector cell function, were significantly higher in Fas KO CAR T cells than in WT or control CAR T cells. Fas KO CAR T cells produced lower level of IL-2 compared with WT and control CAR T cells, but there was no statistical difference ($P > 0.05$). IL-6, a major cytokine for cytokine released syndromes (CRS), was not increased by Fas KO CAR T cells ($P > 0.05$). The production of IL-4, IL-10 and IL-17A were low and comparable among WT and gene-disrupted CAR T cells ($P > 0.05$). These data

indicated that Fas KO CD19.CAR T cells showed enhanced antitumor activity against CD19+ Naml6 cells.
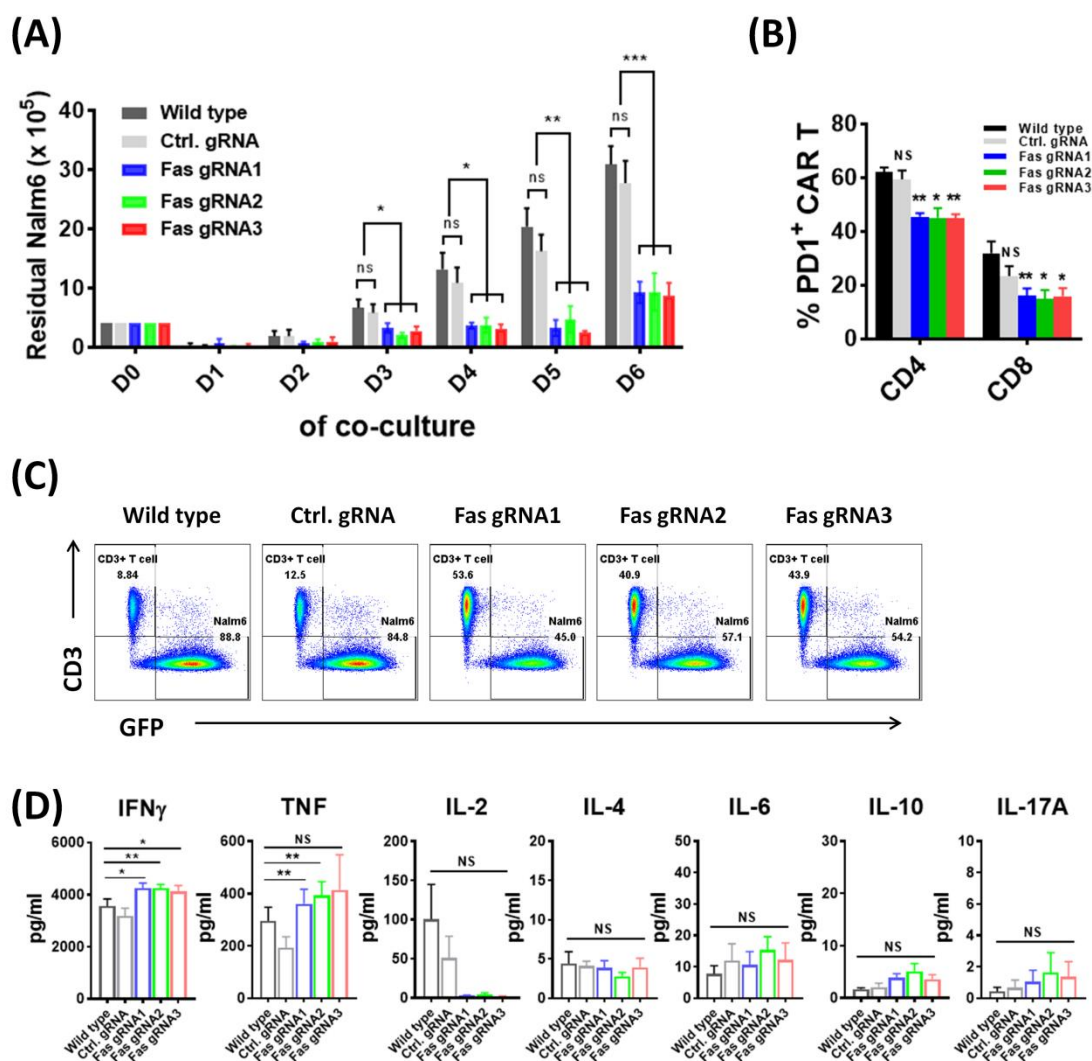


**Figure 3.11 Fas KO CAR T cells exhibit superior killing efficiency.**
(A) WT or gene-disrupted CD19.CAR T cells ($1 \times 10^5$) were re-stimulated with CD19 positive target cells Nalm6 at 1:4 E:T ratio for 6 days, the absolute number of viable Nalm6 GFP cells were assessed by flow cytometry. (B) Expression of PD1 on CAR T cells were analyzed on day 6 by flow cytometry. (C) The percentage of residual Nalm6 GFP cells on day 6 after coculture with WT or gene-disrupted CAR T cells. FACS dot plots were the representative data of 6 independent healthy donors. (D) Cytokine secretion in the coculture supernatant was measured by flow cytometry after 6 days of coculture. Mean values were calculated for each group (n = 6); error bars indicate standard error deviation *, $P < 0.05$; **, $P < 0.01$; ***, $P < 0.001$; NS, no significant difference.

# 4 DISCUSSION

Despite the encouraging outcome of anti-CD19 chimeric antigen receptor T (CAR T) cell therapy in patients with B cell malignancies, *in vivo* CAR T cell persistence remains a major clinical challenge (Schultz and Mackall 2019). In this study, it was demonstrated that CAR T cells highly express the death receptor CD95, which might be sensitive to CD95L-mediated apoptosis and thus impair CAR T cell persistence and anti-tumor efficacy. Thus, inhibition of CD95-CD95L signaling pathway might be a therapeutic option for improving CD19.CAR T cell persistence and might lead to durable clinical responses in patients with B cell malignancies after CD19.CAR T cell therapy. CAR design orchestrates CAR T cell expansion and persistence. To date, second-generation CARs, incorporating a CD3-ζ signal domain and a costimulatory domain (typically CD28 or 4-1BB), are the most common constructs in clinical application. The costimulatory domains bias CAR T cell kinetics. CD28 induces rapid expansion of CAR T cells and better functionality, but this is associated with limited CAR T cell persistence, while 4-1BB confers moderate expansion and prolonged persistence of CAR T cells (Zhao et al. 2015). Third-generation CD19.CAR T cells containing both, the CD28 and the 4-1BB domain have shown superior expansion and longer persistence than second-generation CD19.CAR T cells (Ramos et al. 2018). The safety and favorable outcome of third-generation CD19.CAR T cell therapy in relapsed B cell malignancies has also been proven by the HD-CAR-1 phase I/II clinical trial conducted by our lab (NCT03676504, (Schubert et al. 2019)). Thus, third-generation RV-SFG.CD19.CD28.4-1BB.CD3zeta CAR vector which is well established in our institution was used to produce CD19.CAR T cells for the present study.

In this study, we found that third-generation CD19.CAR T cells generated from healthy donors express high levels of CD95 and are susceptible to CD95L-mediated cell death. Despite the fact that about 57 % freshly isolated peripheral blood T cells express Fas, these cells are not sensitive to CD95L-mediated cell death. The expression of CD95 was rapidly induced in normal T cells upon activation *in vitro*.

Thus, CAR T cells had a high expression level of CD95 due to the activation by anti-CD3 and -CD28 antibodies before transduction with CD19.CAR retroviral vector.

Next, it was investigated whether a blockade of CD95-CD95L signaling by the CD95L inhibitor APG101 would protect the CAR T cells from CD95L-mediated cell death. APG101 (Asunercept ®), is a human fusion protein consisting of the extracellular domain of human CD95 and Fc domain of human IgG antibody. APG101 specifically binds to CD95L and thus blocks CD95/CD95L signaling (Tuettenberg et al. 2012). Apoptosis of CAR T cells induced through CD95L protein could be completely inhibited by APG101. Given that APG101 can effectively block the CD95-CD95L signaling in CD95$^+$ CAR T cells, it was evaluated whether addition of APG101 could optimize culture of CAR T cells. However, APG101 did not increase the viability and expansion of CAR T cells during the cultivation, due to very low levels of CD95L on CAR T cells *ex vivo*.

**CAR constructs and AICD**

Our second aim was to investigate whether the CD19-specific CAR T cells experience activation induce cell death (AICD) upon *in vitro* tumor stimulation, as has been reported in CD171-specific CAR T cells by others (Kunkele et al. 2015). Third-generation CARs have been previously reported to be more prone to AICD due to the potent stimulation induced via signaling domains (Gargett et al. 2016). Künkele *et al*. demonstrated that third-generation CD171-specific CAR (CD28 and 4-1BB) promoted enhanced levels of cytolytic activity as well as CAR T cell apoptosis compared with the second-generation CD171.CAR (4-1BB) upon *in vitro* tumor stimulation (Künkele et al. 2015). However, Hombach and Abken reported that OX40 costimulation alone or in combination with CD28 prevented apoptosis of CD62L$^-$ CAR T cells most efficiently whereas 4-1BB or CD28 costimulation was less effective (Hombach and Abken 2011). Thus, the susceptibility of AICD in CAR T cells is more probably dependent on their specific costimulatory domains rather than

the number of domains.

**The role of APG101 with third generation CD19.CAR T cells**

Using the *in vitro* antigen "stress-test" assay, we found repeated antigenic stimulation promoted CD95L expression including mCD95L and sCD95L in CD19.CAR T cells and resulted in AICD of CD19.CAR T cells, as indicated by increasing CAR T cells undergoing apoptosis following serial tumor stimulation. Addition of APG101 significantly protected CAR T cells from AICD via blockade of CD95-CD95L signaling within CAR T cells. Importantly, APG101 did not hamper the activation and proliferation of CAR T cells but was able to preserve CAR T cells. Exhaustion markers like PD1, TIM3 and LAG3 were also up-regulated in CAR T cells upon stimulation with tumors. PD1 is a well-known immune checkpoint that is induced by T-cell activation and involved in T-cell exhaustion (Zarour 2016). In contrast to the report in CD2-specific CAR T cells (Gargett et al. 2016), PD1 was not involved in CD19.CAR T cell apoptosis as the anti-PD1 antibody pembrolizumab failed to prevent apoptosis of CD19.CAR T cells in our study. APG101 did not affect the surface CD95 expression as well as exhaustion markers PD1, TIM3 and LAG3 expression, but increased the level of soluble CD95L which cleaved from cell surface by metalloproteases upon activation. It has been reported that sCD95L can bind to CD95 but cannot induce apoptosis, thus competitively inhibiting the function of membrane-bound CD95L on T cells (Suda et al. 1997). This was confirmed by no induction of apoptosis on CAR T cell after incubated with sCD95L enriched co-culture supernatant. Engagement of mCD95 with CD95 promotes the recruitment of adaptor protein FADD and pro-caspase-8 and leads to the activation of caspase-8 and caspase-3, which finally induces apoptosis of CD95 expressing T cells (Green and Ferguson 2001). APG101 decreased levels of active caspase-8 in CAR T cells, indicating that APG101 protects CD19.CAR T cells from AICD through disruption of CD95-CD95L signaling.

Based on the above observations, a long-term co-culture assay was used to assess

the *in vitro* survival of CD19.CAR T cells after repeatedly exposed to CD19$^+$ B-ALL cell line Nalm6 cells in the presence of APG101 for 6 days. Addition of APG101 to the co-culture resulted in a significant increase of CAR T cells with an effector memory phenotype. The enhanced survival of CAR T cells after tumor stimulation was attributed to the reduction of AICD on CAR T cells mediated by APG101, resulting in better controlled of tumor cells Nalm6 during the long-term co-culture assay. We found that the enhanced anti-tumor efficacy in the context of APG101 was more pronounced in CAR T cells under high tumor burden, as indicated by comparison of 3 different effector to target (E:T) ratio at the co-culture system. Of note, APG101 alone has no cytotoxic effect on tumor cell Nalm6. The enhanced anti-leukemia efficacy of CAR T cells mediated by APG101 was CD19 antigen dependent, because these effects were also observed in the co-culture of CAR T cells with CD19$^+$ Daudi cells but not CD19$^-$ K562 cells. CD95L blockade also promoted CAR T cell cytokine production including TNF and IFN-γ, as well as IL-10 which has been shown to enhance antitumor CD8$^+$ T-cell responses by promoting CLT persistence in tumor models (Wang et al. 2015). IL-6, a major cytokine for the cytokine released syndrome (CRS), was not increased by APG101. Collectively, these data suggest that CD95 positive CD19.CAR T cells are sensitive to CD95L-mediated cell death, and CD95L blockade by APG101 enhanced CAR T cell survival and promoted killing of tumor cells *in vitro*.

**Fas knockout by CRISPR-Cas9**

CD95 (also known as Fas) is a critical effector for initiating the extrinsic apoptotic signaling cascade, thus genetically knockout of CD95 in CAR T cells was performed to understand whether disruption of CD95/CD95L signaling makes CAR T cells resistant to CD95L-mediated apoptosis. Down-modulation of Fas using a short hairpin RNA approach has been reported in human T cells, but showed relatively poor efficiency of Fas knockdown (Dotti et al. 2005). The CRISPR-Cas9 system is a widely used genome engineering tool for gene knockout (Shalem et al. 2014). Gene

targeting in T cells with lentiviral and adenoviral delivery of CRISPR has low efficiency due to limited transduction rates of Cas9 and gRNA (Li et al. 2015; Wang et al. 2014). In this work, the delivery of CRISPR-Cas9 system via electroporation provides an efficient platform for gene knockout in CD19.CAR T cells. Fas knockout CAR T cells were successfully generated with high efficiency using CRISPR-Cas9 and the cell viability and CAR expression were not changed during *in vitro* culture. Knockout of Fas in CAR T cells resulted in a memory-like T cell phenotype, characterized by a higher fraction of $T_{CM}$ and $T_{EM}$, as well as an increased level of LAG3. However, this effect is probably caused by electroporation given that this feature was also observed in CAR T cells electroporated with Cas9 and control gRNA. Zhang *et al*. also reported that LAG3 knockout CD19.CAR T cells displayed a CD4$^+$ central memory T cell phenotype which is similar to T cells receiving electroporation without Cas9 RNP (Zhang et al. 2017). As expected, Fas disrupted CAR T cells were resistant to apoptosis induced by CD95L protein, unlike WT CAR T and control CAR T cells.

In this study, knockout (KO) of Fas in CAR T cells prevented CAR T cells from undergoing AICD and thus improved their survival upon repetitive tumor stimulation. Moreover, Fas negative population within unselected Fas KO CAR T cells were increased after co-cuture with tumor cells, suggesting a selective advantage for Fas negative CAR T cells upon tumor stimulation. After repetitively being challenged by target tumor cells, Fas KO CAR T cells displayed an effector memory T cell phenotype similar to WT CAR T cells, but associated with an increase of CD4$^+$ central memory T cell subset. It has been reported that central memory T cells confer superior antitumor immunity compared with effector memory T cells (Klebanoff et al. 2005). The killing mechanisms of CAR T cells include: tumor cell lysis by granzyme and perforin, a cytokine-induced killing mechanism, and Fas/FasL pathway associated tumor cell lysis (Benmebarek et al. 2019). Thus, it was evaluated whether disruption of Fas in CD19.CAR T cells would impair their antitumor activity. In this study, knockout of CD95 in CD19.CAR T cells did not impair their killing ability,

suggesting that Fas-FasL killing might not be a major axis by which target cells are lysed by CD19.CAR T cells. Conversely, disruption of Fas in CD19.CAR T cells exhibited superior killing efficiency against CD19$^+$ tumor cells and better contolled of target tumor cells in the long-term. Although tumor cell lysis by CAR T cells is based on the direct T cell-tumor cell interactions, cytokine production by activated CAR T cells could further enhance their anti-tumoral capabilities (Benmebarek et al. 2019). Fas KO CAR T cells produced significantly higher levels of IFN-γ and TNF, key cytokines for effector cell function, compared with wildtype CAR T and control CAR T cells.

Genetic disruption of Fas/FasL signling in adoptive transfered T cells has also been reported by others (Ren et al. 2017; Zhu et al. 2019), and demonstrated Fas/FasL could be a potential therapeutic target for increasing the efficacy of adoptive T cell therapy (ACT). Ren *et al*. have reported that Fas-resistant CAR T cells via a one-shot CRISPR protocol by incorporation of Fas gRNA in a CAR lentiviral vector, exhibited elevation of AICD resistance and prolonged survival when the CAR T cells were challenged with target tumor cells *in vitro* and *in vivo* (Ren et al. 2017). Yamamoto *et al*. developed Fas dominant negative receptors (DNRs) that intrinsically abrogate the apoptosis-inducing functions of Fas/FasL pathway in CAR T cells, resulting in enhanced *in vivo* cellular persistence and augmented antitumor efficacy in murine models (Yamamoto et al. 2019). However, using genetic engineering approaches to disrupt the Fas/FasL signaling could increase the risk of systemic toxicities, which have been reported by others (Cohen and Eisenberg 1991). Mice with germline defects in Fas or FasL can develop profound alterations in normal lymphocyte homeostasis and development, resulting in autoimmune lymphoproliferative syndrome (ALPS) with impaired survival (Cohen and Eisenberg 1991). ALPS is a well characterized human genetic diseases of apoptosis and germline Fas mutations accounting for the majority of ALPS cases (Rao and Oliveira 2011). Furthermore, application of Fas-engineered CAR T cell therapy has the potential to elicit unexpected toxicities including CRS and neurologic toxicity, due to a lack

of control of the highly potent CAR T cells with greater persistence *in vivo*. Preclinical data has shown that cell-extrinsic approaches can also improve the persistence of adoptively transferred T cells through blockade of Fas/FasL signaling, including usage of anti-FasL antibody or soluble form of Fas (Fas-Fc) (Lakins et al. 2018; Motz et al. 2014; Zhu et al. 2017). However, none of them has been tested in clinical trials for evaluation of the safty and efficiency of neutralizing the Fas–FasL pathway. APG101 (Asunercept ®), a soluble CD95-Fc fusion protein which has been used for treating patients with glioblastoma and MDS in the EU (Boch et al. 2018; Wick et al. 2014), has been found to protect CD19.CAR T cells from CD95L-mediated apoptosis and exhibited enhanced survival upon repetitively challenged by tumor cells. Further investigations are needed to define the *in vivo* antitumor capacity of CAR T cells combined with APG101 treatment.

In conclusion, disruption of CD95-CD95L pathway in CD19.CAR T cells through pharmacologic and genetic approaches prevents CAR T cells from CD95L-mediated apoptosis and improves their persistence, resulting in enhanced antitumor efficacy of these CAR T cells. Thus, combining CAR T cell therapy with CD95L inhibitor might improve CAR T cell persistence *in vivo* and thus augments/amplifies the effect of CAR T cell therapy in patients with relapsed or refractory hematologic malignancies.

# 5 SUMMARY

Despite the encouraging outcome of anti-CD19 chimeric antigen receptor T (CAR T) cell therapy in patients with B cell malignancies, CAR T cell persistence remains a major clinical challenge. CAR T cells highly express death receptor CD95 (also known as Fas), which might be sensitive to CD95L-mediated apoptosis and thus impair CAR T cell persistence. Therefore, in this thesis, it was investigated whether disruption of CD95-CD95L signaling within CAR T cells would prevent CAR T cells from CD95L-mediated apoptosis and improve their persistence.

In this study, third-generation CD19.CAR T cells generated from healthy donors expressed high levels of CD95 and were susceptible to CD95L-mediated cell death. CD95 ligand (CD95L) was also expressed on CAR T cells upon tumor stimulation, resulting in activation-induced cell death in CAR T cells via binding to CD95 receptor. The CD95L inhibitor APG101, a soluble CD95-Fc fusion protein, protected CAR T cells from activation-induced cell death through blockade of the CD95-CD95L pathway. CD95L blockade enhanced the survival of CAR T cells after repetitively being challenged by CD19 expressing target tumor cell lines, and promoted killing of tumor cells *in vitro*. In addition, Fas knockout CD19.CAR T cells generated via electroporation-based CRISPR-Cas9 displayed high targeted efficiency and were resistant to CD95L-mediated apoptosis. Moreover, Fas knockout CD19.CAR T cells exhibited prolonged persistence upon repeated antigen stimulation and superior killing efficiency against CD19$^+$ tumor cells.

In conclusion, disruption of the CD95-CD95L pathway in CD19.CAR T cells through pharmacologic and genetic approaches prevents CAR T cells from CD95L-mediated apoptosis and improves their persistence, resulting in enhanced antitumor efficacy of these CAR T cells. Thus, combining CAR T cell therapy with CD95L inhibitor might improve CAR T cell persistence *in vivo* and thus enhance the effect of CAR T cell therapy in patients with relapsed or refractory hematologic malignancies.

# 6 ZUSAMMENFASSUNG

Trotz der ermutigenden Ergebnisse der anti-CD19 chimären Antigenrezeptor T-Zelltherapie (CAR T) bei Patienten mit B-Zell-Malignomen bleibt die Persistenz der CAR T-Zellen eine große klinische Herausforderung. CAR T-Zellen exprimieren in hohem Maße den Todesrezeptor CD95 (auch bekannt als Fas), der über eine CD95L-vermittelte Apoptose die Persistenz der CAR T-Zellen beeinträchtigen könnte. Daher wurde in dieser Arbeit untersucht, ob eine Blockierung des CD95-CD95L Signalwegs innerhalb der CAR T-Zellen die CD95L-vermittelte Apoptose verhindern und so ihre Persistenz verbessern kann.

In dieser Studie wurden CD19.CAR T-Zellen der dritten Generation von gesunden Spendern generiert. Diese CAR T-Zellen zeigten eine hohe CD95-Expression und waren suszeptibel für den CD95L-vermittelten Zelltod. Der CD95-Ligand (CD95L) wurde auf CAR-T-Zellen nach Stimulation mit Tumorzellen exprimiert, was über die Bindung an den CD95-Rezeptor zum aktivierungsinduzierten Zelltod in CAR-T-Zellen führte. Der CD95L-Inhibitor APG101, ein lösliches CD95-Fc-Fusionsprotein, schützte CAR-T-Zellen vor aktivierungsinduziertem Zelltod durch Blockade des CD95-CD95L-Signalwegs. Die CD95L-Blockade erhöhte das Überleben der CAR T-Zellen nach wiederholter Kokultur mit CD19-positiven Tumorzellen und förderte die Elimination von Tumorzellen *in vitro*. In einem weiteren Schritt wurden Fas-knockout-CD19.CAR-T-Zellen mittels Elektroporation auf Basis von CRISPR-Cas9 mit hoher Knockout-Effizienz generiert. Diese CD95-knockout CAR T-Zellen waren resistent gegen CD95L-vermittelte Apoptose. Darüber hinaus zeigten Fas-knockout CD19.CAR T-Zellen gegenüber CD19.CAR T-Zellen ohne Knockout eine verlängerte Persistenz bei wiederholter Antigenstimulation und eine überlegene Zytotoxizität gegen CD19^{+} Tumorzellen.

Insgesamt verhindert die Blockade des CD95-CD95L-Signalwegs in CD19.CAR T-Zellen durch pharmakologische und genetische Ansätze die CD95L-vermittelte Apoptose der CAR T-Zellen und verbessert ihre Persistenz, was zu einer erhöhten

Antitumor-Wirksamkeit dieser CAR T-Zellen führt. Somit könnte die Kombination der CAR T-Zelltherapie mit einem CD95L-Inhibitor die Persistenz der CAR T-Zellen *in vivo* verbessern und damit die Wirkung der CAR T-Zelltherapie bei Patienten mit rezidivierten oder refraktären hämatologischen Neoplasien verstärken.

# 7 REFERENCES

Abbasi, A., Peeke, S., Shah, N., Mustafa, J., Khatun, F., Lombardo, A., Abreu, M., Elkind, R., Fehn, K., de Castro, A., Wang, Y., Derman, O., Nelson, R., Uehlinger, J., Gritsman, K., Sica, R. A., Kornblum, N., Mantzaris, I., Shastri, A., Janakiram, M., Goldfinger, M., Verma, A., Braunschweig, I. and Bachier-Rodriguez, L. (2020). **Axicabtagene ciloleucel CD19 CAR-T cell therapy results in high rates of systemic and neurologic remissions in ten patients with refractory large B cell lymphoma including two with HIV and viral hepatitis**. J Hematol Oncol *13 (1)*, 1, doi: 10.1186/s13045-019-0838-y.

Abramson, J. S., Palomba, M. L., Gordon, L. I., Lunning, M. A., Wang, M., Arnason, J. E., Mehta, A., Purev, E., Maloney, D. G. and Andreadis, C. (2020). **Safety and Efficacy Results from Transcend NHL 001, a Multicenter Phase 1 Study of Lisocabtagene Maraleucel (liso-cel) in Relapsed/Refractory (R/R) Large B-Cell Lymphoma (LBCL)**. Paper presented at: 2020 TCT| Transplantation & Cellular Therapy Meetings of ASTCT and CIBMTR (TCT Meetings).

Allemani, C., Matsuda, T., Di Carlo, V., Harewood, R., Matz, M., Niksic, M., Bonaventure, A., Valkov, M., Johnson, C. J., Esteve, J., Ogunbiyi, O. J., Azevedo, E. S. G., Chen, W. Q., Eser, S., Engholm, G., Stiller, C. A., Monnereau, A., Woods, R. R., Visser, O., Lim, G. H., Aitken, J., Weir, H. K., Coleman, M. P. and Group, C. W. (2018). **Global surveillance of trends in cancer survival 2000-14 (CONCORD-3): analysis of individual records for 37 513 025 patients diagnosed with one of 18 cancers from 322 population-based registries in 71 countries**. Lancet *391 (10125)*, 1023-1075, doi: 10.1016/S0140-6736(17)33326-3.

Benmebarek, M. R., Karches, C. H., Cadilha, B. L., Lesch, S., Endres, S. and Kobold, S. (2019). **Killing Mechanisms of Chimeric Antigen Receptor (CAR) T Cells**. Int J Mol Sci *20 (6)*, doi: 10.3390/ijms20061283.

Blaes, J., Thome, C. M., Pfenning, P. N., Rubmann, P., Sahm, F., Wick, A., Bunse, T., Schmenger, T., Sykora, J., von Deimling, A., Wiestler, B., Merz, C., Jugold, M., Haberkorn, U., Abdollahi, A., Debus, J., Gieffers, C., Kunz, C., Bendszus, M., Kluge, M., Platten, M., Fricke, H., Wick, W. and Lemke, D. (2018). **Inhibition of CD95/CD95L (FAS/FASLG) Signaling with APG101 Prevents Invasion and Enhances Radiation Therapy for Glioblastoma**. Mol Cancer Res *16 (5)*, 767-776, doi: 10.1158/1541-7786.MCR-17-0563.

Blaeschke, F., Stenger, D., Kaeuferle, T., Willier, S., Lotfi, R., Kaiser, A. D., Assenmacher, M., Doring, M., Feucht, J. and Feuchtinger, T. (2018). **Induction of a central memory and stem cell memory phenotype in functionally active CD4(+) and CD8(+) CAR T cells produced in an automated good manufacturing practice system for the treatment of CD19(+) acute lymphoblastic leukemia**. Cancer Immunol Immunother *67 (7)*, 1053-1066, doi: 10.1007/s00262-018-2155-7.

Boch, T., Luft, T., Metzgeroth, G., Mossner, M., Jann, J. C., Nowak, D., Meir, F., Schumann, C., Klemmer, J., Brendel, S., Fricke, H., Kunz, C., Weiss, C., Hofmann, W. K. and Nolte, F.

(2018). **Safety and efficacy of the CD95-ligand inhibitor asunercept in transfusion-dependent patients with low and intermediate risk MDS**. Leuk Res *68*, 62-69, doi: 10.1016/j.leukres.2018.03.007.

Bray, F., Ferlay, J., Soerjomataram, I., Siegel, R. L., Torre, L. A. and Jemal, A. (2018). **Global cancer statistics 2018: GLOBOCAN estimates of incidence and mortality worldwide for 36 cancers in 185 countries**. CA Cancer J Clin *68 (6)*, 394-424, doi: 10.3322/caac.21492.

Cheng, J., Zhao, L., Zhang, Y., Qin, Y., Guan, Y., Zhang, T., Liu, C. and Zhou, J. (2019). **Understanding the Mechanisms of Resistance to CAR T-Cell Therapy in Malignancies**. Front Oncol *9*, 1237, doi: 10.3389/fonc.2019.01237.

Chmielewski, M. and Abken, H. (2015). **TRUCKs: the fourth generation of CARs**. Expert Opin Biol Ther *15 (8)*, 1145-1154, doi: 10.1517/14712598.2015.1046430.

Chmielewski, M. and Abken, H. (2020). **TRUCKS, the fourth-generation CAR T cells: Current developments and clinical translation**. Advances in Cell and Gene Therapy *3 (3)*, doi: 10.1002/acg2.84.

Cohen, P. L. and Eisenberg, R. A. (1991). **Lpr and gld: single gene models of systemic autoimmunity and lymphoproliferative disease**. Annu Rev Immunol *9*, 243-269, doi: 10.1146/annurev.iy.09.040191.001331.

Cong, L., Ran, F. A., Cox, D., Lin, S., Barretto, R., Habib, N., Hsu, P. D., Wu, X., Jiang, W., Marraffini, L. A. and Zhang, F. (2013). **Multiplex genome engineering using CRISPR/Cas systems**. Science *339 (6121)*, 819-823, doi: 10.1126/science.1231143.

Crump, M., Neelapu, S. S., Farooq, U., Van Den Neste, E., Kuruvilla, J., Westin, J., Link, B. K., Hay, A., Cerhan, J. R., Zhu, L., Boussetta, S., Feng, L., Maurer, M. J., Navale, L., Wiezorek, J., Go, W. Y. and Gisselbrecht, C. (2017). **Outcomes in refractory diffuse large B-cell lymphoma: results from the international SCHOLAR-1 study**. Blood *130 (16)*, 1800-1808, doi: 10.1182/blood-2017-03-769620.

Dotti, G., Savoldo, B., Pule, M., Straathof, K. C., Biagi, E., Yvon, E., Vigouroux, S., Brenner, M. K. and Rooney, C. M. (2005). **Human cytotoxic T lymphocytes with reduced sensitivity to Fas-induced apoptosis**. Blood *105 (12)*, 4677-4684, doi: 10.1182/blood-2004-08-3337.

Enblad, G., Karlsson, H., Gammelgard, G., Wenthe, J., Lovgren, T., Amini, R. M., Wikstrom, K. I., Essand, M., Savoldo, B., Hallbook, H., Hoglund, M., Dotti, G., Brenner, M. K., Hagberg, H. and Loskog, A. (2018). **A Phase I/IIa Trial Using CD19-Targeted Third-Generation CAR T Cells for Lymphoma and Leukemia**. Clin Cancer Res *24 (24)*, 6185-6194, doi: 10.1158/1078-0432.CCR-18-0426.

Feins, S., Kong, W., Williams, E. F., Milone, M. C. and Fraietta, J. A. (2019). **An introduction to

**chimeric antigen receptor (CAR) T-cell immunotherapy for human cancer**. Am J Hematol *94 (S1)*, S3-S9, doi: 10.1002/ajh.25418.

Frigault, M. J. and Maus, M. V. (2020). **State of the art in CAR T cell therapy for CD19+ B cell malignancies**. J Clin Invest *130 (4)*, 1586-1594, doi: 10.1172/JCI129208.

Gardner, R. A., Finney, O., Annesley, C., Brakke, H., Summers, C., Leger, K., Bleakley, M., Brown, C., Mgebroff, S., Kelly-Spratt, K. S., Hoglund, V., Lindgren, C., Oron, A. P., Li, D., Riddell, S. R., Park, J. R. and Jensen, M. C. (2017). **Intent-to-treat leukemia remission by CD19 CAR T cells of defined formulation and dose in children and young adults**. Blood *129 (25)*, 3322-3331, doi: 10.1182/blood-2017-02-769208.

Gargett, T., Yu, W., Dotti, G., Yvon, E. S., Christo, S. N., Hayball, J. D., Lewis, I. D., Brenner, M. K. and Brown, M. P. (2016). **GD2-specific CAR T Cells Undergo Potent Activation and Deletion Following Antigen Encounter but can be Protected From Activation-induced Cell Death by PD-1 Blockade**. Mol Ther *24 (6)*, 1135-1149, doi: 10.1038/mt.2016.63.

Gattinoni, L., Lugli, E., Ji, Y., Pos, Z., Paulos, C. M., Quigley, M. F., Almeida, J. R., Gostick, E., Yu, Z., Carpenito, C., Wang, E., Douek, D. C., Price, D. A., June, C. H., Marincola, F. M., Roederer, M. and Restifo, N. P. (2011). **A human memory T cell subset with stem cell-like properties**. Nat Med *17 (10)*, 1290-1297, doi: 10.1038/nm.2446.

Geyer, M. B., Riviere, I., Senechal, B., Wang, X., Wang, Y., Purdon, T. J., Hsu, M., Devlin, S. M., Halton, E., Lamanna, N., Rademaker, J., Sadelain, M., Brentjens, R. J. and Park, J. H. (2018). **Autologous CD19-Targeted CAR T Cells in Patients with Residual CLL following Initial Purine Analog-Based Therapy**. Mol Ther *26 (8)*, 1896-1905, doi: 10.1016/j.ymthe.2018.05.018.

Green, D. R. and Ferguson, T. A. (2001). **The role of Fas ligand in immune privilege**. Nat Rev Mol Cell Biol *2 (12)*, 917-924, doi: 10.1038/35103104.

Grosser, R., Cherkassky, L., Chintala, N. and Adusumilli, P. S. (2019). **Combination Immunotherapy with CAR T Cells and Checkpoint Blockade for the Treatment of Solid Tumors**. Cancer Cell *36 (5)*, 471-482, doi: 10.1016/j.ccell.2019.09.006.

Hofmann, S., Schubert, M. L., Wang, L., He, B., Neuber, B., Dreger, P., Muller-Tidow, C. and Schmitt, M. (2019). **Chimeric Antigen Receptor (CAR) T Cell Therapy in Acute Myeloid Leukemia (AML)**. J Clin Med *8 (2)*, doi: 10.3390/jcm8020200.

Hombach, A. A. and Abken, H. (2011). **Costimulation by chimeric antigen receptors revisited the T cell antitumor response benefits from combined CD28-OX40 signalling**. Int J Cancer *129 (12)*, 2935-2944, doi: 10.1002/ijc.25960.

Hu, Y., Sun, J., Wu, Z., Yu, J., Cui, Q., Pu, C., Liang, B., Luo, Y., Shi, J., Jin, A., Xiao, L. and Huang, H.

(2016). **Predominant cerebral cytokine release syndrome in CD19-directed chimeric antigen receptor-modified T cell therapy**. J Hematol Oncol *9 (1)*, 70, doi: 10.1186/s13045-016-0299-5.

Hyrenius-Wittsten, A. and Roybal, K. T. (2019). **Paving New Roads for CARs**. Trends Cancer *5 (10)*, 583-592, doi: 10.1016/j.trecan.2019.09.005.

Jacoby, E., Bielorai, B., Avigdor, A., Itzhaki, O., Hutt, D., Nussboim, V., Meir, A., Kubi, A., Levy, M., Zikich, D., Zeltzer, L. A., Brezinger, K., Schachter, J., Nagler, A., Besser, M. J. and Toren, A. (2018). **Locally produced CD19 CAR T cells leading to clinical remissions in medullary and extramedullary relapsed acute lymphoblastic leukemia**. Am J Hematol *93 (12)*, 1485-1492, doi: 10.1002/ajh.25274.

Jensen, M. C., Popplewell, L., Cooper, L. J., DiGiusto, D., Kalos, M., Ostberg, J. R. and Forman, S. J. (2010). **Antitransgene rejection responses contribute to attenuated persistence of adoptively transferred CD20/CD19-specific chimeric antigen receptor redirected T cells in humans**. Biol Blood Marrow Transplant *16 (9)*, 1245-1256, doi: 10.1016/j.bbmt.2010.03.014.

Jinek, M., Chylinski, K., Fonfara, I., Hauer, M., Doudna, J. A. and Charpentier, E. (2012). **A programmable dual-RNA-guided DNA endonuclease in adaptive bacterial immunity**. Science *337 (6096)*, 816-821, doi: 10.1126/science.1225829.

Kagoya, Y., Tanaka, S., Guo, T., Anczurowski, M., Wang, C. H., Saso, K., Butler, M. O., Minden, M. D. and Hirano, N. (2018). **A novel chimeric antigen receptor containing a JAK-STAT signaling domain mediates superior antitumor effects**. Nat Med *24 (3)*, 352-359, doi: 10.1038/nm.4478.

Klebanoff, C. A., Gattinoni, L., Torabi-Parizi, P., Kerstann, K., Cardones, A. R., Finkelstein, S. E., Palmer, D. C., Antony, P. A., Hwang, S. T., Rosenberg, S. A., Waldmann, T. A. and Restifo, N. P. (2005). **Central memory self/tumor-reactive CD8+ T cells confer superior antitumor immunity compared with effector memory T cells**. Proc Natl Acad Sci U S A *102 (27)*, 9571-9576, doi: 10.1073/pnas.0503726102.

Kochenderfer, J. N., Somerville, R. P. T., Lu, T., Shi, V., Bot, A., Rossi, J., Xue, A., Goff, S. L., Yang, J. C., Sherry, R. M., Klebanoff, C. A., Kammula, U. S., Sherman, M., Perez, A., Yuan, C. M., Feldman, T., Friedberg, J. W., Roschewski, M. J., Feldman, S. A., McIntyre, L., Toomey, M. A. and Rosenberg, S. A. (2017). **Lymphoma Remissions Caused by Anti-CD19 Chimeric Antigen Receptor T Cells Are Associated With High Serum Interleukin-15 Levels**. J Clin Oncol *35 (16)*, 1803-1813, doi: 10.1200/JCO.2016.71.3024.

Krendyukov, A. and Gieffers, C. (2019). **Asunercept as an innovative therapeutic approach for recurrent glioblastoma and other malignancies**. Cancer Manag Res *11*, 8095-8100, doi: 10.2147/CMAR.S216675.

Kunkele, A., Johnson, A. J., Rolczynski, L. S., Chang, C. A., Hoglund, V., Kelly-Spratt, K. S. and Jensen, M. C. (2015). **Functional Tuning of CARs Reveals Signaling Threshold above Which CD8+ CTL Antitumor Potency Is Attenuated due to Cell Fas-FasL-Dependent AICD**. Cancer Immunol Res *3 (4)*, 368-379, doi: 10.1158/2326-6066.CIR-14-0200.

Künkele, A., Johnson, A. J., Rolczynski, L. S., Chang, C. A., Hoglund, V., Kelly-Spratt, K. S. and Jensen, M. C. J. C. i. r. (2015). **Functional tuning of CARs reveals signaling threshold above which CD8+ CTL antitumor potency is attenuated due to cell Fas–FasL-dependent AICD**. *3 (4)*, 368-379.

Lakins, M. A., Ghorani, E., Munir, H., Martins, C. P. and Shields, J. D. (2018). **Cancer-associated fibroblasts induce antigen-specific deletion of CD8 (+) T Cells to protect tumour cells**. Nat Commun *9 (1)*, 948, doi: 10.1038/s41467-018-03347-0.

Le Gallo, M., Poissonnier, A., Blanco, P. and Legembre, P. (2017). **CD95/Fas, Non-Apoptotic Signaling Pathways, and Kinases**. Front Immunol *8*, 1216, doi: 10.3389/fimmu.2017.01216.

Lee, D. W., Kochenderfer, J. N., Stetler-Stevenson, M., Cui, Y. K., Delbrook, C., Feldman, S. A., Fry, T. J., Orentas, R., Sabatino, M., Shah, N. N., Steinberg, S. M., Stroncek, D., Tschernia, N., Yuan, C., Zhang, H., Zhang, L., Rosenberg, S. A., Wayne, A. S. and Mackall, C. L. (2015). **T cells expressing CD19 chimeric antigen receptors for acute lymphoblastic leukaemia in children and young adults: a phase 1 dose-escalation trial**. Lancet *385 (9967)*, 517-528, doi: 10.1016/S0140-6736(14)61403-3.

Li, C., Guan, X., Du, T., Jin, W., Wu, B., Liu, Y., Wang, P., Hu, B., Griffin, G. E., Shattock, R. J. and Hu, Q. (2015). **Inhibition of HIV-1 infection of primary CD4+ T-cells by gene editing of CCR5 using adenovirus-delivered CRISPR/Cas9**. J Gen Virol *96 (8)*, 2381-2393, doi: 10.1099/vir.0.000139.

Li, S., Young, K. H. and Medeiros, L. J. (2018). **Diffuse large B-cell lymphoma**. Pathology *50 (1)*, 74-87, doi: 10.1016/j.pathol.2017.09.006.

Lim, S. C. (2002). **Expression of Fas ligand and sFas ligand in human gastric adenocarcinomas**. Oncol Rep *9 (1)*, 103-107.

Locke, F. L., Ghobadi, A., Jacobson, C. A., Miklos, D. B., Lekakis, L. J., Oluwole, O. O., Lin, Y., Braunschweig, I., Hill, B. T., Timmerman, J. M., Deol, A., Reagan, P. M., Stiff, P., Flinn, I. W., Farooq, U., Goy, A., McSweeney, P. A., Munoz, J., Siddiqi, T., Chavez, J. C., Herrera, A. F., Bartlett, N. L., Wiezorek, J. S., Navale, L., Xue, A., Jiang, Y., Bot, A., Rossi, J. M., Kim, J. J., Go, W. Y. and Neelapu, S. S. (2019). **Long-term safety and activity of axicabtagene ciloleucel in refractory large B-cell lymphoma (ZUMA-1): a single-arm, multicentre, phase 1-2 trial**. Lancet Oncol *20 (1)*, 31-42, doi: 10.1016/S1470-2045(18)30864-7.

Louis, C. U., Savoldo, B., Dotti, G., Pule, M., Yvon, E., Myers, G. D., Rossig, C., Russell, H. V., Diouf, O., Liu, E., Liu, H., Wu, M. F., Gee, A. P., Mei, Z., Rooney, C. M., Heslop, H. E. and Brenner, M. K. (2011). **Antitumor activity and long-term fate of chimeric antigen receptor-positive T cells in patients with neuroblastoma**. Blood *118 (23)*, 6050-6056, doi: 10.1182/blood-2011-05-354449.

Lynch, D. H., Ramsdell, F. and Alderson, M. R. (1995). **Fas and FasL in the homeostatic regulation of immune responses**. Immunol Today *16 (12)*, 569-574, doi: 10.1016/0167-5699(95)80079-4.

Maher, S., Toomey, D., Condron, C. and Bouchier-Hayes, D. (2002). **Activation-induced cell death: the controversial role of Fas and Fas ligand in immune privilege and tumour counterattack**. Immunol Cell Biol *80 (2)*, 131-137, doi: 10.1046/j.1440-1711.2002.01068.x.

Mali, P., Aach, J., Stranges, P. B., Esvelt, K. M., Moosburner, M., Kosuri, S., Yang, L. and Church, G. M. (2013). **CAS9 transcriptional activators for target specificity screening and paired nickases for cooperative genome engineering**. Nat Biotechnol *31 (9)*, 833-838, doi: 10.1038/nbt.2675.

Mamonkin, M. and Heslop, H. E. (2017). **Exhausting alloreactivity of donor-derived CAR T cells**. Nat Med *23 (2)*, 147-148, doi: 10.1038/nm.4276.

Marks, D. I., van Oostrum, I., Mueller, S., Welch, V., Vandendries, E., Loberiza, F. R., Bohme, S., Su, Y., Stelljes, M. and Kantarjian, H. M. (2019). **Burden of hospitalization in acute lymphoblastic leukemia patients treated with Inotuzumab Ozogamicin versus standard chemotherapy treatment**. Cancer Med *8 (13)*, 5959-5968, doi: 10.1002/cam4.2480.

Maude, S. L., Laetsch, T. W., Buechner, J., Rives, S., Boyer, M., Bittencourt, H., Bader, P., Verneris, M. R., Stefanski, H. E., Myers, G. D., Qayed, M., De Moerloose, B., Hiramatsu, H., Schlis, K., Davis, K. L., Martin, P. L., Nemecek, E. R., Yanik, G. A., Peters, C., Baruchel, A., Boissel, N., Mechinaud, F., Balduzzi, A., Krueger, J., June, C. H., Levine, B. L., Wood, P., Taran, T., Leung, M., Mueller, K. T., Zhang, Y., Sen, K., Lebwohl, D., Pulsipher, M. A. and Grupp, S. A. (2018). **Tisagenlecleucel in Children and Young Adults with B-Cell Lymphoblastic Leukemia**. N Engl J Med *378 (5)*, 439-448, doi: 10.1056/NEJMoa1709866.

Morrison, S. J. and Scadden, D. T. (2014). **The bone marrow niche for haematopoietic stem cells**. Nature *505 (7483)*, 327-334, doi: 10.1038/nature12984.

Motz, G. T., Santoro, S. P., Wang, L. P., Garrabrant, T., Lastra, R. R., Hagemann, I. S., Lal, P., Feldman, M. D., Benencia, F. and Coukos, G. (2014). **Tumor endothelium FasL establishes a selective immune barrier promoting tolerance in tumors**. Nat Med *20 (6)*, 607-615, doi: 10.1038/nm.3541.

Muschen, M., Moers, C., Warskulat, U., Even, J., Niederacher, D. and Beckmann, M. W. (2000). **CD95**

**ligand expression as a mechanism of immune escape in breast cancer**. Immunology *99 (1)*, 69-77, doi: DOI 10.1046/j.1365-2567.2000.00921.x.

Navani, V., Graves, M. C., Bowden, N. A. and Van Der Westhuizen, A. (2020). **Immune checkpoint blockade in solid organ tumours: Choice, dose and predictors of response**. Br J Clin Pharmacol *86 (9)*, 1736-1752, doi: 10.1111/bcp.14352.

Neelapu, S. S., Locke, F. L., Bartlett, N. L., Lekakis, L. J., Miklos, D. B., Jacobson, C. A., Braunschweig, I., Oluwole, O. O., Siddiqi, T., Lin, Y., Timmerman, J. M., Stiff, P. J., Friedberg, J. W., Flinn, I. W., Goy, A., Hill, B. T., Smith, M. R., Deol, A., Farooq, U., McSweeney, P., Munoz, J., Avivi, I., Castro, J. E., Westin, J. R., Chavez, J. C., Ghobadi, A., Komanduri, K. V., Levy, R., Jacobsen, E. D., Witzig, T. E., Reagan, P., Bot, A., Rossi, J., Navale, L., Jiang, Y., Aycock, J., Elias, M., Chang, D., Wiezorek, J. and Go, W. Y. (2017). **Axicabtagene Ciloleucel CAR T-Cell Therapy in Refractory Large B-Cell Lymphoma**. N Engl J Med *377 (26)*, 2531-2544, doi: 10.1056/NEJMoa1707447.

Nozoe, T., Yasuda, M., Honda, M., Inutsuka, S. and Korenaga, D. (2003). **Fas ligand expression is correlated with metastasis in colorectal carcinoma**. Oncology *65 (1)*, 83-88, doi: 10.1159/000071208.

Park, J. H., Riviere, I., Gonen, M., Wang, X., Senechal, B., Curran, K. J., Sauter, C., Wang, Y., Santomasso, B., Mead, E., Roshal, M., Maslak, P., Davila, M., Brentjens, R. J. and Sadelain, M. (2018). **Long-Term Follow-up of CD19 CAR Therapy in Acute Lymphoblastic Leukemia**. N Engl J Med *378 (5)*, 449-459, doi: 10.1056/NEJMoa1709919.

Paul, S., Kantarjian, H. and Jabbour, E. J. (2016). **Adult Acute Lymphoblastic Leukemia**. Mayo Clin Proc *91 (11)*, 1645-1666, doi: 10.1016/j.mayocp.2016.09.010.

Porter, D. L., Hwang, W. T., Frey, N. V., Lacey, S. F., Shaw, P. A., Loren, A. W., Bagg, A., Marcucci, K. T., Shen, A., Gonzalez, V., Ambrose, D., Grupp, S. A., Chew, A., Zheng, Z., Milone, M. C., Levine, B. L., Melenhorst, J. J. and June, C. H. (2015). **Chimeric antigen receptor T cells persist and induce sustained remissions in relapsed refractory chronic lymphocytic leukemia**. Sci Transl Med *7 (303)*, 303ra139, doi: 10.1126/scitranslmed.aac5415.

Ramos, C. A., Rouce, R., Robertson, C. S., Reyna, A., Narala, N., Vyas, G., Mehta, B., Zhang, H., Dakhova, O., Carrum, G., Kamble, R. T., Gee, A. P., Mei, Z., Wu, M. F., Liu, H., Grilley, B., Rooney, C. M., Heslop, H. E., Brenner, M. K., Savoldo, B. and Dotti, G. (2018). **In Vivo Fate and Activity of Second- versus Third-Generation CD19-Specific CAR-T Cells in B Cell Non-Hodgkin's Lymphomas**. Mol Ther *26 (12)*, 2727-2737, doi: 10.1016/j.ymthe.2018.09.009.

Rao, V. K. and Oliveira, J. B. (2011). **How I treat autoimmune lymphoproliferative syndrome**. Blood *118 (22)*, 5741-5751, doi: 10.1182/blood-2011-07-325217.

Redondo, P., Solano, T., B, V. A., Bauza, A. and Idoate, M. (2002). **Fas and Fas ligand: expression and soluble circulating levels in cutaneous malignant melanoma**. Br J Dermatol *147 (1)*, 80-86, doi: 10.1046/j.1365-2133.2002.04745.x.

Ren, J., Zhang, X., Liu, X., Fang, C., Jiang, S., June, C. H. and Zhao, Y. (2017). **A versatile system for rapid multiplex genome-edited CAR T cell generation**. Oncotarget *8 (10)*, 17002-17011, doi: 10.18632/oncotarget.15218.

Schubert, M. L., Schmitt, A., Sellner, L., Neuber, B., Kunz, J., Wuchter, P., Kunz, A., Gern, U., Michels, B., Hofmann, S., Huckelhoven-Krauss, A., Kulozik, A., Ho, A. D., Muller-Tidow, C., Dreger, P. and Schmitt, M. (2019). **Treatment of patients with relapsed or refractory CD19+ lymphoid disease with T lymphocytes transduced by RV-SFG.CD19.CD28.4-1BBzeta retroviral vector: a unicentre phase I/II clinical trial protocol**. BMJ Open *9 (5)*, e026644, doi: 10.1136/bmjopen-2018-026644.

Schultz, L. and Mackall, C. (2019). **Driving CAR T cell translation forward**. Sci Transl Med *11 (481)*, doi: 10.1126/scitranslmed.aaw2127.

Schuster, S. J., Bishop, M. R., Tam, C. S., Waller, E. K., Borchmann, P., McGuirk, J. P., Jager, U., Jaglowski, S., Andreadis, C., Westin, J. R., Fleury, I., Bachanova, V., Foley, S. R., Ho, P. J., Mielke, S., Magenau, J. M., Holte, H., Pantano, S., Pacaud, L. B., Awasthi, R., Chu, J., Anak, O., Salles, G., Maziarz, R. T. and Investigators, J. (2019). **Tisagenlecleucel in Adult Relapsed or Refractory Diffuse Large B-Cell Lymphoma**. N Engl J Med *380 (1)*, 45-56, doi: 10.1056/NEJMoa1804980.

Shalem, O., Sanjana, N. E., Hartenian, E., Shi, X., Scott, D. A., Mikkelson, T., Heckl, D., Ebert, B. L., Root, D. E., Doench, J. G. and Zhang, F. (2014). **Genome-scale CRISPR-Cas9 knockout screening in human cells**. Science *343 (6166)*, 84-87, doi: 10.1126/science.1247005.

Sharma, P. and Allison, J. P. (2020). **Dissecting the mechanisms of immune checkpoint therapy**. Nat Rev Immunol *20 (2)*, 75-76, doi: 10.1038/s41577-020-0275-8.

Siddiqi, T., Dorritie, K. A., Soumerai, J. D., Stephens, D. M., Dubovsky, J. A., Gillenwater, H. H., Gong, L., Thorpe, J., Yang, L. and Wierda, W. G. (2019). **TRANSCEND CLL 004: Minimal residual disease (MRD) negative responses after lisocabtagene maraleucel (Liso-Cel; JCAR017), a CD19-directed CAR T cell product, in patients (pts) with relapsed/refractory chronic lymphocytic leukemia or small lymphocytic lymphoma (CLL/SLL)**. Journal of Clinical Oncology *37 (15_suppl)*, 7501-7501, doi: 10.1200/JCO.2019.37.15_suppl.7501.

Sive, J. I., Buck, G., Fielding, A., Lazarus, H. M., Litzow, M. R., Luger, S., Marks, D. I., McMillan, A., Moorman, A. V., Richards, S. M., Rowe, J. M., Tallman, M. S. and Goldstone, A. H. (2012). **Outcomes in older adults with acute lymphoblastic leukaemia (ALL): results from the international MRC UKALL XII/ECOG2993 trial**. Br J Haematol *157 (4)*, 463-471, doi:

10.1111/j.1365-2141.2012.09095.x.

Skorka, K., Ostapinska, K., Malesa, A. and Giannopoulos, K. (2020). **The Application of CAR-T Cells in Haematological Malignancies**. Arch Immunol Ther Exp (Warsz) *68 (6)*, 34, doi: 10.1007/s00005-020-00599-x.

Sommermeyer, D., Hudecek, M., Kosasih, P. L., Gogishvili, T., Maloney, D. G., Turtle, C. J. and Riddell, S. R. (2016). **Chimeric antigen receptor-modified T cells derived from defined CD8+ and CD4+ subsets confer superior antitumor reactivity in vivo**. Leukemia *30 (2)*, 492-500, doi: 10.1038/leu.2015.247.

Song, M. K., Park, B. B. and Uhm, J. E. (2019). **Resistance Mechanisms to CAR T-Cell Therapy and Overcoming Strategy in B-Cell Hematologic Malignancies**. Int J Mol Sci *20 (20)*, doi: 10.3390/ijms20205010.

Suda, T., Hashimoto, H., Tanaka, M., Ochi, T. and Nagata, S. (1997). **Membrane Fas ligand kills human peripheral blood T lymphocytes, and soluble Fas ligand blocks the killing**. J Exp Med *186 (12)*, 2045-2050, doi: 10.1084/jem.186.12.2045.

Tuettenberg, J., Seiz, M., Debatin, K. M., Hollburg, W., von Staden, M., Thiemann, M., Hareng, B., Fricke, H. and Kunz, C. (2012). **Pharmacokinetics, pharmacodynamics, safety and tolerability of APG101, a CD95-Fc fusion protein, in healthy volunteers and two glioma patients**. Int Immunopharmacol *13 (1)*, 93-100, doi: 10.1016/j.intimp.2012.03.004.

Turtle, C. J., Hay, K. A., Hanafi, L. A., Li, D., Cherian, S., Chen, X., Wood, B., Lozanski, A., Byrd, J. C., Heimfeld, S., Riddell, S. R. and Maloney, D. G. (2017). **Durable Molecular Remissions in Chronic Lymphocytic Leukemia Treated With CD19-Specific Chimeric Antigen Receptor-Modified T Cells After Failure of Ibrutinib**. J Clin Oncol *35 (26)*, 3010-3020, doi: 10.1200/JCO.2017.72.8519.

Vardiman, J. W., Thiele, J., Arber, D. A., Brunning, R. D., Borowitz, M. J., Porwit, A., Harris, N. L., Le Beau, M. M., Hellstrom-Lindberg, E., Tefferi, A. and Bloomfield, C. D. (2009). **The 2008 revision of the World Health Organization (WHO) classification of myeloid neoplasms and acute leukemia: rationale and important changes**. Blood *114 (5)*, 937-951, doi: 10.1182/blood-2009-03-209262.

Viardot, A., Wais, V., Sala, E. and Koerper, S. (2019). **Chimeric antigen receptor (CAR) T-cell therapy as a treatment option for patients with B-cell lymphomas: perspectives on the therapeutic potential of Axicabtagene ciloleucel**. Cancer Manag Res *11*, 2393-2404, doi: 10.2147/CMAR.S163225.

Wang, H., Kaur, G., Sankin, A. I., Chen, F., Guan, F. and Zang, X. (2019). **Immune checkpoint blockade and CAR-T cell therapy in hematologic malignancies**. J Hematol Oncol *12 (1)*, 59, doi: 10.1186/s13045-019-0746-1.

Wang, L., Liu, J. Q., Talebian, F., Liu, Z., Yu, L. and Bai, X. F. (2015). **IL-10 enhances CTL-mediated tumor rejection by inhibiting highly suppressive CD4(+) T cells and promoting CTL persistence in a murine model of plasmacytoma**. Oncoimmunology *4 (7)*, e1014232, doi: 10.1080/2162402X.2015.1014232.

Wang, W., Ye, C., Liu, J., Zhang, D., Kimata, J. T. and Zhou, P. (2014). **CCR5 gene disruption via lentiviral vectors expressing Cas9 and single guided RNA renders cells resistant to HIV-1 infection**. PLoS One *9 (12)*, e115987, doi: 10.1371/journal.pone.0115987.

Wick, W., Fricke, H., Junge, K., Kobyakov, G., Martens, T., Heese, O., Wiestler, B., Schliesser, M. G., von Deimling, A., Pichler, J., Vetlova, E., Harting, I., Debus, J., Hartmann, C., Kunz, C., Platten, M., Bendszus, M. and Combs, S. E. (2014). **A phase II, randomized, study of weekly APG101+reirradiation versus reirradiation in progressive glioblastoma**. Clin Cancer Res *20 (24)*, 6304-6313, doi: 10.1158/1078-0432.CCR-14-0951-T.

Xu, X., Sun, Q., Liang, X., Chen, Z., Zhang, X., Zhou, X., Li, M., Tu, H., Liu, Y., Tu, S. and Li, Y. (2019). **Mechanisms of Relapse After CD19 CAR T-Cell Therapy for Acute Lymphoblastic Leukemia and Its Prevention and Treatment Strategies**. Front Immunol *10*, 2664, doi: 10.3389/fimmu.2019.02664.

Yamamoto, T. N., Lee, P. H., Vodnala, S. K., Gurusamy, D., Kishton, R. J., Yu, Z., Eidizadeh, A., Eil, R., Fioravanti, J., Gattinoni, L., Kochenderfer, J. N., Fry, T. J., Aksoy, B. A., Hammerbacher, J. E., Cruz, A. C., Siegel, R. M., Restifo, N. P. and Klebanoff, C. A. (2019). **T cells genetically engineered to overcome death signaling enhance adoptive cancer immunotherapy**. J Clin Invest *129 (4)*, 1551-1565, doi: 10.1172/JCI121491.

Yi, F., Frazzette, N., Cruz, A. C., Klebanoff, C. A. and Siegel, R. M. (2018). **Beyond Cell Death: New Functions for TNF Family Cytokines in Autoimmunity and Tumor Immunotherapy**. Trends Mol Med *24 (7)*, 642-653, doi: 10.1016/j.molmed.2018.05.004.

Zarour, H. M. (2016). **Reversing T-cell Dysfunction and Exhaustion in Cancer**. Clin Cancer Res *22 (8)*, 1856-1864, doi: 10.1158/1078-0432.CCR-15-1849.

Zhang, Y., Zhang, X., Cheng, C., Mu, W., Liu, X., Li, N., Wei, X., Liu, X., Xia, C. and Wang, H. (2017). **CRISPR-Cas9 mediated LAG-3 disruption in CAR-T cells**. Front Med *11 (4)*, 554-562, doi: 10.1007/s11684-017-0543-6.

Zhao, Z., Condomines, M., van der Stegen, S. J. C., Perna, F., Kloss, C. C., Gunset, G., Plotkin, J. and Sadelain, M. (2015). **Structural Design of Engineered Costimulation Determines Tumor Rejection Kinetics and Persistence of CAR T Cells**. Cancer Cell *28 (4)*, 415-428, doi: 10.1016/j.ccell.2015.09.004.

Zhu, J., Petit, P. F. and Van den Eynde, B. J. (2019). **Apoptosis of tumor-infiltrating T lymphocytes:**

**a new immune checkpoint mechanism**. Cancer Immunol Immunother *68 (5)*, 835-847, doi: 10.1007/s00262-018-2269-y.

Zhu, J., Powis de Tenbossche, C. G., Cane, S., Colau, D., van Baren, N., Lurquin, C., Schmitt-Verhulst, A. M., Liljestrom, P., Uyttenhove, C. and Van den Eynde, B. J. (2017). **Resistance to cancer immunotherapy mediated by apoptosis of tumor-infiltrating lymphocytes**. Nat Commun *8 (1)*, 1404, doi: 10.1038/s41467-017-00784-1.

# CURRICULUM VITAE

## PERSONAL INFORMATION

| | |
|---|---|
| Name | Bailin He |
| Date of birth | August 10, 1990 |
| Place of birth | Dongguan, PR China |
| Nationality | Chinese |

## EDUCATION

07.2018 - present
Heidelberg University, Heidelberg, Germany
Supervisor: Prof. Dr. med. Michael Schmitt

PhD candidate

09.2014 – 07.2017
Degree: Master of Medicine
Major: Internal Medicine
Southern Medical University, Guangzhou, China
Mentor: Prof. Dr. med. Xiaoli Liu

09.2009 – 07.2014
Degree: Bachelor of Medicine
Major: Medicine Laboratory
Guangdong Medical College, Dongguan, China

## EXPERIENCE

07.2018 - present
Doctoral research
AG Cellular Immunotherapy, Dept. of Internal Medicine V
Heidelberg University Hospital, Heidelberg, Germany
Supervisor: Prof. Dr. med. Michael Schmitt

11.2017- 06.2018
Research training
Dept. of Hematology, Hemostasis, Oncology, and Stem
Cell Transplantation.
Hannover Medical School, Hannover, Germany
Mentor: Prof. Dr. med. Zhixiong Li

01.2016 – 05.2017
Research training
Laboratory of Hematology, Nanfang Hospital
Southern Medical University, Guangzhou, China
Mentor: Prof. Dr. med. Xiaoli Liu

| 01.2015 – 12.2015 | Clinical traineeships |
| | Nanfang Hospital |
| | Southern Medical University, Guangzhou, China |

| 01.2013 – 01.2014 | Internship |
| | Shenzhen Hospital of Peking University, Shenzhen, China |

## HONORS

| 2017 | Study-abroad Scholarship by Guangzhou Elite Project |
| 2017 | Southern Medical University Outstanding Graduate |
| 2014 | Guangdong Medical College Outstanding Graduate |

## CONFERENCES ATTENDED

| 2019 | 61st American Society of Hematology (ASH) Annual Meeting (Poster presentation), Orlando, the US |
| 2019 | Research Day of Medical Clinic V, Heidelberg University Hospital (Poster presentation), Heidelberg, Germany |
| 2018, 2019 | 2nd and 3rd Cell Therapy Symposium, Heidelberg University Hospital, Heidelberg, Germany |

## PUBLICATIONS

(1) He, B., Wang, Q., Liu, X., Lu, Z., Han, J., Pan, C., Carter, B. Z., Liu, Q., Xu, N. and Zhou, H. (2020). A novel HDAC inhibitor chidamide combined with imatinib synergistically targets tyrosine kinase inhibitor resistant chronic myeloid leukemia cells. Biomed Pharmacother *129*, 110390.

(2) Hofmann, S., Schubert, M. L., Wang, L., He, B., Neuber, B., Dreger, P., Muller-Tidow, C. and Schmitt, M. (2019). Chimeric Antigen Receptor (CAR) T Cell Therapy in Acute Myeloid Leukemia (AML). J Clin Med *8 (2)*.

(3) Stock, S., Ubelhart, R., Schubert, M. L., Fan, F., He, B., Hoffmann, J. M., Wang, L., Wang, S., Gong, W., Neuber, B., Huckelhoven-Krauss, A., Gern, U., Christ, C., Hexel, M., Schmitt, A., Schmidt, P., Krauss, J., Jager, D., Muller-Tidow, C., Dreger, P., Schmitt, M. and Sellner, L. (2019). Idelalisib for optimized CD19-specific chimeric antigen receptor T cells in chronic lymphocytic leukemia patients. Int J Cancer *145 (5)*, 1312-1324.

(4) Lu, Z., Xu, N., He, B., Pan, C., Lan, Y., Zhou, H. and Liu, X. (2017). Inhibition of autophagy enhances the selective anti-cancer activity of tigecycline to overcome drug resistance in the treatment of chronic myeloid leukemia. J Exp Clin Cancer Res *36 (1)*, 43.

# ACKNOWLEDGMENT

# EIDESSTATTLICHE VERSICHERUNG

1.  Bei der eingereichten Dissertation zu dem Thema „Blockade of CD95/CD95L Death Signaling Enhances CAR T Cell Persistence and Antitumor Efficacy" handelt es sich um meine eigenständig erbrachte Leistung.

2.  Ich habe nur die angegebenen Quellen und Hilfsmittel benutzt und mich keener unzulässigen Hilfe Dritter bedient. Insbesondere habe ich wörtlich oder sinngemäß aus anderen Werken übernommene Inhalte als solche kenntlich gemacht.

3.  Die Arbeit oder Teile davon habe ich bislang nicht an einer Hochschule des In- oder Auslands als Bestandteil einer Prüfungs- oder Qualifikationsleistung vorgelegt.

4.  Die Richtigkeit der vorstehenden Erklärungen bestätige ich.

5.  Die Bedeutung der eidesstattlichen Versicherung und die strafrechtlichen Folgen einer unrichtigen oder unvollständigen eidesstattlichen Versicherung sind mir bekannt. Ich versichere an Eides statt, dass ich nach bestem Wissen die reine Wahrheit erklärt und nichts verschwiegen habe.

Ort und Datum                                                    Unterschrift